Superconductivity, Superfluids and Condensates

James F. Annett

University of Bristol

Contents

1
Superconductivity

1.1 Introduction

This chapter describes some of the most fundamental experimental facts about superconductors, together with the simplest theoretical model: the **London equation**. We shall see how this equation leads directly to the expulsion of magnetic fields from superconductors, the Meissner-Ochsenfeld effect, which usually considered to be is the fundamental property which defines superconductivity.

The chapter starts with a brief review of the Drude theory of conduction in normal metals. We shall also show how it is possible to use the Drude theory to make the London equation plausible. We shall also explore some of the consequences of the London equation, in particular the existence of vortices in superconductors and the differences between type I and II superconductors.

1.2 Conduction in metals

The idea that metals are good electrical conductors because the electrons move freely between the atoms was first developed by Drude in 1905, only five years after the original discovery of the electron.

Although Drude's original model did not include quantum mechanics, his formula for the conductivity of metals remains correct even in the modern quantum theory of metals. To briefly recap the key ideas in the theory of metals, we recall that the wave functions of the electrons in crystalline solids obey **Bloch's theorem**,[1].

$$\psi_{n\mathbf{k}}(\mathbf{r}) = u_{n\mathbf{k}}(\mathbf{r})e^{i\mathbf{k}.\mathbf{r}}. \tag{1.1}$$

Where here $u_{n\mathbf{k}}(\mathbf{r})$ is a function which is periodic, $\hbar\mathbf{k}$ is the crystal momentum, and $\mathbf{k}$ takes values in the first Brillouin zone of the reciprocal lattice. The energies of these Bloch wave states give the **energy bands**, $\epsilon_{n\mathbf{k}}$, where n counts the different electron bands. Electrons are fermions, and

---

[1]See for example, the text *Band theory and electronic properties of solids* by J. Singleton (2002), or other textbooks on Solid State Physics, such as Kittel (1996), or Ashcroft and Mermin(1976)

so at temperature T a state with energy ϵ is occupied according to the **Fermi-Dirac** distribution

$$f(\epsilon) = \frac{1}{e^{\beta(\epsilon - \mu)} + 1}. \tag{1.2}$$

The chemical potential, μ, is determined by the requirement that the total density of electrons per unit volume is

$$\frac{N}{V} = \frac{2}{(2\pi)^3} \sum_n \int \frac{1}{e^{\beta(\epsilon_{n\mathbf{k}} - \mu)} + 1} d^3 k \tag{1.3}$$

where the factor of 2 is because of the two spin states of the $s = 1/2$ electron. Here the integral over $\mathbf{k}$ includes all of the first Brillouin zone of the reciprocal lattice and, in principle, the sum over the band index n counts all of the occupied electron bands.

In all of the metals that we are interested the temperature is such that this Fermi gas is in a highly degenerate state, in which $k_\mathrm{B} T << \mu$. In this case $f(\epsilon_{n\mathbf{k}})$ is nearly 1 in the region 'inside' the Fermi surface, and is 0 outside. The Fermi surface can be defined by the condition $\epsilon_{n\mathbf{k}} = \epsilon_F$, where $\epsilon_F = \mu$ is the Fermi energy. In practice, for simplicity, in this book we shall usually assume that there is only one conduction band at the Fermi surface, and so we shall ignore the band index n from now on. In this case the density of **conduction electrons**, n, is given by

$$n = \frac{2}{(2\pi)^3} \int \frac{1}{e^{\beta(\epsilon_\mathbf{k} - \mu)} + 1} d^3 k \tag{1.4}$$

where $\epsilon_\mathbf{k}$ is the energy of the single band which crosses the Fermi surface. In cases where the single band approximation is not sufficient, it is quite easy to add back a sum over bands to the theory whenever necessary.

Metallic conduction is dominated by the thin shell of quantum states with energies $\epsilon_F - k_\mathrm{B} T < \epsilon < \epsilon_F + k_\mathrm{B} T$, since these are the only states which can be thermally excited at temperature T. We can think of this as a low density gas of 'electrons' excited into empty states above ϵ_F and of 'holes' in the occupied states below ϵ_F. In this **Fermi gas** description of metals the electrical conductivity, σ, is given by the Drude theory as,

$$\sigma = \frac{ne^2 \tau}{m}, \tag{1.5}$$

where m is the effective mass of the conduction electrons[2], $-e$ is the electron charge and τ is the average lifetime for free motion of the electrons between collisions with impurities or other electrons.

---

[2]Note that the band mass of the Bloch electrons, m, need not be the same as the bare mass of an electron in vacuum, m_e. The effective mass is typically $2 - 3$ times greater. In the most extreme case, the **heavy fermion materials** m can be as large as $50 - 100 m_e$!

The conductivity is defined by the **constitutive equation**

$$\mathbf{j} = \sigma \boldsymbol{\mathcal{E}}. \tag{1.6}$$

Here $\mathbf{j}$ is the electrical current density which flows in response to the external electric field, $\mathcal{E}$. The resistivity ρ obeys

$$\boldsymbol{\mathcal{E}} = \rho \mathbf{j}, \tag{1.7}$$

and so ρ is simply the reciprocal of the conductivity, $\rho = 1/\sigma$. Using the Drude formula we see that

$$\rho = \frac{m}{ne^2} \tau^{-1}, \tag{1.8}$$

and so the resistivity is proportioal to the scattering rate, τ^{-1} of the conduction electrons. In the SI system the resistivity has units of Ωm, or is more often quoted in Ωcm.

Eq. 1.5 shows that the electrical conductivity depends on temperature mainly via the different scattering processes which enter into the mean lifetime τ. In a typical metal there will be three main scattering processes, scattering by impurities, by electron-electron interactions and by electron-phonon collisions. These are independent processes, and so we should add the scattering rates to obtain the total effective scattering rate

$$\tau^{-1} = \tau_{imp}^{-1} + \tau_{el-el}^{-1} + \tau_{el-ph}^{-1}, \tag{1.9}$$

where τ_{imp}^{-1} is the rate of scattering by impurities, τ_{el-el}^{-1} the electron-electron scattering rtae, and τ_{el-ph}^{-1} the electron phonon scattering rate. Using Eq. 1.8 we see that the total resistivity is just a sum of independent contributions from each of these different scattering processes,

$$\rho = \frac{m}{ne^2} \left(\tau_{imp}^{-1} + \tau_{el-el}^{-1} + \tau_{el-ph}^{-1} \right). \tag{1.10}$$

Each of these lifetimes is a characteristic function of temperature. The impuri ty scattering rate, τ_{imp}^{-1}, will be essentially independent of temperature, at least for the case of non-magnetic impurities. The electron-electron scattering rate, τ_{el-el}^{-1}, is proportional to T^2, where T is the temperature. While at low temperatures (well below the phonon Debye temperature) the electron-phonon scattering rate, τ_{el-ph}^{-1}, is proportional to T^5. Therefore we would expect that the resistivity of a metal is of the form

$$\rho = \rho_0 + aT^2 + \dots \tag{1.11}$$

at very low temperatures. The zero temperature resistivity, the residual resistivity, ρ_0, depends only on the concentration of impurities.

For most metals the resistivity does indeed behave in this way at low temperatures. However for a superconductor something dramatically different happens. Upon cooling the resistivity first follows the simple smooth

behaviour, Eq. 1.11, but then suddenly vanishes entirely, as sketched in Fig. 1.1. The temperature where the resistivity vanishes is called the critical temperature, T_c. Below this temperature the resistivity is not just small, but is, as far as can be measured, **e**xactly zero.

This phenomenon was a complete surprise when it was first observed by H. Kammerling Onnes in 1911. He had wanted to test the validity of the Drude theory by measuring the resistivity at the lowest temperatures possible. The first measurements on samples of platinum and gold were quite consistent with the Drude model. But then he then turned his attention to mercury, because of its especially high purity. Based on Eq. 1.11 one could expect a very small, perhaps even zero, residual resisitivity in exceptionally pure substances. But what Kammerling Onnes actually observed was completly unexpected, and not consistent with Eq. 1.11. Surprisingly he discovered that all signs of resistance appeared to suddenly vanished suddenly below about 4K. This was quite unexpected from the Drude model, and was, in fact, the discovery of a new state of matter: superconductivity.

1.3   Superconducting materials

A number of the elements in the periodic table become superconducting at low temperatures, as summarized in Table 1.1. Of the elements, Niobium (Nb) has the highest critical temperature T_c of 9.2K at atmospheric pressure. Interestingly, some while common metals such as aluminium (1.2K), tin (3.7K) and lead (7.2K) become superconducting, other equally good, or better, metals (such as copper, silver or gold) show no evidence for superconductivity at all. It is still a matter of debate whether or not they would eventually become superconducting if made highly pure and cooled to sufficiently low temperatures. As recently as 1998 it was discovered that extremely pure platinum becomes superconducting, but only when it is prepared into small nano-particles at temperatures of a few miliKelvin.

Another recent discovery is that quite a few more elments also become superconducting when they are subjected to extremely high pressures. Samples must be pressurized between two anvil shaped diamonds. Using this techni que it is possible to obtain such high pressures that substances which are normally insulators become metallic, and some of these novel metals become superconductin g. Sulphur and oxygen both become superconducting at surprisingly high temperatures . Even iron becomes superconducting under pressure. At normal pressures iron is, of course, magnetic, and the magnetism prevents superconductivity from occuring . However, at high pressures a non-magnetic phase can be found, and this becomes superconducting. For many years the "holy grail" for this sort of high pressu re work has been to looks for superconductivity in metallic hydrogen. It has been predicted that metallic hydrogen could become superconducting at as high as 300K, which would be the first room temperature superconductor! To date, high pressure phases of metallic hydrogen have indeed been produced, but, so far at least, superconductivity has not been found.

Table 1.1 Some selected superconducting elements and compounds

substance	Tc (K)	
Al	1.2	
Hg	4.1	first superconductor, discovered 1911
Nb	9.3	higest T_c of an element at normal pressure
Pb	7.2	
Sn	3.7	
Ti	0.39	
Tl	2.4	
V	5.3	
W	0.01	
Zn	0.88	
Zr	0.65	
Fe	2	high pressure
H	300	predicted, under high pressure
O	30	high pressure, maximum T_c of any element
S	10	high pressure
Nb_3Ge	23	A15 structure, highest known T_c before 1986
$Ba_{1-x}Pb_xBiO_3$	12	first perovskite oxide structure
$La_{2-x}Sr_xCuO_4$	35	first high T_c superconductor
$YBa_2Cu_3O_{7-\delta}$	92	first superconductor above 77K
$HgBa_2Ca_2Cu_3O_{8+\delta}$	135-165	highest T_c ever recorded
$K_3 C_{60}$	30	fullerene molecules
YNi_2B_2C	17	borocarbide superconductor
MgB_2	38	discovery announced in January 2001
Sr_2RuO_4	1.5	possible p-wave superconductor
UPt_3	0.5	"heavy fermion" exotic superconductor
$(TMTSF)_2ClO_4$	1.2	organic molecular superconductor
ET-BEDT	12	organic molecular superconductor

Superconductivity appears to be fairly common in nature, and there are perhaps several hundred known superconducting materials. Before 1986 the highest known T_c values were in the A-15 type materials, including Nb_3Ge with $T_c = 23K$. This, and the closely related compound Nb_3Sn ($T_c = 18K$ are widely used in the superconducting magnet industry.

In 1986 Bednorz and Müller discovered that the material $La_{2-x}Ba_x$-CuO_4 becomes superconducting with a T_c which is maximum at 38K for $x \approx 0.15$. Within a matter of months the related compound $YBa_2Cu_3O_7$ was discovered to have $T_c = 92K$, ushering in the era of 'high temperature

superconductivity'.[3] This breakthrough was especially important in terms of possible commercial applications of superconductivity, since these superconductors are the first which can operate in liquid nitrogen (boiling point 77K) rather than requiring liquid helium (4K) . Other high temperature superconductors have been discovered in chemically related systems. Currently $HgBa_2Ca_2Cu_3O_{8+\delta}$ has the highest confirmed value of T_c at 135K at room pressure, shown in Fig. 1.2, rising to 165K when the material is subjected to high pressures. The reason why these particular materials are so unique is still not completely understood, as we shall see in later chapters of this book.

As well as high temperature superconductors, there are also many other interesting superconducting materials. Some of these have exotic properties which are still not understood and are under very active investigation. These include other oxide-based superconducting materials, organic superconductors, C_{60} based fullerene superconductors, and 'heavy fermion' superconductors (typically compounds containing the elements U or Ce) which are dominated by strong electron-electron interaction effects. Other superconductors have surprising properties, such as coexitence of magnetism and superconductivity, or evidence of exotic "unconventional" superconducting phases. We shall discuss some of these strange materials in chapter 7.

1.4 Zero-resistivity

As we have seen, in superconductors the resistivity, ρ, becomes zero, and so the conductivity σ appears to become infinite below T_c. To be consistent with the constitutive relation, Eq. 1.6, we must always have zero electric field,

$$\boldsymbol{\mathcal{E}} = 0,$$

at all points inside a superconductor. In this way the current, $\mathbf{j}$, can be finite. So we have current flow without electric field.

Notice that the change from finite to zero resistivity at the superconducting critical temperature T_c is very sudden, as shown in Fig. 1.1. This represents a thermodynamic phase transition from one state to another. As for other phase transitions, such as from liquid to gas, the properties of the phases on either side of the transition can be completely different. The change from one to the other occurs sharply at a fixed temperature

---

[3]Bednorz and Müller received the 1987 Nobel prize for physics, within a year of publication of their results. At the first major condensed matter physics conference after these discoveries, the 1987 American Physical Society March Meeting held in New York city, there was a special evening session devoted to the discoveries. The meeting hall was packed with hundreds of delegates sitting in the gangways, others had to watch the proceedings on TV screens in the hallways. The number of speakers was so great that the session lasted all through the night until the following morning, when the hall was needed for next offical session of the conference! The following day's New York Times newpaper headline reported the meeting as the "Woodstock of Physics".

rather than being a smooth cross-over from one type of behaviour to another. Here the two different phases are referred to as the "normal state" and the "superconducting state". In the normal state the resistivity and other properties behaves similarly to a normal metal, while in the superconducting state many physical properties, including resistivity, are quite different.

In some cases, notably the high temperature superconductors, looking closely at the $\rho(T)$ curve near to T_c shows a small range of temperatures where the resistance starts to decrease before becoming truly zero. This is visible in Fig. 1.2 as a slight bend just above T_c. This bend is due to thermodynamic critical fluctuations associated with the phase transition. The precise thermodynamic phase transition temperature T_c can be defined as the temperature where the resistivity first becomes exactly zero. [4]

The key characteristic of the superconducting state is that the resistivity is **exactly** zero,

$$\rho = 0, \tag{1.12}$$

or the conductivity, σ, is infinite. How do we know that the resistivity is exactly zero? After all, zero is rather difficult to distinguish from some very very small, but finite, number.

Consider how one might actually measure the resistivity of a superconductor. The simplest measurement would be a basic "two terminal" geometry shown in Fig. 1.3(a). The sample resistance, R, is related to the resisitvity

$$R = \rho \frac{L}{A} \tag{1.13}$$

and L is the sample length and A is its cross sectional area. But the problem with the two-terminal geometry shown in Fig. 1.3(a) is that even if the sample resistance is zero the overall resistance is finite, because the sample resistance is in series with resistances from the connecting leads and from the electrical contacts between the sample and the leads. A much better experimental technique is the four terminal measurement of Fig. 1.3(b). There there are four leads connected to the sample. Two of them are used to provide a current, I, through the sample. The second pair of lead are then used to measure a voltage, V. Since no current flows in the second pair of leads the contact resistances will not matter. The resistance of the part of the sample between the second pair of contacts will be $R = V/I$ by Ohm's law, at least in the idealized geometry shown. In any case if

---

[4]One could perhaps imagine the existence of materials where the resistivity approached zero smoothly without a thermodynamic phase transition. For example in a completely pure metal with no impurities one might expect the $\rho \to 0$ as temperature approaches absolute zero. Such system would not be classified as a superconductor in the standard terminology, even though it might have infinite conductivity. The word superconductor is used only to mean a material with a definite phase transition and critical temperature T_c. A true superconductor must also exhibit the Meissner-Ochsenfeld effect.

the sample is superconducting we should definitely observe $V = 0$ when I is finite implying that $\rho = 0$. (Of course the current I must not be too large. All superconductors have a critical current, I_c, above which the superconductivity is destroyed and the resistance becomes finite again).

The most convincing evidence that superconductors really have $\rho = 0$ is the observation of **persistent currents**. If we have a closed loop of superconducting wire, such as the ring shown in Fig. 1.4 then it is possible to set up a current, I, circulating in the loop. Because there is no dissipation of energy due to finite resistance, the energy stored in the magnetic field of the ring will remain constant and the current never decays.

To see how this persistent current can be set up, consider the flux of magnetic field through the centre of the superconducting ring. The flux is defined by the surface integral

$$\Phi = \int \mathbf{B} . \mathbf{dS} \tag{1.14}$$

where $\mathbf{dS}$ is a vector perpendicular to the plane of the ring. Its length dS, is an infinitesimal element of the area enclosed by the ring. But, by using the Maxwell equation

$$\boldsymbol{\nabla} \times \boldsymbol{\varepsilon} = -\frac{\partial \mathbf{B}}{\partial t} \tag{1.15}$$

and Stokes's theorem

$$\int (\boldsymbol{\nabla} \times \boldsymbol{\varepsilon}) d\mathbf{S} = \oint \boldsymbol{\varepsilon} . \mathbf{dr} \tag{1.16}$$

we can see that

$$-\frac{d\Phi}{dt} = \oint \boldsymbol{\varepsilon} . \mathbf{dr} \tag{1.17}$$

where the line integral is taken around the closed path around the inside of the ring. This path can be taken to be just inside the superconductor, and so $\boldsymbol{\varepsilon} = 0$ everywhere along the path. Therefore

$$\frac{d\Phi}{dt} = 0 \tag{1.18}$$

and hence the magnetic flux through the ring stays constant as a function of time.

We can use this property to set up a persistent current in a superconducting ring. In fact it is quite analogous to the way we saw in Chapter 2 how to set up a persistent superfluid flow in ^{4}He. The difference is that now we use a magnetic field rather than rotation of the ring. First we start with the superconductor at a temperature above T_c, so that it is in its normal state. Then apply an external magnetic field, $\mathbf{B}_{ext}$. This passes easily through the superconductor since the system is normal. Now cool the system to below T_c. The flux in the ring is given by $\Phi = \int \mathbf{B}_{ext} . \mathbf{dS}$. But we

know from Eq. 1.18 that this remains constant, no matter what. Even if we turn off the source of external magnetic field, so that now $\mathbf{B}_{ext} = 0$, the flux Φ must remain constant. The only way the superconductor can keep Φ constant is to generate its own magnetic field $\mathbf{B}$ through the centre of the ring, which it must achieve by having a circulating current, I, around the ring. The value of I will be exactly the one required to induce a magnetic flux equal to Φ inside the ring. Further, because Φ is constant the current I must also be constant. We therefore have a set up circulating persistent current in our superconducting ring.

Furthermore if there were any electrical resistance at all in the ring there would be energy dissipation and hence the current I would decay gradually over time. But experiments have been done in which persistent currents were observed to remain constant over a period of years. Therefore the resistance must really be exactly equal to zero to all intents and purposes!

1.5 The Meissner-Ochsenfeld Effect

Nowadays, the fact the the resistivity is zero, $\rho = 0$, is not taken as the true definition of superconductivity. The fundamental proof that superconductivity occurs in a given material is the demonstration of the Meissner-Ochsenfeld effect.

This effect is the fact the a superconductor **expels** a weak external magnetic field. First, consider the situation illustrated in Fig. 1.5 in which a small spherical sample of material is held at temperature T and placed in a small external magnetic field, $\mathbf{B}_{ext}$. Suppose initially we have the sample in its normal state, $T > T_c$, and the external field is zero, as illustrated in the top part of the diagram in Fig. 1.5. Imagine that we first cool to a temperature below T_c (left diagram) while keeping the field zero. Then later as we gradually turn on the external field the field inside the sample must remain zero (bottom diagram). This is because, by the Maxwell equation Eq. 1.15 combined with $\boldsymbol{\mathcal{E}} = 0$ we must have

$$\frac{\partial \mathbf{B}}{\partial t} = 0 \qquad (1.19)$$

at all points inside the superconductor. Thus by applying the external field to the sample after it is already superconducting we must arrive at the state shown in the bottom diagram in Fig. 1.5 where the magnetic field $\mathbf{B} = 0$ is zero everywhere inside the sample.

But now consider doing things in the other order. Suppose we take the sample above T_c and first turn on the external field, $\mathbf{B}_{ext}$. In this case the magnetic field will easily penetrate into the sample, $\mathbf{B} = \mathbf{B}_{ext}$, as shown in the right hand picture in Fig. 1.5. What happens then we now cool the sample? The Meissner-Ochsenfeld effect is the observation that upon cooling the system to below T_c the magnetic field is **expelled**. So that by cooling we move from the situation depicted on right to the one shown at the bottom of Fig. 1.5. This fact cannot be deduced from the simple

fact of zero resistivity ($\rho = 0$) and so this is a new and separate physical phenomenon assosciated with superconductors.

There are several reasons why the existence of the Meissner-Ochsenfeld effecting a sample is taken as definitive proof of superconductivity. At a practical level it is perhaps clearer to experimentally demonstrate the flux expulsion than zero resistivity, because, for example, it is not necessary to attach any electrical leads to the sample. A more fundamental reason is that the Meissner-Ochsenfeld effect is a property of **thermal equilibrium**, while resistivity is a non-equilibrium transport effect. In fact one can see in Fig. 1.5 that we reach the same final state of the system (bottom picture in Fig. 1.5) whether we first cool and then apply the field, or the other way around. Therefore the final state of the system does not depend on the history of the sample, which is a necessary condition for thermal equilibrium. It is perhaps possible to imagine exotic systems for which the resistivity vanishes, but for which there is no Meissner-Ochsenfeld effect. In fact some quantum Hall effect states may possess this property. But, for the purposes of this book however we shall always define a **superconductor** as a system which exhibits the Meissner-Ochsenfeld effect.

1.6 Perfect Diamagnetism

In order to maintain $\mathbf{B} = 0$ inside the sample whatever (small) external fields are imposed as required by the Meissner-Ocshenfeld effect there obviously must be screening currents flowing around the edges of the sample. These produce a magnetic field which is equal and opposite to the applied external field, leaving zero field in total.

The simplest way to describe these screening currents is to use Maxwell's equations in a magnetic medium (see Blundell (2002) or other texts on magnetic materials). The total current is separated into the externally applied currents (for example in the coils producing the external field), $\mathbf{j}_{ext}$, and the internal screening currents, $\mathbf{j}_{int}$,

$$\mathbf{j} = \mathbf{j}_{ext} + \mathbf{j}_{int}. \tag{1.20}$$

The screening currents produce a magnetization in the sample, $\mathbf{M}$ per unit volume, defined by

$$\boldsymbol{\nabla} \times \mathbf{M} = \mathbf{j}_{int}. \tag{1.21}$$

As in the theory of magnetic media (Blundell 2002) we also define a magnetic field $\mathbf{H}$ in terms of the external currents only

$$\boldsymbol{\nabla} \times \mathbf{H} = \mathbf{j}_{ext}. \tag{1.22}$$

The three vectors $\mathbf{M}$ and $\mathbf{H}$ and $\mathbf{B}$ are related by [5]

---

[5]Properly the name "magnetic field" is applied to $\mathbf{H}$ in a magnetic medium. Then the field $\mathbf{B}$ is called the magnetic induction or the magnetic flux density. Many people find this terminology confusing. Following Blundell (2002), in this book we shall simply call them the "H-field" and "B-field" respectively whenever there is a need to distinguish between them.

$$\mathbf{B} = \mu_o(\mathbf{H} + \mathbf{M}). \tag{1.23}$$

Maxwell's equations also tell us that

$$\mathbf{\nabla}.\mathbf{B} = 0. \tag{1.24}$$

The magnetic medium Maxwell's equations above are supplemented by boundary conditions at the sample surface. From Eq. 1.24 it follows that the component of $\mathbf{B}$ perpendicular to the surface must remain constant; while from the condition Eq. 1.22 one can prove that components of $\mathbf{H}$ parallel to the surface remain constant. The two boundary conditions are therefore,

$$\Delta\mathbf{B}_\perp = 0 \tag{1.25}$$
$$\Delta\mathbf{H}_\parallel = 0. \tag{1.26}$$

Note that we are using SI units here. In SI units $\mathbf{B}$ is in Tesla, while $\mathbf{M}$ and $\mathbf{H}$ are in units of Amperes per metre, Am^{-1}. The constant $\mu_o = 4\pi \times 10^{-7}$.

One should take note that many books and research papers on superconductivity still use the older c.g.s. units. In c.g.s. units $\mathbf{B}$ and $\mathbf{H}$ are in gauss and oersteds, respectively. $1\text{gauss} = 10^{-4}\text{T}$, $1\text{oersted} = 10^3/4\pi$ Am^{-1} and in cgs units

$$\mathbf{B} = \mathbf{H} + 4\pi\mathbf{M}$$

and

$$\nabla \times \mathbf{H} = 4\pi\mathbf{j}.$$

In these units the susceptibility of a superconductor is $\chi = -1/(4\pi)$ rather than the SI value of -1.

Note that there is no μ_o or ϵ_o in the c.g.s. system of units. Instead, the speed of light, $c = 1/\sqrt{\epsilon_0\mu_0}$, often appears explicitly. For example the Lorentz force on a charge q particle, moving with velocity $\mathbf{v}$ in a magnetic field $\mathbf{B}$ is

$$\mathbf{F} = \frac{1}{c}q\mathbf{v} \times \mathbf{B}$$

in c.g.s. units, compared to the SI unit equivalent

$$\mathbf{F} = q\mathbf{v} \times \mathbf{B}.$$

Also note that the unit of electrical charge is the Coulomb (C) in SI units, but it is the statcoulomb in cgs units, where $1\text{statcoulomb} = 3.336 \times 10^{-10} C$.

For simplicity we shall usually assume that the sample is an infinitely long solenoid as sketched in Fig. 1.6. The external current flows in solenoid

coils around the sample. In this case the field **H** is uniform inside the sample,

$$\mathbf{H} = I\frac{N}{L}\mathbf{e}_z \tag{1.27}$$

where I is the current flowing through the solenoid coil and there are N coil turns in length L. $\mathbf{e}_z$ is a unit vector along the solenoid axis.

Imposing the Meissner condition $\mathbf{B} = 0$ in Eq. 1.23 immediately leads to the magnetization

$$\mathbf{M} = -\mathbf{H}. \tag{1.28}$$

The magnetic susceptibility is defined by

$$\chi = \left.\frac{dM}{dH}\right|_{H=0} \tag{1.29}$$

and so we find that for superconductors

$$\chi = -1 \tag{1.30}$$

(or $-1/4\pi$ in cgs units!).

Solids with a negative value of χ are called diamagnets (in contrast positive χ is a paramagnet). Diamagnets screen out part of the external magnetic field, and so they become magnetized oppositely to the external field. In superconductors the external field is completely screened out. Therefore we can say that superconductors are **perfect diamagnets**.

The best way to detect superconductivity in some unknown sample is therefore to measure its susceptibility. If the sample is fully superconducting then χ as a function of T will something like the sketch giving in Fig. 1.7 sketch. Thus by measuring χ one will find $\chi = -1$ in a superconductor, evidence for perfect diamagnetism, or the Meissner effect. This is usually considered much more reliable evidence for superconductivity in a sample than zero resistance alone would be.

1.7   Type I and Type II Superconductivity

This susceptibility χ is defined in the limit of very weak external fields, **H**. As the field becomes stronger it turns out that either one of two possible things can happen.

The first case, called a type I superconductor, is that the **B** field remains zero inside the superconductor until suddenly the superconductivity is destroyed. The field where this happens is called the **critical field**, H_c. The way the magnetization M changes with H in a type I superconductor is shown in Fig. 1.8. As shown, the magnetization obeys $M = -H$ for all fields less than H_c, and then becomes zero (or very close to zero) for fields above H_c.

Many superconductors, however, behave differently. In a type II superconductor there are two different critical fields, denoted H_{c1}, the **lower**

critical field, and H_{c2} the **upper critical field**. For small values of applied field H the Meissner-Ochsenfeld effect again leads to $M = -H$ and there is no magnetic flux density inside the sample, $B = 0$. However in a type II superconductor once the field exceeds H_{c1}, magnetic flux does start to enter the superconductor and hence $B \neq 0$, and M is closer to zero than the full Meissner-Ochsenfeld value of $-H$. Upon increasing the field H further the magnetic flux density gradually increases, until finally at H_{c2} the superconductivity is destroyed and $M = 0$. This behaviour is sketched on the right hand side of Fig. 1.8

As a function of the temperature the critical fields vary, and they all approach zero at the critical temperature T_c. The typical phase diagrams of type I and type II superconductors, as a function of H and T are shown in Fig. 1.9.

The physical explanation of the thermodynamic phase between H_{c1} and H_{c2} was given by Abrikosov. He showed that the magnetic field can enter the superconductor in the form of **vortices**, as shown in fig. 1.10. Each vortex consists of a region of circulating supercurrent around a small central core which has essentially become normal metal. The magnetic field is able to pass through the sample inside the vortex cores, and the circulating currents server to screen out the magnetic field from the rest of the superconductor outside the vortex.

It turns out that each vortex carries a fixed unit of magnetic flux, $\Phi_0 = h/2e$ (see below), and hence, if there are a total of N_v vortices in a sample of total area, A, then the average magnetic flux density, B, is

$$B = \frac{N_v}{A} \frac{h}{2e}. \tag{1.31}$$

It is instructive to compare this result for the number of vortices per unit area,

$$\frac{N_v}{A} = \frac{2eB}{h}. \tag{1.32}$$

with the similar expression derived earlier for the density of vortices in rotating superfluid ^{4}He, Eq. **??**. There is in fact a direct mathematical analogy between the effect of a uniform rotation at angular frequency ω in a neutral superfluid, and the effect of a magnetic field, B, in a superconductor.

1.8   The London Equation

The first theory which could account for the existence of the Meissner-Ochsenfeld effect was developed by two brothers, F. London and H. London, in 1935. Their theory was was originally motivated by the two-fluid model of superfluid ^{4}He. They assumed that some fraction of the conduction electrons in the solid become superfluid while the rest remain normal. They then assumed that the superconducting electrons could move without dissipation, while the normal electrons would continue to act as if they had a finite resistivity. Of course the superfluid electrons always 'short circuit'

the normal ones and make the overall resistivity equal to zero. As in the theory of superfluid ^{4}He discussed in chapter 2, we denote the number density of superfluid electrons by n_s and the density of normal electrons by $n_n = n - n_s$, where n is the total density of electrons per unit volume.

Although this model is simple several of its main predictions are indeed correct. Most importantly it leads to the **London equation** which relates the electric current density inside a superconductor, **j**, to the magnetic vector potential, **A**, by

$$\mathbf{j} = -\frac{n_s e^2}{m_e}\mathbf{A}. \tag{1.33}$$

This is one of the most important equations describing superconductors. Nearly twenty years after it was originally introduced by the London brothers it was eventually derived from the full microscopic quantum theory of superconductivity by Bardeen Cooper and Schrieffer.

Let us start to make the London equation Eq. 1.33 plausible by reexamining the Drude model of conductivity. This time consider the Drude theory for finite frequency electric fields. Using the complex number represntation of the a.c. currents and fields, d.c. formula becomes modified to:

$$\mathbf{j}e^{-i\omega t} = \sigma(\omega)\boldsymbol{\mathcal{E}}e^{-i\omega t} \tag{1.34}$$

where the conductivity is also complex. Its real part corresponds to currents which are in phase with the applied electrical field (resistive), while the imaginary part corresponds to out of phase currents (inductive and capacitive).

Generalizing the Drude theory to the case of finite frequency, the conductivity turns out to be

$$\sigma(\omega) = \frac{ne^2\tau}{m}\frac{1}{1 - i\omega\tau}, \tag{1.35}$$

Ashcroft and Mermin (1976). This is essentially like the response of a damped Harmonic oscillator with a resonant frequency at $\omega = 0$. Taking the real part we get

$$\text{Re}[\sigma(\omega)] = \frac{ne^2}{m}\frac{\tau}{1 + \omega^2\tau^2}, \tag{1.36}$$

a Lorentzian function of frequency. Note that the width of the Lorentzian is $1/\tau$ and its maximum height is τ. Integrating over frequency, we see that the area under this Lorentzian curve is a constant

$$\int_{-\infty}^{+\infty} Re[\sigma(\omega)]d\omega = \frac{\pi ne^2}{m} \tag{1.37}$$

independent of the lifetime τ.

Now is is interesting to consider what would be the corresponding Drude model $\sigma(\omega)$ in the case of a perfect conductor, where there is no scattering of the electrons. We can we can obtain this by taking the limit $\tau^{-1} \to 0$ in the Drude model. Taking this limit Eq. 1.35 gives:

$$\sigma(\omega) = \frac{ne^2}{m}\frac{1}{\tau^{-1} - i\omega} \to -\frac{ne^2}{i\omega m} \tag{1.38}$$

at any finite frequency, ω. There is no dissipation since the current is always out of phase with the applied electric field and $\sigma(\omega)$ is always imaginary. There is a purely inductive response to an applied electric field. The real part of the conductivity $\mathrm{Re}[\sigma(\omega)]$ is therefore zero at any finite frequency, ω in this $\tau^{-1} \to 0$ limit. But the sum rule, Eq. 1.37, must be obeyed whatever the value of τ. Therefore the real part of the conductivity, $Re[\sigma(\omega)]$ must be a function which is zero almost everywhere but which has a finite integral. This must be, of course, a Dirac delta function,

$$\mathrm{Re}[\sigma(\omega)] = \frac{\pi ne^2}{m}\delta(\omega). \tag{1.39}$$

One can see that this is correct by considering the $\tau^{-1} \to 0$ limit of the Lorentzian peak in $\mathrm{Re}[\sigma(\omega)]$ in Eq. 1.36. The width of the peak is of order τ^{-1} and goes to zero, but the maximum height increases keeping a constant total area because of the sum rule. The τ^{-1} limit is thus a Dirac delta function located at $\omega = 0$.

Inspired by the two fluid model of superfluid ^{4}He, the London brothers assumed that we can divide the total electron density, n, into a normal part, n_n and a superfluid part, n_s,

$$n = n_s + n_n. \tag{1.40}$$

They assumed that the 'normal' electrons would still have a typical metallic damping time τ, but the superfluid electrons would move without dissipation, corresponding to $\tau = \infty$. They assumed that this superfluid component will give rise to a Dirac delta function peak in the conductivity located at $\omega = 0$ and a purely imaginary response elsewhere,

$$\sigma(\omega) = \frac{\pi n_s e^2}{m_e}\delta(\omega) - \frac{n_s e^2}{i\omega m_e}. \tag{1.41}$$

Note that we effectively **define** n_s by the weight in this delta function peak, and (by convention) we use the bare electron mass in vacuum, m_e, rather than the effective band mass, m, in this definition.

In fact the experimentally measured finite frequency conductivity $Re\sigma(\omega)$ in superconductors does indeed have a delta function located at zero frequency. But other aspects of the two fluid model conductivity assumed by London and London are not correct. In particular the 'normal' fluid component is not simply like the conductivity of a normal metal. In fact the

complete $Re[\sigma(\omega)]$ of a superconductor looks something like the sketch in Fig. 1.11. There is a delta function peak located at $\omega = 0$, and the amplitude of the peak defines n_s, the superfluid density or or condensate density. At higher frequencies the real part of the conductivity is zero, $Re[\sigma(\omega)] = 0$, corresponding to dissipationless current flow. However above a certain frequency, corresponding to $\hbar\omega = 2\Delta$ (where 2Δ is the 'energy gap') the conductivity again becomes finite. The presence of an energy gap was observed shortly before the Bardeen Cooper and Schrieffer (BCS) theory was completed, and the energy gap was a central feature of the theory, as we shall see later.

Derivation of the London Equation

If we restrict our attention to frequencies below the energy gap, then the conductivity is exactly given by Equation 1.41. In this regime we can derive the London equation relating the supercurrent $\mathbf{j}$ to the magnetic field $\mathbf{B}$.

Taking the curl of both sides of the equation $\mathbf{j} = \sigma\boldsymbol{\mathcal{E}}$ we find

$$
\begin{aligned}
(\nabla \times \mathbf{j})e^{-i\omega t} &= \sigma(\omega)(\nabla \times \boldsymbol{\mathcal{E}})e^{-i\omega t} \\
&= -\sigma(\omega)\frac{d(\mathbf{B}e^{-i\omega t})}{dt} \\
&= i\omega\sigma(\omega)\mathbf{B}e^{-i\omega t} \\
&= -\frac{n_s e^2}{m_e}\mathbf{B}e^{-i\omega t},
\end{aligned} \tag{1.42}
$$

where in the final step we use Eq. 1.38 for the finite frequency conductivity of the superconductor.

We now take the $\omega = 0$ limit of the above equations. The last line effectively relates a d.c. current, $\mathbf{j}$ to a static external magnetic field $\mathbf{B}$ by,

$$
\nabla \times \mathbf{j} = -\frac{n_s e^2}{m_e}\mathbf{B}. \tag{1.43}
$$

This equation completely determines $\mathbf{j}$ and $\mathbf{B}$ because they are also related by the static Maxwell equation:

$$
\nabla \times \mathbf{B} = \mu_o \mathbf{j}. \tag{1.44}
$$

Combining these two equations gives

$$
\nabla \times (\nabla \times \mathbf{B}) = -\mu_o \frac{n_s e^2}{m_e}\mathbf{B} \tag{1.45}
$$

or

$$
\nabla \times (\nabla \times \mathbf{B}) = -\frac{1}{\lambda^2}\mathbf{B} \tag{1.46}
$$

where λ has dimensions of length, and is the **penetration depth** of the superconductor,

$$\lambda = \left(\frac{m_e}{\mu_o n_s e^2} \right)^{1/2}.$$ (1.47)

It is the distance inside the surface over which an external magnetic field is screened out to zero, given that $B = 0$ in the bulk.

Finally, the London equation can also be rewritten in terms of the magnetic vector potential $\mathbf{A}$ defined by

$$\mathbf{B} = \nabla \times \mathbf{A},$$ (1.48)

giving

$$\mathbf{j} = -\frac{n_s e^2}{m_e} \mathbf{A}$$ (1.49)

$$= -\frac{1}{\mu_o \lambda^2} \mathbf{A}.$$ (1.50)

Note that this only works provided that we choose the correct **g**auge for the vector potential, $\mathbf{A}$. Recall that $\mathbf{A}$ is not uniquely defined from Eq. 1.48 since $\mathbf{A} + \nabla \chi(\mathbf{r})$ leads to exactly the same $\mathbf{B}$ for any scalar function, $\chi(\mathbf{r})$. But conservation of charge implies that the current and charge density, ρ, obey the continuity equation

$$\frac{\partial \rho}{\partial t} + \nabla . \mathbf{j} = 0.$$ (1.51)

In a static, d.c., situation the first term is zero, and so $\nabla . \mathbf{j} = 0$. Comparing with the London equation in the form, Eq. 1.49 we see that this is satisfied provided that the gauge is chosen so that $\nabla . \mathbf{A} = 0$. This is called the **London gauge**.

For superconductors this form of the London equation effectively replaces the normal metal $\mathbf{j} = \sigma \boldsymbol{\mathcal{E}}$ constitutive relation by something which is useful when σ is infinite. It is interesting to speculate about whether or not it would be possible to find other states of matter which are perfect conductors with $\sigma = \infty$, but which do not obey the London equation. If such exotic states exist (and they may indeed occur in the Quantum Hall Effect) they would not be superconductors in the sense in which we are using that word here.

The most important consequence of the London equation is to explain the Meissner-Ochsenfeld effect. In fact one can easily show that any external magnetic field is screened out inside the superconductor, as

$$B = B_0 e^{-x/\lambda}$$ (1.52)

where x is the depth inside the surface of the superconductor. This is illustrated in Fig. 1.12. The derivation of this expression from the London equation is very straightforward, and is left to exercise 3.1 at the end of this chapter. The implication of this result is that magnetic fields only penetrate

a small distance, λ, inside the surface of a superconductor, and thus the field is equal to zero far inside the bulk of a large sample.

A modified form of the London equation was later proposed by Pippard. This form generalizes the London equation by relating the current at a point $\mathbf{r}$ in the solid, $\mathbf{j}(\mathbf{r})$, to the vector potential at nearby points $\mathbf{r}'$. The expression he proposed was

$$\mathbf{j}(\mathbf{r}) = -\frac{n_s e^2}{m_e} \frac{3}{4\pi\xi_0} \int \frac{\mathbf{R}(\mathbf{R}.\mathbf{A}(\mathbf{r}'))}{R^4} e^{-R/r_0} d^3 r', \tag{1.53}$$

where $\mathbf{R} = \mathbf{r} - \mathbf{r}'$. The points which contribute to the integral are separated by distances of order r_0 or less, with r_0 defined by

$$\frac{1}{r_0} = \frac{1}{\xi_0} + \frac{1}{l}. \tag{1.54}$$

Here l is the **mean free path** of the electrons at the Fermi surface of the metal,

$$l = v_F \tau, \tag{1.55}$$

with τ the scattering time from the Drude conductivity formula, and v_F the electron band velocity at the Fermi surface. The length ξ_0 is called the **coherence length**. After the Bardeen Cooper Schrieffer theory of superocnductivity was completed, it became clear that this length is closely related to the value of the energy gap, Δ, by

$$\xi_0 = \frac{\hbar v_F}{\pi\Delta}. \tag{1.56}$$

It also has the physical interpretation that it represents the physical size of the Cooper pair bound state in the BCS theory.

The existence of the Pippard coherence length implies that a superconductor is characterized by no fewer than **three different length scales**. We have the penetration depth, λ, the coherence length, ξ_0, and the mean free path, l. We shall see in the next chapter than the dimensionless ratio $\kappa = \lambda/\xi_0$ determines whether a superconductor is type I or type II. Similarly, if the mean free path is much longer than the coherence length , $l \gg \xi_0$ the superconductor is said to be in the **clean limit**, while if $l < \xi_0$ the superconductor is said to be in the **dirty limit**. It is a surprising and very important property of most superconductors that they can remain superconducting even when there are large numbers of impurities making the mean free path l very short. In fact even many alloys are superconducting despite the strongly disordered atomic structure.

1.9   The London vortex

We can use the London equation to find a simple mathematical description of a superconducting vortex, as in Fig. 1.10. The vortex will have a cylindrical core of normal material, with a radius of approximately the coherence

length, ξ_0. Inside this core we will have a finite magnetic field, say B_0. Outside the vortex core we can use the London equation in the form of Eq. 1.46 to write a differential equation for the magnetic field , $\mathbf{B} = (0, 0, B_z)$. Using cylindrical polar coordinates (r, θ, z), and the expression for curl in cylndrical polars, Eq. **??** we obtain (exercise 3.3)

$$\frac{d^2 B_z}{dr^2} + \frac{1}{r}\frac{dB_z}{dr} - \frac{B_z}{\lambda^2} = 0. \tag{1.57}$$

This is a form of Bessel's equation (Boas 1983, Matthews and Walker 1970). The solutions to equations of this type are called modified, or hyperbolic Bessel functions, $K_\nu(z)$ and they can be found in many standard texts of mathematical physics. In this particular case the solution is $K_0(z)$. The resulting magnetic field can be written in the form,

$$B_z(r) = \frac{\Phi_0}{2\pi\lambda^2} K_0\left(\frac{r}{\lambda}\right) \tag{1.58}$$

where Φ_0 is the total magnetic flux enclosed by the vortex core,

$$\Phi_0 = \int B_z(r) d^2 r. \tag{1.59}$$

We shall see in the next chapter that the magnetic flux is quantized, resulting in the universal value $\Phi_0 = h/2e$ of flux per vortex line.

For small values of z the function $K_0(z)$ becomes

$$K_0(z) \sim -\ln z$$

(Abromowitz and Stegun, 1965) and so

$$B_z(r) = \frac{\Phi_0}{2\pi\lambda^2} \ln\left(\frac{\lambda}{r}\right) \tag{1.60}$$

when $r << \lambda$. Using $\mu_0 \mathbf{j} = \nabla \times \mathbf{B}$ we find (problem 3.3) that the corresponding circulating current is irrotational,

$$\mathbf{j} \sim \frac{1}{r}\mathbf{e}_\phi \tag{1.61}$$

exactly as we found earlier for vortices in superfluid helium.

The divergence at $r = 0$ in these expressions is not physical, and is cut off by the finite coherence length of the superconductor, ξ_0. Effectively this defines a small core size for the vortex (again similar to the vortex core in superfluid ^{4}He). Superconductivity is suppressed inside the vortex core, for $r < \xi_0$, which is effectively normal material. Therefore, Eq. 1.60 is valid in the region $\xi_0 << r << \lambda$, and this simple London vortex model is only valid in superconductors where $\xi_0 << \lambda$.

For the case of large z the modified Bessel function becomes

$$K_0(z) \sim \sqrt{\frac{\pi}{2z}} e^{-z}$$

asymptotically (Abromowitz and Stegun, 1965). Therefore the magnetic field very far from the core of a London vortex is of the form (exercise 3.3)

$$B_z(r) = \frac{\Phi_0}{2\pi\lambda^2} \sqrt{\frac{\pi\lambda}{2r}} e^{-r/\lambda}. \tag{1.62}$$

Qualitatively this is similar to the penetration of a magnetic field near a surface as shown in Fig. 1.12.

Overall then, in this London vortex model the magnetic field has some large constant value B_0 inside the vortex core, $r < \xi$, then decreases logarithmically between $\xi_0 < r < \lambda$ and then goes to zero exponentially outside the vortex on a length scale of order λ. Clearly this picture is only useful in the limit $\lambda > \xi_0$, corresponding to a type II superconductor.

It is also instructive to calculate the energy of the rotating supercurrents in the vortex. The result[6] is that the energy of the vortex is approximately

$$E = \frac{\Phi_0^2}{4\pi\mu_0\lambda^2} \ln\left(\frac{\lambda}{\xi_0}\right) \tag{1.63}$$

per unit length.

1.10   Further Reading

To review the basic concepts of band theory of metals, see *Band theory and electronic properties of solids*, Singleton (2002), a companion volume to this book in the Oxford Master Series in Condensed Matter.

There are many text books dealing with superconductivity. Probably the ones which are especially good for beginners are *Supercondctivity Today*, Ramakrishnan and Rao 1992, and it Superconductivity and Superfluidity by Tilley and Tilley (1990).

Among the more advanced books, *Superconductivity of metals and Alloys*, de Gennes (1966), has the most extensive discussion of the topics covered in this chapter, especially vortices and the vortex lattice.

Bessel functions and their mathematical properties are described in many texts. Their definitions and propoerties are given in depth by Abromowitz and Stegun (1965). Good introductions are given by Boas (1983) and Matthews and Walker (1970).

---

[6]See exercise 3.4 below for the proof.

1.11 Exercises

(3.1) (a) Using the London equation show that

$$\mathbf{\nabla} \times (\mathbf{\nabla} \times \mathbf{B}) = -\frac{1}{\lambda^2}\mathbf{B}$$

in a superconductor.

(b) In Fig. 1.12, the surface of the superconductor lies in the $y - z$ plane. A magnetic field is applied in the z direction parallel to the surface, $\mathbf{B} = (0, 0, B_0)$. Given that inside the superconductor the magnetic field is a function of x only, $\mathbf{B} = (0, 0, B_z(x))$ show that

$$\frac{d^2 B_z(x)}{dx^2} = \frac{1}{\lambda^2}B_z(x).$$

(c) Solving the ordinary differential equation in (b) show that the magnetic field near a surface of a superconductor has the form

$$B = B_0 \exp\left(-x/\lambda\right)$$

as shown in Fig. 1.12.

(3.2) Consider a thin superconducting slab, of thickness $2L$, as shown in Fig. 1.13. If an external parallel magnetic field, B_0, is applied parallel to the slab surfaces, show that inside the slab the magnetic field becomes

$$B_z(x) = B_0 \frac{\cosh\left(x/\lambda\right)}{\cosh\left(L/\lambda\right)}.$$

(3.3) (a) A vortex in a superconductor can be modelled as having a cylindrical core of normal metal of radius ξ_0. Use $\mathbf{\nabla} \times (\mathbf{\nabla} \times \mathbf{B}) = -\mathbf{B}/\lambda^2$ and the expression for curl in cylindrical polar coordinates (Eq. **??** to show that the magnetic field $B_z(r)$ outside of the core obeys the Bessel equation:

$$\frac{1}{r}\frac{d}{dr}\left(r\frac{dB_z}{dr}\right) = \frac{B_z}{\lambda^2}.$$

(b) For small r, obeying $\xi < r << \lambda$, the right hand side of the Bessel equation in (a) can be approximated by zero. Show that this approximation leads to

$$B_z(r) = a\ln\left(r\right) + b.$$

where a and b are unknown constants.

(c) Show that the current corresponding to the field $B_z(r)$ found in (b) is equal to

$$\mathbf{j} = \frac{a}{\mu_0 r}\mathbf{e}_\phi$$

similar to the superfluid current in a ^{4}He vortex. Hence find the vector potential $\mathbf{A}$ and find a as a function of the magnetic flux enclosed by the vortex core, Φ.

(d) For larger values of r ($r \sim \lambda$ and above) assume that we can approximate the Bessel equation from (a) by:

$$\frac{d}{dr}\left(\frac{dB_z}{dr}\right) = \frac{B_z}{\lambda^2}.$$

Hence show that $B_z(r) \sim e^{-r/\lambda}$ for large r.

(e) The large r solution given in part (d) is not exactly the correct asymptotic form of the solution, as described in section 3.9. For large values of r, assume that

$$B_z(r) \sim r^p e^{-r/\lambda}$$

and hence show that the correct exponent is $p = -1/2$, as described above.

(3.4) Suppose that any supercurrent flow corresponds to an effective superfluid flow velocity $\mathbf{v}$ of the electrons, where $\mathbf{j} = -en_s\mathbf{v}$. Assume that the corresponding kinetic energy is $\frac{1}{2}mv^2 n_s$ per unit volume. Hence, using the results from exercise 3.3 parts (c) and (d), show that the total energy of a vortex line is roughly of order

$$E = \frac{\Phi^2}{4\pi\mu_0\lambda^2}\ln\left(\frac{\lambda}{\xi_0}\right)$$

per unit length.

(3.5) The complex conductivity $\sigma(\omega)$ has real and imaginary parts that are related together by **Kramers-Kronig** relations

$$\mathrm{Re}[\sigma(\omega)] = \frac{1}{\pi}\mathcal{P}\int_{-\infty}^{\infty}\frac{\mathrm{Im}[\sigma(\omega')]}{\omega' - \omega}d\omega'$$

and

$$\mathrm{Im}[\sigma(\omega)] = -\frac{1}{\pi}\mathcal{P}\int_{-\infty}^{\infty}\frac{\mathrm{Re}[\sigma(\omega')]}{\omega' - \omega}d\omega'.$$

Where, here $\mathcal{P}\int$ means the **principal value** of the integral (Boas 1983, Matthews and Walker 1970). Therefore an experimental measurement of the real part is sufficient to determine the imaginary part, and *vice versa*.

(a) Using these expressions, and assuming that the real part of the conductivity $\text{Re}\sigma(\omega)$ is a Dirac delta function

$$\text{Re}[\sigma(\omega)] = \frac{\pi n_s e^2}{m_e}\delta(\omega)$$

show that the imaginary part is given by

$$\text{Im}[\sigma(\omega)] = -\frac{n_s e^2}{\omega m_e}$$

exactly as given in Eq. 1.41.

(b) *Exercise for those who have studied analytic complex function theory.* We can derive the Kramers-Kronig relations as follows. Consider the contour integral

$$I = \oint \frac{\sigma(\omega')}{\omega' - \omega}d\omega'$$

around the contour shown in Fig. 1.14. Find the poles of $\sigma(\omega')$ according to Eq. 1.38 and show that is is analytic in the upper half plane $(\text{Im}[\omega'] > 0)$ in Fig. 1.14.

(c) Use the result from (b) to show that $I = 0$, and thus prove that

$$0 = \mathcal{P}\int_{-\infty}^{\infty} \frac{\sigma(\omega')}{\omega' - \omega}d\omega' - i\pi\sigma(\omega) = 0,$$

where the integral is now just along the real ω' axis. Take the real and imaginary parts of this expression and show that this results in the Kramer's Kronig equations given above.[7]

---

[7]The proof is actually very general. The fact that $\sigma(\omega')$ is analytic in the upper half plane is in fact just a consequence of **causality**, i.e. the applied current always responds to the applied external field. Effect follows cause, never the reverse! Therefore the Kramers-Kronig relations are always true for any such response function.
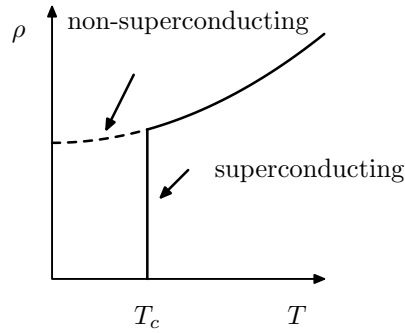
Fig. 1.1 Resistivity of a typical metal as a function of temperature. If it is a non-superconducting metal (such as copper or gold) the resistivity approaches a finite value at zero temperature, while for a superconductor (such as lead, or mercury) all signs of resistance disappear suddenly below a certain temperature, T_c.
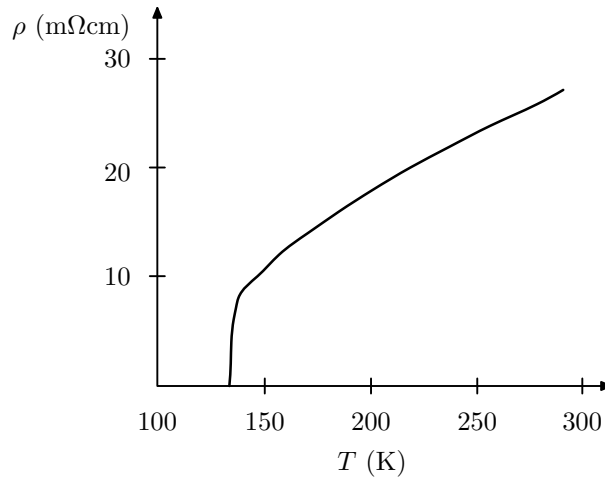
Fig. 1.2 Resistivity of $HgBa_2Ca_2Cu_3O_8 + \delta$ as a function of temperature (adapted from data of Chu (1993). Zero resistance is obtained at about 135K, the highest known T_c in any material at normal pressure. In this material T_c approaches a maximum of about 165K under high pressure. Note the rounding of the resistivity curve just above T_c, which is due to superconducting fluctuation effects. Also, well above T_c the resistivity does not follow the expected Fermi liquid behaviour.
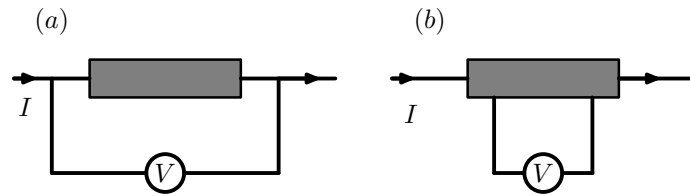
Fig. 1.3 Measurement of resistivity by (a) the two terminal method, (b) the four terminal method. The second method, (b), is much more accurate since no current flows through the leads measuring the voltage drop across the resistor, and so the resistances of the leads and contacts is irrelevant.
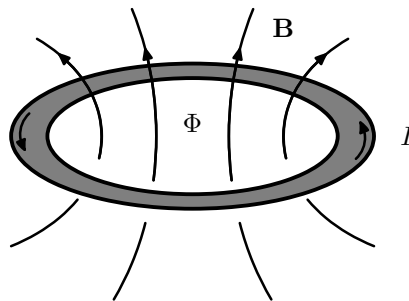
**Fig. 1.4** Persistent current around a superconducting ring. The current maintains a constant magnetic flux, Φ, through the superconducting ring.
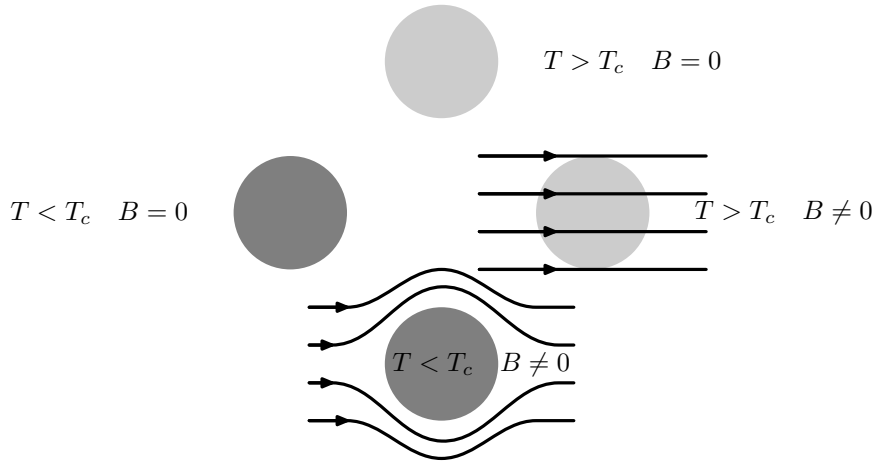
Fig. 1.5 The Meissner-Ochsenfeld effect in superconductors. If a sample initially at high temperature and in zero magnetic field (top) is first cooled (left) and then placed in a magnetic field (bottom), then the magnetic field cannot enter the material (bottom). This is a consequence of zero resistivity. On the other hand a normal sample (top) can be first placed in a magnetic field (right) and **then** cooled (bottom). In the case the magnetic field is **expelled** from the system.
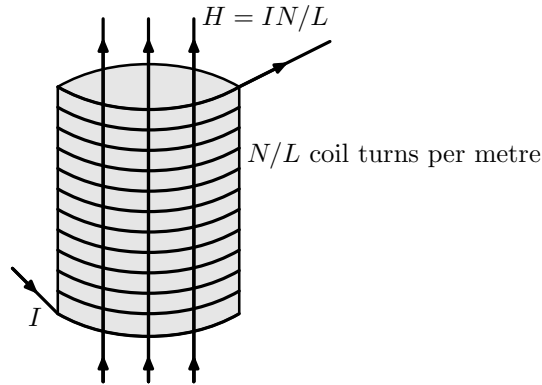
Fig. 1.6 Measurement of **M** as a function of **H** for a sample with solenoidal geometry. A long solenoid coil of N/L turns per metre leads to a uniform field $H = IN/L$ Amperes per metre inside the solenoid. The sample has magnetization, M, inside the solenoid, and the magnetic flux density is $B = \mu_0(H + M)$. Increasing the current in the coils from I to $I + dI$, by dI leads to an inductive e.m.f. $\mathcal{E} = -d\Phi/dt$ where $\Phi = NBA$ is the total magnetic flux threading the N current turns of area A. This inductive e.m.f. can be measured directly, since it is simply related to the differential self-inductance of the coil, $\mathcal{L}$, via $\mathcal{E} = -\mathcal{L}dI/dt$. Therefore, by measuring the self-inductance $\mathcal{L}$ one can deduce the B-field and hence M as a function of I or H.
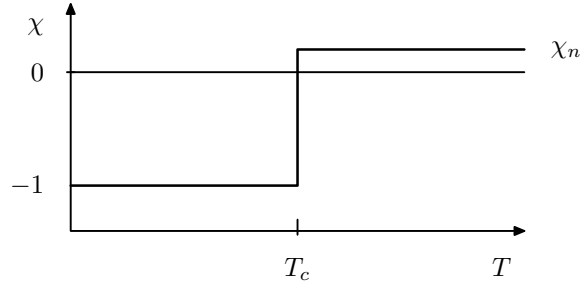
Fig. 1.7 Magnetic susceptibility, χ, of a superconductor as a function of temperature. Above T_c it is a constant normal state value, χ_n, which is usually small and positive (paramagetic). Below T_c the susceptibility is large and negative, $\chi = -1$, signifying perfect diamagnetism.
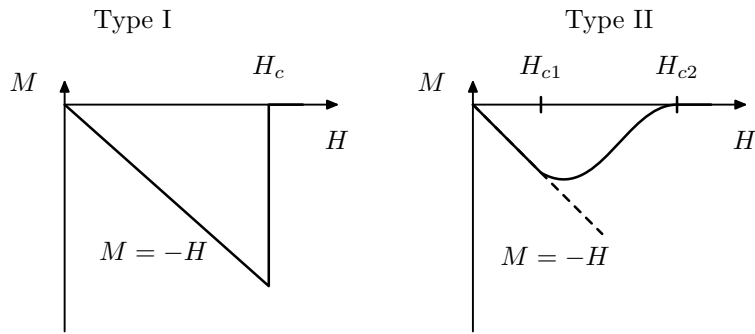
Fig. 1.8 The magnetization M as a function of H in type I and type II superconductors. For type I perfect Meissner diamagnetism is continued until H_c, beyond which superconductivity is destroyed. For type II materials perfect diamagnetism occurs only below H_{c1}. Between H_{c1} and H_{c2} Abrikosov vortices enter the material, which is still superconducting.
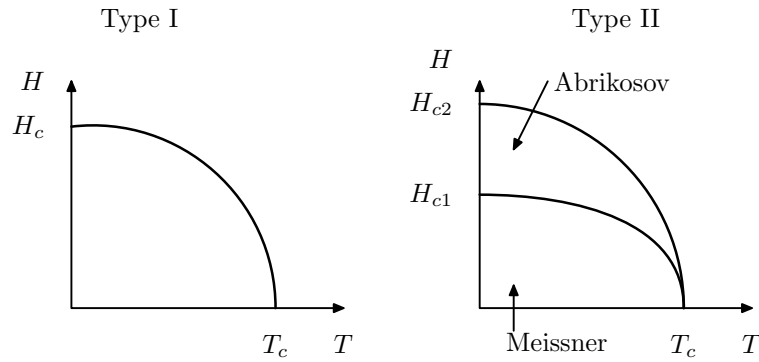
Fig. 1.9 The $H - T$ phase diagram of type I and type II superconductors. In type II superconductors the phase below H_{c1} is normally denoted the Meissner state, while the phase between H_{c1} and $Hc2$ is the Abrikosov or mixed state.
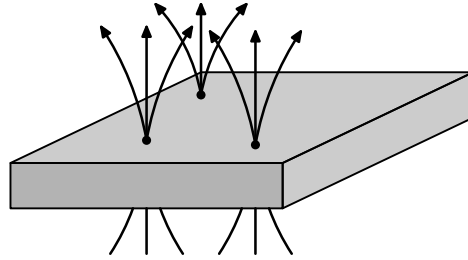
Fig. 1.10 Vortices in a type II superconductor. The magnetic field can pass through the superconductor, provided it is channelled through a small "vortex core". The vortex core is normal metal. This allows the bulk of the material to remain superconducting, while also allowing a finite average magnetic flux density B to pass through.
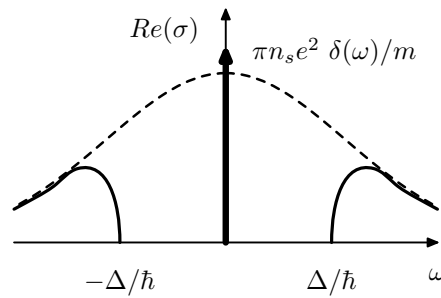
Fig. 1.11 The finite frequency conductivity of a normal metal (dashed line) and a superconductor (solid line). In the superconducting case an energy gap leads to zero conductivity for frequencies below $\Delta/\hbar$. The remaining spectral weight becomes concentrated in a Dirac delta function at $\omega = 0$.
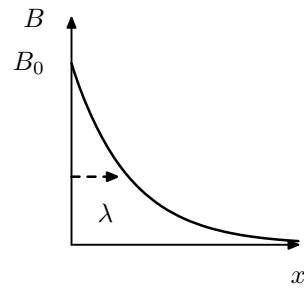
Fig. 1.12 The magnetic field near a surface of a superconductor in the Meissner state. The field decays exponentially on a length scale given by the penetration depth λ.
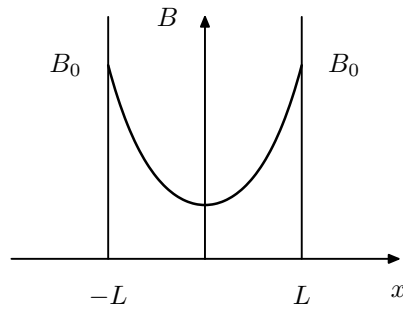
Fig. 1.13 Exercise 3.2. The magnetic field inside a superconducting slab of hickness $2L$.
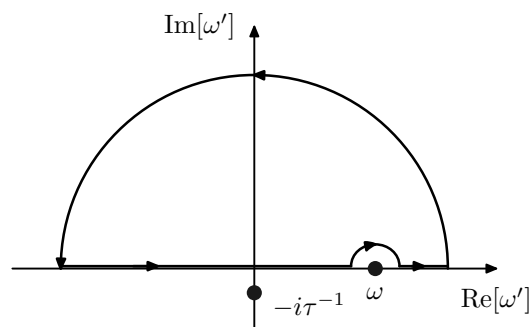
Fig. 1.14 Complex integration contour for Exercise 3.5.

2

The Ginzburg-Landau model

2.1 Introduction

The superconducting state and the normal metallic state are separate thermodynamic phases of matter in just the same way as gas, liquid and solid are different phases. Similarly, the normal Bose gas and BEC, or normal liquid He^4 and superfluid He II are separated by a thermodynamic phase transitions. Each such phase transition can be characterized by the nature of the singularities in specific heat and other thermodynamic variables at the transition, T_c. We can therefore examine the problems of superfluidity and superconductivity from the point of view of the thermodynamics of phase transitions.

The theory of superconductivity introduced by Ginzburg and Landau in 1950 describes the superconducting phase transition from this thermodynamic point of view. It was originally introduced as a phenomenological theory, but later Gor'kov showed that it can be derived from full the microscopic BCS theory in a suitable limit.[1]

In this chapter we shall first discuss the superconducting phase transition from the point of view of equilibrium thermodynamics. Then we gradually build up towards the full Ginzburg Landau model. First we discuss spatially uniform systems, then spatially varying systems and finally systems in an external magnetic field. The Ginzburg Landau theory makes many useful and important predictions. Here we focus on just two applications: to flux quantization, and to the Abrikosov flux lattice in type II superconductors.

The Ginzubrg Landau theory as originally applied to superconductors was *par excellance* a **mean-field theory** of the thermodynamic state. However, in fact, one of its most powerful features is that it can be used to go beyond the original mean-field limit, so as to include the effects of thermal fluctuations. We shall see below that such fluctuations are largely negligible in the case of conventional "low-T_c" superconductors, making the

---

[1]In fact, the Ginzburg Landau model is very general and has applications in many different areas of physics. It can be modified to describe many different physical systems, including magnetism, liquid crystal phases and even the symmetry breaking phase transitions which took place in the early universe as matter cooled following the big bang!

mean-field approximation essentially exact. However in the newer high T_c superconductors these fluctuations lead to many important phenomena, such as flux flow, and the melting of the Abrikosov vortex lattice.

2.2   The condensation energy

We already have enough information about superconductivity to derive some important thermodynamic properties about the superconducting phase transition. We can analyze the phase diagram of superconductors in exactly the same manner as one would consider the well known thermodynamics of a liquid gas phase transition problem, such as given by the van der Waals equation of state. However, for the superconductor instead of the pair of thermodynamic variables P, V (pressure and volume) we have the magnetic variables $\mathbf{H}$ and $\mathbf{M}$ as the relevant thermodynamic parameters.

Let us first briefly review the basic thermodynamics of magnetic materials. This is covered in several undergraduate text books on thermodynamics such as Mandl (1987) or Callen (1960), Blundell (2001). If we consider a long cylindrical sample in a solenoidal field, as shown in Fig. 1.6, then the magnetic field $\mathbf{H}$ inside the sample is given by

$$\mathbf{H} = \frac{N}{L} I \mathbf{e}_z, \tag{2.1}$$

where the coil has N/L turns per metre, I is the current and $\mathbf{e}_z$ is a unit vector along the axis of the cylinder. The total work done, $\dj W$, on increasing the current infinitesimally from I to $I + dI$ can be calculated as

$$
\begin{aligned}
\dj W &= -N \int \mathcal{E} I dt \\
&= +N \int \frac{d\Phi}{dt} I dt \\
&= +N I d\Phi \\
&= +N A I dB \\
&= +N V \mathbf{H}.d\mathbf{B} \\
&= +\mu_0 V \left(\mathbf{H}.d\mathbf{M} + \mathbf{H}.d\mathbf{H} \right)
\end{aligned}
\tag{2.2}
$$

where A is the cross sectional area of the coli, $V = AL$ is its volume, $\mathcal{E} = -d\Phi/dt$ is the e.m.f. induced in the coil by the change in the total magnetic flux, Φ, through the sample. We also used the identity $\mathbf{B} = \mu_0(\mathbf{M} + \mathbf{H})$ in writing the last step in Eq. 2.2.

This analysis shows that we can divide the total work done by increasing the current in the coil into two separate parts. The first part,

$$\mu_0 \mathbf{H}.d\mathbf{M}$$

per unit volume, is the **magnetic work** done on the sample. The second part,

$$\mu_0\mathbf{H}.d\mathbf{H}$$

is the work per unit volume which would have been done even if no sample had been present inside the coil; it is the work done by the **self-inductance** of the coil. If the coil is empty, $\mathbf{M} = 0$ and so $\mathbf{B} = \mu_0\mathbf{H}$ and one can easily see that the work done is exactly the change in the vacuum field energy of the electromagnetic field

$$E_B = \frac{1}{2\mu_0} \int B^2 d^3r \qquad (2.3)$$

due to the change of current in the solenoid coils. By convention[2] we shall not include this vacuum field energy, as work done "on the sample". Therefore we define the magnetic work done on the sample as $\mu_0\mathbf{H}d\mathbf{M}$ per unit volume.

With this definition of magnetic work the first law of thermodynamics for a magnetic material reads,

$$dU = TdS + \mu_0 V\mathbf{H}.d\mathbf{M} \qquad (2.4)$$

where U is the total internal energy, TdS is the heat energy with T the temperature and S the entropy. We see that the magnetic work is analogous to the work, $-PdV$, in a gas. As in the usual thermodynamics of gases the internal energy, U, is most naturally thought of as a function of the entropy and volume: $U(S,V)$. The analogue of the first law for a magnetic system, Eq. 2.4, shows that the internal energy of a magnetic substance is most naturally thought of as a function of S and $\mathbf{M}$, $U(S,\mathbf{M})$. In terms of this function the temperature and field $\mathbf{H}$ are given by

$$T = \frac{\partial U}{\partial S} \qquad (2.5)$$

$$\mathbf{H} = \frac{1}{\mu_0 V}\frac{\partial U}{\partial \mathbf{M}}. \qquad (2.6)$$

However S and $\mathbf{M}$ are usually not the most convenient variables to work with. In a solenoidal geometry such as Fig. 1.6 it is the H-field which is directly fixed by the current, not $\mathbf{M}$. It is therefore useful to define magnetic analogues of the Helmholtz and Gibbs free energies

$$F(T,\mathbf{M}) = U - TS \qquad (2.7)$$

$$G(T,\mathbf{H}) = U - TS - \mu_0 V\mathbf{H}.\mathbf{M}. \qquad (2.8)$$

As indicated, the Gibbs free energy G is naturally viewed as a function of T and $\mathbf{H}$ since,

---

[2]Unfortunately there is no single standard convention used by all books and papers in this field. Different contributions to the total energy are either included or not, and so one must be very careful when comparing similar looking equations from different texts and research papers. Our convention follows Mandl (1987) and Callen (1960).

$$dG = -SdT - \mu_0 V \mathbf{M}.d\mathbf{H}. \tag{2.9}$$

In terms of G one can calculate the entropy and magnetization,

$$S = -\frac{\partial G}{\partial T} \tag{2.10}$$

$$\mathbf{M} = -\frac{1}{\mu_0 V}\frac{\partial G}{\partial \mathbf{H}}. \tag{2.11}$$

$G(T, \mathbf{H})$ is usually the most convenient thermodynamic quantity to work with since T and $\mathbf{H}$ are the variables which are most naturally controlled experimentally. Furthermore from $G(T, \mathbf{H})$ one can also reconstruct the free energy, $F = G + \mu_0 V \mathbf{H}.\mathbf{M}V$ or the internal energy $U = F + TS$.

The Gibbs free energy allows us to calculate the free energy difference between the superconducting state and the normal state. Consider the H, T phase diagram of a type I superconductor, as sketched above in Fig. 2.1. We can evaluate the change in Gibbs free energy in the superconducting state by integrating along the vertical line drawn. Along this line $dT = 0$, and so, clearly,

$$G_s(T, H_c) - G_s(T, 0) = \int_0^{H_c} dG = -\mu_0 V \int_0^{H_c} \mathbf{M}.d\mathbf{H},$$

where the subscript s implies that $G(T, \mathbf{H})$ is in the superconducting state. But for a type I superconductor in the superconducting state we know from the Meissner-Ochsenfeld effect that $\mathbf{M} = -\mathbf{H}$ and thus,

$$G_s(T, H_c) - G_s(T, 0) = \mu_0 \frac{H_c^2}{2} V.$$

Now, at the critical field H_c in Fig. 2.1 the normal state and the superconducting state are in thermodynamic equilibrium. Equilibrium between phases implies that the two Gibbs free energies are equal:

$$G_s(T, H_c) = G_n(T, H_c).$$

Furthermore, in the normal state $M \approx 0$ (apart from the small normal metal paramagnetism or diamagnetism which we neglect). So if the normal metal state had persisted below H_c down to zero field, it would have had a Gibbs free energy of,

$$G_n(T, H_c) - G_n(T, 0) = \int_0^{H_c} dG = -\mu_0 V \int_0^{H_c} M dH \approx 0.$$

Putting these together we find the difference in Gibbs free energies of superconducting and normal states at zero field:

$$G_s(T, 0) - G_n(T, 0) = -\mu_0 V \frac{H_c^2}{2} \tag{2.12}$$

The Gibbs potential for the superconducting state is lower, so it is the stable state.

We can also write the above results in terms of the more familiar Helmholtz free energy. Using $F = G - \mu_0 V \mathbf{H}.\mathbf{M}$ and substituting $\mathbf{H} = \mathbf{M} = 0$ we can see that the difference in Helmholtz free energies $F(T, \mathbf{M})$ is the same as for the Gibbs potentials, and hence

$$F_s(T, 0) - F_n(T, 0) = -\mu_0 V \frac{H_c^2}{2}. \tag{2.13}$$

The quantity $\mu_0 H_c^2/2$ is the **condensation energy**. It is a measure of the gain in free energy per unit volume in the superconducting state compared to the normal state at the same temperature.

As an example lets consider niobium. Here $T_c = 9$K, and $H_c = 160$kA/m ($B_c = \mu_0 H_c = 0.2T$). The condensation energy $\mu_0 H_c^2/2 = 16.5$kJ/m^3. Given that Nb has a bcc crystal structure with a 0.33nm lattice constant we can work out the volume per atom and find that the condensation energy is only around 2μeV/atom! Such tiny energies were a mystery until the BCS theory, which shows that the condensation energy is of order $(k_B T_c)^2 g(E_F)$, where $g(\epsilon_F)$ is the density of states at the Fermi level. The energy is so small because $k_B T_c$ is many orders of magnitude smaller than the Fermi energy, ϵ_F.

The similar thermodynamic arguments can also be applied to calculate the condensation energy of type II superconductors. Again the magnetic work per unit volume is calculated as an integral along a countour, as shown in the right panel of Fig. 2.1,

$$G_s(T, H_{c2}) - G_s(T, 0) = \mu_0 V \int_0^{H_{c2}} \mathbf{M}.d\mathbf{H} \tag{2.14}$$

The integral is simply the area under the curve of M as a function of H drawn in Fig. 1.8 (assuming that $\mathbf{M}$ and $\mathbf{H}$ have the same vector directions). **Defining** the value of H_c for a type II superconducting from the value of the integral

$$\frac{1}{2}H_c^2 \equiv \int_0^{H_{c2}} \mathbf{M}.d\mathbf{H} \tag{2.15}$$

we again can express the zero field condensation energy in terms of H_c,

$$F_s(T, 0) - F_n(T, 0) = -\mu_0 V \frac{H_c^2}{2}. \tag{2.16}$$

Here H_c is called the **thermodynamic critical field**. Note that there is no phase transition at H_c in a type II superconductor. The only real transitions are at H_{c1} and H_{c2}, and H_c is merely a convenient measure of the condensation energy.

We can also calculate the entropy of the superconducting state using the same methods. A simple calculation (Exercise 4.1) shows that in a type

I superconductor there is a finite change in entropy between the normal and superconducting states at H_c,

$$S_s(T, H_c) - S_n(T, H_c) = -\mu_0 H_c \frac{dH_c}{dT}. \tag{2.17}$$

This shows that the phase transition is generally **first-order**, i.e. it has a finite latent heat. But, in zero external field, at the point $(T, H) = (T_c, 0)$ in Fig. 2.1, this entropy difference goes to zero, and so in this case the phase transition is **second-order**.

2.3   Ginzburg-Landau theory of the bulk phase transition

The Ginzburg-Landau theory of superconductivity is built upon a general approach to the theory of second order phase transitions which Landau had developed in the 1930's. Landau had noticed that typically second order phase transitions, such as the Curie temperature in a ferromagnet, involve some change in symmetry of the system. For example a magnet above the Curie temperature, T_c, has no magnetic moment. But below T_c a spontaneous magnetic moment develops. In principle could point in any one of a number of different directions, each with an equal energy, but the system spontaneously chooses one particular direction. In Landau's theory such phase transitions are characterized by an **order parameter** which is zero in the disordered state above T_c, but becomes non-zero below T_c. In the case of a magnet the magnetization, $\mathbf{M}(\mathbf{r})$, is a suitable order parameter.

For superconductivity Ginzburg and Landau (GL) postulated the existence of an order parameter denoted by ψ. This characterizes the superconducting state, in the same way as the magnetization does in a ferromagnet. The order parameter is assumed to be some (unspecified) physical quantity which characterizes the state of the system. In the normal metallic state above the critical temperature T_c of the superconductor it is zero. While in the superconducting state below T_c it is non-zero. Therefore it is assumed to obey:

$$\psi = \begin{cases} 0 & T > T_c \\ \psi(T) \neq 0 & T < T_c. \end{cases} \tag{2.18}$$

Ginzburg and Landau postulated that the order parameter ψ should be a complex number, thinking of it as a macroscopic wave function for the superconductor in analogy with superfluid ^{4}He. At the time of their original work the physical significance of this complex ψ in superconductors was not at all clear. But, as we shall see below, in the microscopic BCS theory of superconductivity there appears a parameter, Δ, which is also complex. Gor'kov was able to derive the Ginzburg-Landau theory from BCS theory, and show that ψ is essentially the same as Δ, except for some constant numerical factors. In fact, we can even identify $|\psi|^2$ as the density of BCS "Cooper pairs" present in the sample.

Ginzburg and Landau assumed that the free energy of the superconductor must depend smoothly on the parameter ψ. Since ψ is complex and the

free energy must be real, the energy can only depend on $|\psi|$. Furthermore, since ψ goes to zero at the critical temperature, T_c, we can Tailor expand the free energy in powers of $|\psi|$. For temperatures close to T_c only the first two terms in the expansion should be necessary, and so the free energy density ($f = F/V$) must be of the form:

$$f_s(T) = f_n(T) + a(T)|\psi|^2 + \frac{1}{2}b(T)|\psi|^4 + \ldots \qquad (2.19)$$

since $|\psi|$ is small. Here $f_s(T)$ and $f_n(T)$ are the superconducting state and normal state free energy densities, respectively. Clearly Eq. 2.19 is the only possible function which is real for any complex ψ near $\psi = 0$ and which is a differentiable function of ψ and ψ^* near to $\psi = 0$. The parameters $a(T)$ and $b(T)$ are, in general, temperature dependent pheonomenological parameters of the theory. However it is assumed that they must be smooth functions of temperature. We must also assume that $b(T)$ is positive, since otherwise the free energy density would have no minimum, which would be unphysical (or we would have to extend the expansion to include higher powers such as $|\psi|^6$).

Plotting $f_s - f_n$ as a function of ψ is easy to see that there are two possible curves, depending on the sign of the parameter $a(T)$, as shown in Fig. 2.2. In the case $a(T) > 0$, the curve has one minimum at $\psi = 0$. On the other hand, for $a(T) < 0$ there are minima wherever $|\psi|^2 = -a(T)/b(T)$. Landau and Ginzburg assumed that at high temperatures, above T_c, we have $a(T)$ positive, and hence the minimum free energy solution is one with $\psi = 0$, i.e. the normal state. But if $a(T)$ gradually decreases as the temperature T is reduced, then the state of the system will change suddenly when we reach the point $a(T) = 0$. Below this temperature the minimum free energy solution changes to one with $\psi \neq 0$. Therefore we can identify the temperature where $a(T)$ becomes zero as the critical temperature T_c.

Near to this critical temperature, T_c, assuming that the coefficients $a(T)$ and $b(T)$ change smoothly with temperature, we can make a Taylor expansion,

$$\begin{aligned} a(T) &\approx \dot{a} \times (T - T_c) + \ldots \\ b(T) &\approx b + \ldots, \end{aligned} \qquad (2.20)$$

where $\dot{a}$ and b are two pheonomenological constants. Then for temperatures just above T_c, $a(T)$ will be positive, and we have the free energy minimum, $\psi = 0$. On the other hand, just below T_c we will have minimum energy solutions with non-zero $|\psi|$, a s seen in Fig. 2.2. In terms of the parameters $\dot{a}$ and b it is easy to see that

$$|\psi| = \begin{cases} \left(\frac{\dot{a}}{b}\right)^{1/2}(T_c - T)^{1/2} & T < T_c \\ 0 & T > T_c \end{cases} . \qquad (2.21)$$

The corresponding curve of $|\psi|$ as a function of temperature, T, is shown in Fig 2.3. One can see the abrupt change from zero to non-zero values at

the critical temperature T_c. In fact, this curve is qualitatively similar to those obtained with other types of second order phase transitions within Landau's general theory. For example the behaviour of the order parameter ψ near T_c in Fig. 2.3 resembles closely change in the magnetization $\mathbf{M}$ in a ferromagnet near its Curie point in the Stoner theory of magnetism (Blundell 2001).

It turns out to be very important that, because ψ is complex, there are in fact an infinite set of minima corresponding to all possible values of the complex phase θ,

$$\psi = |\psi|e^{i\theta}. \tag{2.22}$$

The phase value, θ is arbitrary, since all values lead to the same total free energy. But, just as in the case of the direction of magnetization $\mathbf{M}$ in a ferromagnet the system spontaneously chooses one particular value. A magnet heated to above T_c and then cooled again will almost certainly adopt a different random direction of magnetization, and the same would be true for the angle θ in a superconductor. In fact we have met this same concept before, in Chapter 2, when we discussed the XY symmetry of the macroscopic wave function in superfluid He II (Fig. **??**).

The value of the minimum free energy in Fig. 2.2, is easily found to be $-a(T)^2/2b(T)$. This is the free energy difference (per unit volume) between the superconducting and non-superconducting phases of the system at temperature T. This corresponds to the condensation energy of the superconductor, and so we can writ e

$$f_s(T) - f_n(T) = -\frac{\dot{a}^2(T - T_c)^2}{2b} = -\mu_0 \frac{H_c^2}{2}, \tag{2.23}$$

giving the thermodynamic critical field,

$$H_c = \frac{\dot{a}}{(\mu_0 b)^{1/2}}(T_c - T) \tag{2.24}$$

near to T_c.

From this free energy we can also obtain other relevant physical quantities, such as the entropy and heat capacity. Differentiating f with respect to T gives the entropy per unit volume, $s = S/V$,

$$s_s(T) - s_n(T) = -\frac{\dot{a}^2}{b}(T_c - T), \tag{2.25}$$

below T_c. At T_c there is no discontinuity in entropy, or latent heat, confirming that the Ginzburg-Landau model corresponds to a second order thermodynamic phase transition. But there is a sudden change in specific heat at T_c. Differentiating the entropy to find the heat capacity $C_V = Tds/dT$ per unit volume we obtain

$$C_{Vs} - C_{Vn} = \begin{cases} T\frac{\dot{a}^2}{b} & T < T_c \\ 0 & T > T_c \end{cases} \tag{2.26}$$

and so the heat capacity has a discontinuity

$$\Delta C_V = T_c \frac{\dot{a}^2}{b} \tag{2.27}$$

at T_c. The metallic normal state heat capacity is linear in T, $C_{Vn} = \gamma T$, with γ the Sommerfeld constant, and so the full heat capacity curve looks like Fig. 2.4 near to T_c.[3]

Interestingly the specific heat for superconductors shown in Fig. 2.4 is qualitatively quite very different from both the case of Bose-Einstein condensation, shown in Fig. **??**, and the λ point of superfluid ^{4}He, Fig. **??**.[4]

2.4 Ginzburg-Landau theory of inhomogenous systems

The complete Ginzburg and Landau theory of superconductivity also allows for the possibility that the order parameter depends on position, $\psi(\mathbf{r})$. This, of course, now really begins to resemble the macroscopic condensate wave function introduced in chapter 2 for the case of superfluid helium.

Ginzburg and Landau postulated that the Free energy is as given above, together with a new term depending on the gradient of $\psi(\mathbf{r})$. With this term free energy density becomes,

$$f_s(T) = f_n(T) + \frac{\hbar^2}{2m^*}|\boldsymbol{\nabla}\psi(\mathbf{r})|^2 + a(T)|\psi(\mathbf{r})|^2 + \frac{b(T)}{2}|\psi(\mathbf{r})|^4 \tag{2.28}$$

at point $\mathbf{r}$ in the absence of any magnetic fields. Setting $\psi(\mathbf{r})$ to a constant value, $\psi(\mathbf{r}) = \psi$, we see that the parameters $a(T)$ and $b(T)$ are the same as for the bulk theory described in the previous section. The new parameter m^* determines the energy cost associated with gradients in $\psi(\mathbf{r})$. It has dimensions of mass, and it plays the role of an effective mass for the quantum system with macroscopic wave function $\psi(\mathbf{r})$.

In order to find the order parameter $\psi(\mathbf{r})$ we must minimize the total free energy of the system,

$$F_s(T) = F_n(T) + \int d^3r \left(\frac{\hbar^2}{2m^*}|\boldsymbol{\nabla}\psi|^2 + a(T)|\psi(\mathbf{r})|^2 + \frac{b(T)}{2}|\psi(\mathbf{r})|^4 \right) d^3r. \tag{2.29}$$

To find the minimum we must consider an infinitesimal variation in the function $\psi(\mathbf{r})$

---

[3] The Ginzburg Landau theory can only be reliably used at temperatures close to T_c. Therefore our calculated specific heat is only correct near to T_c, and we cannot legitimately continue the Ginzburg-Landau line in Fig. 2.4 down from T_c all the way to $T = 0$.

[4] In fact the differences are deceptive! Our theory rests on a mean-field approximation and has neglected important thermal fluctuation effects, as we shall see below. When these fluctuations are large, as in the case of high temperature superconductors, the observed specific heat near T_c appears to show exactly the same XY universality class as the lambda point in superfluid helium (Overend 1994).

$$\psi(\mathbf{r}) \to \psi(\mathbf{r}) + \delta\psi(\mathbf{r}) \tag{2.30}$$

relative to some function $\psi(\mathbf{r})$. Evaluating the change in the total free energy due to $\delta\psi$ and dropping all terms of higher than linear order in the variation $\delta\psi$ we find after some lengthy algebra

$$
\begin{aligned}
\delta F_s &= \int \left[\frac{\hbar^2}{2m^*}(\boldsymbol{\nabla}\delta\psi^*).(\boldsymbol{\nabla}\psi) + \delta\psi^*(a\psi + b\psi|\psi^2|) \right] d^3r \\
&\quad + \int \left[\frac{\hbar^2}{2m^*}(\boldsymbol{\nabla}\psi^*).(\boldsymbol{\nabla}\delta\psi) + (a\psi^* + b\psi^*|\psi^2|)\delta\psi \right] d^3r. \tag{2.31}
\end{aligned}
$$

The two terms involving gradients can be integrated by parts, to obtain

$$
\begin{aligned}
\delta F_s &= \int \delta\psi^* \left(-\frac{\hbar^2}{2m^*}\nabla^2\psi + a\psi + b\psi|\psi^2| \right) d^3r \\
&\quad + \int \left(-\frac{\hbar^2}{2m^*}\nabla^2\psi + a\psi + b\psi|\psi^2| \right)^* \delta\psi \, d^3r. \tag{2.32}
\end{aligned}
$$

The condition for $\psi(\mathbf{r})$ to produce a minimum in free energy is that $\delta F = 0$ for any arbitrary variation $\delta\psi(\mathbf{r})$. From Eq. 2.32 this can only be when $\psi(\mathbf{r})$ obeys

$$-\frac{\hbar^2}{2m^*}\nabla^2\psi + a\psi + b\psi|\psi^2| = 0. \tag{2.33}$$

We can obtain this same result more formally by noting that the total Free energy of the solid is a **functional** of $\psi(\mathbf{r})$, denoted $F_s[\psi]$, meaning that the scalar number F_s depends on the whole function $\psi(\mathbf{r})$ at all points in the system, $\mathbf{r}$. It will be minimized by a function $\psi(\mathbf{r})$ which satisfies

$$\frac{\partial F_s[\psi]}{\partial\psi(\mathbf{r})} = 0 \qquad \frac{\partial F_s[\psi]}{\partial\psi^*(\mathbf{r})} = 0. \tag{2.34}$$

where the derivatives are mathematically **functional derivatives**. Functional derivative can be defined by analogy with the idea of a partial derivative. For a function of many variables, $f(x_1, x_2, x_3, \ldots)$ we can express changes in the function value due to infinitesimal variations of the parameters using the standard expression

$$df = \frac{\partial f}{\partial x_1}dx_1 + \frac{\partial f}{\partial x_2}dx_2 + \frac{\partial f}{\partial x_3}dx_3 + \ldots. \tag{2.35}$$

Considering the free energy as a function of infinitely many variables, $\psi(\mathbf{r})$ and $\psi^*(\mathbf{r})$ at all possible points $\mathbf{r}$ we can write the analogue of Eq. 2.35 as,

$$dF_s = \int \left(\frac{\partial F_s[\psi]}{\partial\psi(\mathbf{r})}d\psi(\mathbf{r}) + \frac{\partial F_s[\psi]}{\partial\psi^*(\mathbf{r})}d\psi^*(\mathbf{r}) \right) d^3r. \tag{2.36}$$

In comparison with Eq. 2.32 we see that

$$\frac{\partial F_s[\psi]}{\partial \psi^*(\mathbf{r})} = -\frac{\hbar^2}{2m^*}\nabla^2\psi + a(T)\psi + b(T)\psi|\psi^2| \tag{2.37}$$

and

$$\frac{\partial F_s[\psi]}{\partial \psi(\mathbf{r})} = (-\frac{\hbar^2}{2m^*}\nabla^2\psi + a(T)\psi + b(T)\psi|\psi^2|)^* \tag{2.38}$$

which is just the complex conjugate of Eq. 2.37. Perhaps it seems surprising that we can effectively treat $\psi(\mathbf{r})$ and $\psi^*(\mathbf{r})$ as independent variables in the differentiation, but this is correct because there are two independent real functions, $\mathrm{Re}[\psi(\mathbf{r})]$ and $\mathrm{Im}[\psi(\mathbf{r})]$, which can be varied separately.

Thus we have found that minimizing the total Free energy leads to the following Schrödinger like equation for $\psi(\mathbf{r})$,

$$-\frac{\hbar^2}{2m^*}\nabla^2\psi(\mathbf{r}) + \left(a + b|\psi(\mathbf{r})|^2\right)\psi(\mathbf{r}) = 0. \tag{2.39}$$

However, unlike the usual Schrödinger equation, this is a non-linear equation because of the second term in the bracket. Because of this non-linearity the quantum mechanical principle of superposition does not apply, and the normalization of ψ is different from the usual one in quantum mechanics.

2.5 Surfaces of Superconductors

The effective non-linear Schödinger equation, Eq. 2.39, has several useful applications. In particular, it can be used to study the response of the superconducting order parameter to external perturbations. Important examples of this include the properties of the surfaces and interfaces of superconductors.

Consider a simple model for the interface between a normal metal and a superconductor. Suppose that the interface lies in the yz plane separating the normal metal in the $x < 0$ region from the superconductor in the $x > 0$ region. On the normal metal side of the interface the superconducting order parameter, $\psi(\mathbf{r})$, must be zero. Assuming that $\psi(\mathbf{r})$ must be continuous, we must therefore solve the non-linear Schrödinger equation,

$$-\frac{\hbar^2}{2m^*}\frac{d^2\psi(x)}{dx^2} + a(T)\psi(x) + b(T)\psi^3(x) = 0 \tag{2.40}$$

in the region $x > 0$ with the boundary condition at $\psi(0) = 0$. It turns out that one can solve this equation directly (exercise 4.2) to find

$$\psi(x) = \psi_0 \tanh\left(\frac{x}{\sqrt{2}\xi(T)}\right), \tag{2.41}$$

as shown in Fig. 2.5. Here ψ_0 is the value of the order parameter in the bulk far from the surface and the parameter $\xi(T)$ is defined by

$$\xi(T) = \left(\frac{\hbar^2}{2m^*|a(T)|}\right)^{1/2}. \qquad (2.42)$$

This quantity, which has dimensions of length, is called the **Ginzburg-Landau coherence length**. It is an important physical parameter characterizing the superconductor. In Fig. 2.5 one can see that $\xi(T)$ is a measure of the distance from the surface over which the order parameter has recovered back to nearly its bulk value.

The Ginzburg-Landau coherence length arises in almost all problems of inhomogenous superconductors, including surfaces, interfaces, defects and vortices. Using $a(T) = \dot{a}(T - T_c)$ the coherence length $\xi(T)$ can be rewritten,

$$\xi(T) = \xi(0)|t|^{-1/2}, \qquad (2.43)$$

where

$$t = \frac{T - T_c}{T_c} \qquad (2.44)$$

is called the reduced temperature. This expression makes it clear that the coherence length $\xi(T)$ diverges at the critical temperature T_c, and that its divergence is characterized by a critical exponent of $1/2$. This exponent is typical for mean-field theories such as the Ginzburg-Landau model. The zero temperature value of ξ, $\xi(0)$, is apart from some numerical factors of order unity, essentially the same as the Pippard coherence length for superconductors, as introduced in Chapter 3. In BCS theory the coherence length relates to the physical size of a single Cooper pair.

It is also possible to calculate the contribution to the total free energy due to the surface in Fig. 2.5. The surface contribution to the total free energy is

$$\sigma = \int_0^\infty \left(\frac{\hbar^2}{2m^*}\left(\frac{d\psi(x)}{dx}\right)^2 + a\psi^2(x) + \frac{b}{2}\psi^4(x) + \frac{1}{2}\mu_0 H_c^2\right) dx \qquad (2.45)$$

with $\psi(x)$ given by Eq. 2.41. Here $-\mu_0 H_c^2/2 = -a^2/2b$ is the bulk free energy density. Evaluating the integral (de Gennes 1960) gives

$$\sigma = \frac{1}{2}\mu_0 H_c^2 \times 1.89\xi(T) \qquad (2.46)$$

free energy per unit area of the surface.

This theory can also be used to model the **proximity effect** between two superconductors. At an interface between two different superconducting materials the one with the higher T_c will become superconducting first, and will nucleate superconductivity at the surface of the second one. Superconductivity will nucleate at temperatures above the T_c for the second superconductor. If one makes the lower T_c superconductor a thin layer, of order the coherence length $\xi(T)$ in thickness, then the whole system will

become superconducting at a temperature above the natural critical temperature of the lower T_c material. Effectively the order parameter $\psi(\mathbf{r})$ has been forced to become non-zero in the thin film material by its proximity to the higher T_c material.

2.6 Ginzburg-Landau theory in a magnetic field

The full power of the GL approach to superconductors only becomes apparent when we include one final term, the effect of a magnetic field. It is this which truly shows that this is a fully fledged theory of superconductivity, complete with Meissner-Ochsenfeld effect, London equation and so on. Effectively, the Ginzburg-Landau theory as developed given in the previous sections did not include any effects of the charge of the superconducting condensate. Therefore it would be appropriate for systems of neutral particles, such as a superfliud, or for situations where there are no supercurrents. But in the presence of supercurrents of charged particles we must extend the theory to include the interaction of the current and magnetic field.

What is needed is to include the effects of magnetic fields in the free energy. Ginzburg and Landau postulated that the magnetic field enters as if $\psi(\mathbf{r})$ were the wave function for charged particles, i.e with the usual replacement in quantum mechanics

$$\frac{\hbar}{i}\boldsymbol{\nabla} \to \frac{\hbar}{i}\boldsymbol{\nabla} - q\mathbf{A} \qquad (2.47)$$

where q is the charge and $\mathbf{A}$ is the magnetic vector potential. For all known superconductors it turns out that the appropriate charge q is $-2e$. Why this is the case only became clear after the BCS theory was developed, and the link between the BCS theory and the Ginzburg-Landau model had been explained by Gor'kov. He showed that the correct physical interpretation of the GL order parameter $\psi(\mathbf{r})$ is that it can be understood as the wave function for the centre of mass motion of Cooper pairs of electrons. Since each Cooper pair has a net charge of $-2e$, then this is is the correct effective charge q.[5] Actually the sign can equally well be taken as $q = +2e$, since we can think of Cooper pairs of holes as readily as pairs of electrons. In fact no observable effects in the Ginzburg-Landau theory differ when we take a different convention for the sign.

With this replacement the Ginzburg-Landau free energy density of the superconductor becomes,

$$f_s(T) = f_n(T) + \frac{\hbar^2}{2m^*}|(\frac{\hbar}{i}\boldsymbol{\nabla} + 2e\mathbf{A})\psi|^2 + a|\psi|^2 + \frac{b}{2}|\psi|^4. \qquad (2.48)$$

---

[5]In fact, in their original paper Ginzburg and Landau assumed that the effective charge would be e, not $2e$. Reputedly, Ginzburg, then a young PhD student, told his famous advisor Landau that $2e$ fitted the available experimental data better than e, but Landau overruled him and insisted that he was sure that it must be e!

To obtain the total free energy we must integrate this over the system, but we must also include an additional term, corresponding to the electromagnetic field energy of the field $\mathbf{B}(\mathbf{r}) = \boldsymbol{\nabla} \times \mathbf{A}$ at each point $\mathbf{r}$. Therefore the total free energy of both the superconductor and the magnetic field is,[6]

$$
\begin{aligned}
F_s(T) \quad = \quad & F_n(T) + \int \left(\frac{\hbar^2}{2m^*} |(\frac{\hbar}{i}\boldsymbol{\nabla} + 2e\mathbf{A})\psi|^2 + a|\psi|^2 + \frac{b}{2}|\psi|^4 \right) d^3r \\
& + \frac{1}{2\mu_0} \int B(\mathbf{r})^2 d^3r.
\end{aligned} \tag{2.49}
$$

The first integral is carried out over points $\mathbf{r}$ inside the sample, while the second is performed over all space.

The condition for the minimum free energy state is again found by performing a functional differentiation to minimize with respect to $\psi(\mathbf{r})$ and $\psi^*(\mathbf{r})$. The resulting equation for $\psi(\mathbf{r})$ is again a non-linear Schrödinger equation, but now with a term containing the magnetic vector potential $\mathbf{A}$,

$$
-\frac{\hbar^2}{2m^*}(\nabla + \frac{2ei}{\hbar}\mathbf{A})^2 \psi(\mathbf{r}) + \left(a + b|\psi|^2\right)\psi(\mathbf{r}) = 0. \tag{2.50}
$$

The supercurrents due to the magnetic field can be found from functional derivative of the Ginzburg Landau superconductor free energy with respect to the vector potential,

$$
\mathbf{j}_s = -\frac{\partial F_s}{\partial \mathbf{A}(\mathbf{r})} \tag{2.51}
$$

which leads to the supercurrent

$$
\mathbf{j}_s = -\frac{2e\hbar i}{2m^*}(\psi^*\boldsymbol{\nabla}\psi - \psi\boldsymbol{\nabla}\psi^*) - \frac{(2e)^2}{m^*}|\psi|^2\mathbf{A}. \tag{2.52}
$$

Note the close similarity to the superfluid current flow that we found earlier in the case of ^4He, Eq. **??**. The differences from Eq. **??** are firstly the charge of the condensate particles, $-2e$, and the presence of the last term which provides the effect of the vector potential $\mathbf{A}$. Finally, the vector potential must be obtained from the magnetic field arising from both the supercurrents and any other currents, such as the external currents, $\mathbf{j}_{ext}$, in the solenoid coils of Fig. 1.6,

$$
\boldsymbol{\nabla} \times \mathbf{B} = \mu_0(\mathbf{j}_{ext} + \mathbf{j}_s), \tag{2.53}
$$

as given by Maxwell's equations.

---

[6]Note that in the definition of the magnetic work given in Eq. 2.4, we excluded the part of this field energy, $\mu_0 H^2/2$ per unit volume, that would be present even with no sample present inside the coil in Fig. 1.6. From now on, it will be more convenient to include this energy explicitly, making F_s the total free energy of both sample and vacuum fields.

2.7 Gauge Symmetry and Symmetry Breaking

The Ginzburg-Landau order parameter for superconductors has both an amplitude and a complex phase

$$\psi(\mathbf{r}) = |\psi(\mathbf{r})|e^{i\theta(\mathbf{r})}. \tag{2.54}$$

This is similar to the macroscopic wave function for superfluid He II, introduced in Chapter 2. However, unlike superfluids of neutral particles , something very interesting happens now when we consider gauge invariance.

If we make a **gauge transformation** of the magnetic vector potential

$$\mathbf{A}(\mathbf{r}) \rightarrow \mathbf{A}(\mathbf{r}) + \boldsymbol{\nabla}\chi(\mathbf{r}) \tag{2.55}$$

then we must make a corresponding change in the phase of the order parameter, θ. Consider the term in the Ginzburg-Landau free energy density containing the canonical momentum operator

$$\hat{p} = \frac{\hbar}{i}\boldsymbol{\nabla} + 2e\mathbf{A}.$$

If we change the phase of the order parameter by

$$\psi(\mathbf{r}) \rightarrow \psi(\mathbf{r})e^{i\theta(\mathbf{r})} \tag{2.56}$$

then we obtain

$$
\begin{aligned}
\hat{p}\psi(\mathbf{r})e^{i\theta(\mathbf{r})} &= e^{i\theta(\mathbf{r})}\left(\frac{\hbar}{i}\boldsymbol{\nabla} + 2e\mathbf{A}\right)\psi(\mathbf{r}) + \psi(\mathbf{r})e^{i\theta(\mathbf{r})}\hbar\boldsymbol{\nabla}\theta(\mathbf{r}) \\
&= e^{i\theta(\mathbf{r})}\left(\frac{\hbar}{i}\boldsymbol{\nabla} + 2e(\mathbf{A} + \frac{\hbar}{2e}\boldsymbol{\nabla}\theta)\right)\psi(\mathbf{r}).
\end{aligned}
\tag{2.57}
$$

From this it follows that the free energy will be unchanged when we simultaneously change $\psi(\mathbf{r})$ to $\psi(\mathbf{r})e^{i\theta(\mathbf{r})}$ and the vector potential according to,

$$\mathbf{A}(\mathbf{r}) \rightarrow \mathbf{A}(\mathbf{r}) + \frac{\hbar}{2e}\boldsymbol{\nabla}\theta. \tag{2.58}$$

This shows that the theory satisfies **local gauge invariance**. Both the phase of the order parameter and the magnetic vector potential depend on the choice of gauge, but all physical observables (free energy, magnetic field $\mathbf{B}$ etc.) are gauge invariant.

So far this is all completely general. But we saw earlier that a bulk superconductor has a ground state with a constant order parameter, ψ. Therefore it must have the same θ everywhere. There must be a **phase-stiffness**, or an energy cost associated with changing θ from one part of the solid to another. If we consider a superconductor in which the order parameter has a constant magnitude, $|\psi|$, and a phase $\theta(\mathbf{r})$ which varies

only slowly with position $\mathbf{r}$, then (using Eq. 2.57) we obtain the total free energy

$$F_s = F_s^0 + \rho_s \int d^3r \left(\boldsymbol{\nabla}\theta + \frac{2e}{\hbar}\mathbf{A} \right)^2 . \qquad (2.59)$$

Here the **superfluid stiffness** is defined by,

$$\rho_s = \frac{\hbar^2}{2m^*}|\psi|^2 \qquad (2.60)$$

and F_s^0 is the total free energy in the ground state ($\theta = constant$, $\mathbf{A} = 0$). Now if we choose some particular gauge for $\mathbf{A}(\mathbf{r})$, such as the London gauge, $\boldsymbol{\nabla}.\mathbf{A} = 0$, then within this fixed gauge there is now a free energy cost associated with further gradients in $\theta(\mathbf{r})$. To minimize the gradient energy, we must minimize the gradients, by making $\theta(\mathbf{r})$ as constant as possible throughout the system. In the case of zero applied magnetic field, we can choose $\mathbf{A} = 0$, and clearly then $\theta(\mathbf{r})$ will be constant everywhere in the system. Again we are back to the XY symmetry of Fig. **??**. Since the system effectively chooses an (arbitrary) constant order parameter phase everywhere in the system, we can say that the system exhibits **long ranged order** in the order parameter phase, just as a ferromagnet has long ranged order in its magnetization $\mathbf{M}(\mathbf{r})$.

Because the long ranged order is in the phase variable (which is not normally a physical observable in quantum mechanics) we say that the system has **spontaneously broken global gauge symmetry**. The point is that *global* gauge symmetry refers to changing $\theta(\mathbf{r})$ by a constant amount everywhere in the whole solid (which does not require any change in $\mathbf{A}$). This is in contrast to *local* gauge symmetry in which $\theta(\mathbf{r})$ and $\mathbf{A}(\mathbf{r})$ are changed simultaneously, consistent with Eq. 2.58.

Eq. 2.59 also implies the London equation, and hence the Meissner-Ochsenfeld effect, bringing us full circle back to Chapter 3. The current can be calculated from a functional derivative of the free energy

$$\begin{aligned} \mathbf{j}_s &= -\frac{\partial F_s[\mathbf{A}]}{\partial \mathbf{A}(\mathbf{r})} \\ &= -\frac{2e}{\hbar}\rho_s \left(\nabla\theta + \frac{2e}{\hbar}\mathbf{A} \right). \end{aligned} \qquad (2.61)$$

Starting in the ground state, where θ is constant, we directly find that with a small constant external vector potential, $\mathbf{A}$, the current is,

$$\mathbf{j}_s = -\rho_s \frac{(2e)^2}{\hbar^2}\mathbf{A} \qquad (2.62)$$

which is exactly the same as the London equation. The superfluid stiffness, ρ_s, is essentially just the London superfluid density, n_s, in disguise!

To make the connection between ρ_s and the London superfluid fraction, n_s, more clear, consider the London equation

$$\mathbf{j}_s = -\frac{n_s e^2}{m_e}\mathbf{A}.\tag{2.63}$$

If we rewrite Eq. 2.61 in the form

$$\mathbf{j}_s = -\frac{(2e)^2}{2m^*}|\psi|^2\mathbf{A},\tag{2.64}$$

then clearly these are the same. It is conventional to define the constants so that the London superfluid density is $n_s = 2|\psi|^2$ and the Ginzburg-Landau effective mass is $m^* = 2m_e$ (where m_e is the bare electron mass). With this choice the equation can be interpreted physically as implying that $|\psi|^2$ is the density of pairs of electrons in the ground state. Therefore in comparison with the BCS theory of superconductivity we can interpret $|\psi|^2$ with the density of Cooper pairs in the ground state, and n_s as the density of electrons belonging to these Cooper pairs. The normal fraction, $n_n = n - n_s$ coresponds to the density of unpaired electrons. The Ginzburg-Landau parameter m^* is the mass of the Cooper pair, which is naturally twice the original electron mass.

In terms of the original free energy Ginzburg-Landau parameters, $\dot{a}$ and b, the superfluid density, n_s is given by

$$n_s = 2|\psi^2| = 2\frac{\dot{a}(T_c - T)}{b}.\tag{2.65}$$

Therefore the London penetration depth, $\lambda(T)$ is given by

$$\lambda(T) = \left(\frac{m_e b}{2\mu_0 e^2 \dot{a}(T_c - T)}\right)^{1/2}.\tag{2.66}$$

Clearly this will diverge at the critical temperature, T_c, since it is proportional to $(T_c - T)^{-1/2}$. We saw earlier that the Ginzburg Landau coherence length, $\xi(T)$, also diverges with the same power of $(T_c - T)$, and so the dimensionless ratio,

$$\kappa = \frac{\lambda(T)}{\xi(T)},\tag{2.67}$$

is independent of temperature within the Ginzburg Landau theory. Table 2.1 summarizes the measured values of penetration depth and coherence length at zero temperature, $\lambda(0)$, $\xi(0)$, for a selection of superconductors.

2.8 Flux quantization

Let us now apply the Ginzburg-Landau theory to the case of a superconducting ring, as shown in Fig. 1.4. Describing the system using cylindrical polar coordinates, $\mathbf{r} = (r, \phi, z)$, with the z-axis perpendicular to the plane

Table 2.1 Penetration depth, $\lambda(0)$, and coherence length, $\xi(0)$, at zero temperature for some important superconductors. Data values are taken from Poole (2000).

	T_c (K)	$\lambda(0)$ (nm)	$\xi(0)$(nm)	κ
Al	1.18	1550	45	0.03
Sn	3.72	180	42	0.23
Pb	7.20	87	39	0.48
Nb	9.25	39	52	1.3
Nb_3Ge	23.2	3	90	30
YNi_2B_2C	15	8.1	103	12.7
K_3C_{60}	19.4	2.8	240	95
$YBa_2Cu_3O_{7-\delta}$	91	1.65	156	95

of the ring, we see that the order parameter $\psi(\mathbf{r})$ must be periodic in the angle ϕ,

$$\psi(r, \phi, z) = \psi(r, \phi + 2\pi, z). \tag{2.68}$$

We assume that the variations of $\psi(\mathbf{r})$ across the cross section of the ring are unimportant, and so we can neglect and r and z dependence. Therefore the possible order parameters inside the superconductor are of the form

$$\psi(\phi) = \psi_0 e^{in\phi} \tag{2.69}$$

where n is an integer and ψ_0 is a constant. We can interpret n as a **winding number** of the macroscopic wave function, exactly as for the case of superfluid helium in Fig. **??**.

However, unlike the case of superfluid helium, a circulating current in a superconductor will induce magnetic fields. Assuming that there is a magnetic flux Φ through the ring, then the vector potential can be chosen to be in the tangential direction, $\mathbf{e}_\phi$ and is given by

$$A_\phi = \frac{\Phi}{2\pi R}, \tag{2.70}$$

where R is the radius of the area enclosed by the ring. This follows from

$$\Phi \equiv \int \mathbf{B}.\mathbf{dS} = \int (\boldsymbol{\nabla} \times \mathbf{A}).\mathbf{dS} = \oint \mathbf{A}.\mathbf{dr} = 2\pi R A_\phi. \tag{2.71}$$

The free energy corresponding to this wave function and vector potential is

$$F_s(T) = F_n(T) + \int d^3r \left(\frac{\hbar^2}{2m^*} |(\boldsymbol{\nabla} + \frac{2ei}{\hbar}\mathbf{A})\psi|^2 + a|\psi|^2 + \frac{b}{2}|\psi|^4 \right) + E_B$$

$$= F_s^0(T) + V\left(\frac{\hbar^2}{2m^*}\left|\frac{in}{R} - \frac{2ei\Phi}{2\pi\hbar R}\right|^2 |\psi|^2\right) + \frac{1}{2\mu_0}\int B^2 d^3r \quad (2.72)$$

where we have used the expression to gradient in cylindrical polar coordinates

$$\boldsymbol{\nabla} X = \frac{\partial X}{\partial r}\mathbf{e}_r + \frac{1}{r}\frac{\partial X}{\partial \phi}\mathbf{e}_\phi + \frac{\partial X}{\partial z}\mathbf{e}_z \quad (2.73)$$

(Boas 1983), V is the total volume of the superconducting ring, and $F_s^0(T)$ is the ground state free energy of the ring in the absence of any currents and magnetic fluxes. The vacuum magnetic field energy $E_B = (1/2\mu_0)\int B^2 d^3r$ can be expressed in terms of the inductance, L of the ring and the current I,

$$E_B = \frac{1}{2}LI^2. \quad (2.74)$$

Clearly, it will be proportional to the square of the total flux, Φ through the ring

$$E_B \propto \Phi^2.$$

On the other hand, the energy of the superconductor contains a term depending on both the flux ϕ and the winding number, n. This term can be expressed as,

$$V\frac{\hbar^2}{2m^*R^2}|\psi|^2(\Phi - n\Phi_0)^2,$$

where the **flux quantum** is $\Phi_0 = h/2e = 2.07 \times 10^{-15}$Wb.

We therefore see that the free energy is equal to the bulk free energy plus two additional terms depending only on the winding number n and the flux Φ. The energy of the superconducting ring is therefore of the general form,

$$F_s(T) = F_s^{bulk}(T) + const.(\Phi - n\Phi_0)^2 + const.\Phi^2. \quad (2.75)$$

This energy is sketched in Fig. 2.6. We can see from the figure that the free energy is a minimum whenever the flux through the loop obeys $\Phi = n\Phi_0$. This is the phenomenon of **flux quantization** in superconductors.

Taking a ring in its normal state above T_c and cooling it to below T_c will result in the system adopting one of the meta-stable minima in Fig. 2.6, depending on the applied field. It will then be trapped in the minimum, and a persistent current will flow around the ring to maintain a constant flux $\Phi = n\Phi_0$. Even if any external magnetic fields are turned off, the current in the ring must maintain a constant flux Φ in the ring. It is possible to directly measure the magnetic flux directly in such rings, and hence confirm that it is indeed quantized in units of Φ_0, or multiples of 2×10^{-15} Wb. Incidentally, the fact that flux quantization is observed in units of $\Phi_0 = h/2e$ and not units of h/e is clear experimental proof that the relevant charge is $2e$ not e, hence implying the existence of Cooper pairs.

Given that a system is prepared in one of the meta-stable minima, it can, in principle, escape over the energy barriers to move into a neighbouring lower energy minimum. This would be a mechanism for the persistent current to decay, and hence for dissipation. Such an event corresponds to a change in the winding number, n, and is called a **phase-slip**. However the rate for thermally hopping over these barriers is exponentially small, of order

$$\frac{1}{\tau} \sim e^{-E_0/k_{\mathrm{B}}T} \tag{2.76}$$

where E_0 is the barrier height between minima in Fig. 2.6. Clearly this thermal hopping rate can be made negligibly small. For example, E_0 is formally proportional to the ring volume, V, and so can be made arbitrarily large in a macroscopic system. In practice persistent currents have been observed to flow for years, with essentially no decay!

Another interesting possible mechanism for a phase slip would be a quantum tunnelling from one minimum to another. This would be possible at any temperature. But again the rate is impractically small in macroscopic systems. However, a very interesting recent development has been the direct observation of these tunnelling events in small **mesoscopic** superconducting rings. hese experiments have demonstrated **macroscopic quantum coherence** and are discussed briefly in the next chapter.

2.9   The Abrikosov flux lattice

The great beauty of the Ginzburg-Landau theory is that it allows one to solve many difficult problems in superconductvity, without any reference to the underlying microscopic BCS theory. In some sense one could argue that it is more general, for example it would almost certainly applies to exotic superconductors, such as the high T_c cuprates, even though the original BCS theory does not seem to explain these systems. The other great advantage of the Ginzburg-Landau theory is that is considerably easier to work with than the BCS theory, especially in cases where the order parameter has complicated spatial variations. The *tour de force* example of this is the **Abrikosov flux lattice**.

Abrikosov found a solution to the Ginzburg-Landau equations in the case of a bulk superconductor in a magnetic field. The result he obtained is remarkable in many respects. It is essentially an exact solution for type II superconductors, valid close to H_{c2}. Furthermore, it predicted a striking result, that just below H_{c2} the order parameter forms into a periodic structure of vortices. Each vortex carries a magnetic flux, hence explaining how magnetic flux enters superconductors in the **mixed state** between H_{c1} and H_{c2}. Abrikosov's prediction of the flux lattice was confirmed experimentally, showing not just that vortices occur, but they also tend to align in a regular triangular lattice, as predicted by the theory. This periodic lattice of vortices was perhaps the first example in physics of *emergent phenomena* in *complex systems*; the fact that sufficiently complex systems exhibit

a variety of novel phenomena on different length scales. These phenomena effectively arise from *self-organization* on the macroscopic length scale.

In type II superconductors the thermodynamic phase transition at H_{c2} is second order (see problem 4.1). Therefore we can expect that the Ginzburg-Landau order parameter ψ is small in magnitude just below H_{c2} and reaches zero exactly at H_{c2}.[7] Therefore, the magnetization M will also be small at a magnetic field just below H_{c2} (since ψ is near zero, the superfluid density n_s and the screening supercurrents will also vanish at H_{c2}),as can be seen in Fig. 1.8. Therefore to a good approximation we can assume that

$$\mathbf{B} = \mu_0 \mathbf{H}, \tag{2.77}$$

where $\mathbf{H}$ is, as usual, the applied field given by the external apparatus as in Fig. 1.6. This also implies that sufficiently near to H_{c2} we can neglect any spatial variations in the B-field, $\mathbf{B}(\mathbf{r})$ and just treat it as a constant,

$$\mathbf{B} = (0, 0, B). \tag{2.78}$$

It will be convenient to express the corresponding vector potential $\mathbf{A}$ in the **Landau gauge** as

$$\mathbf{A}(\mathbf{r}) = (0, xB, 0). \tag{2.79}$$

In which case the Ginzburg-Landau equation, Eq. **??** becomes

$$-\frac{\hbar^2}{2m^*}\left(\boldsymbol{\nabla} + \frac{2eBi}{\hbar}x\mathbf{j}\right)\cdot\left(\boldsymbol{\nabla} + \frac{2eBi}{\hbar}x\mathbf{j}\right)\psi(\mathbf{r}) + a(T)\psi + b|\psi|^2\psi = 0, \tag{2.80}$$

where, as usual, $\mathbf{j}$ is the unit vector in the y direction.

Now if we are infinitesimally below H_{c2}, then ψ is essentially zero and we can drop the cubic term, $b|\psi|^2\psi$. All the other terms are liner in ψ and so we have **linearized** the equation. Expanding out the bracket (paying attention to the commutation of $\boldsymbol{\nabla}$ and $x\mathbf{j}$) gives

$$-\frac{\hbar^2}{2m^*}\left(\nabla^2 + \frac{4eBi}{\hbar}x\frac{\partial}{\partial y} - \frac{(2eB)^2}{\hbar^2}x^2\right)\psi(\mathbf{r}) + a(T)\psi = 0. \tag{2.81}$$

Introducing the cyclotron frequency,

$$\omega_c = \frac{2eB}{m^*}, \tag{2.82}$$

and noting that $a(T)$ is negative since we are at a temperature below the zero field T_c, the equation can be written in the form,

$$\left(-\frac{\hbar^2}{2m^*}\nabla^2 - \hbar\omega_c ix\frac{\partial}{\partial y} + \frac{m^*\omega_c^2}{2}x^2\right)\psi(\mathbf{r}) = |a|\psi(\mathbf{r}). \tag{2.83}$$

where $\xi(T)$ is the Ginzburg-Landau coherence length.

---

[7]In contrast this would not be the case for a type I superconductor, where the transition at H_c is first order. In these superconductors ψ jumps from discontinuously from zero to a finite value at H_c.

Now Eq. 2.83 has the form of an eigenvalue equation, and is well known in quantum mechanics. It is equivalent to the Scrödinger equation for the wave function of a charged particle in a magnetic field, which has well known **Landau level** solutions (Ziman 1979). The solution has the form,

$$\psi(\mathbf{r}) = e^{i(k_y y + k_z z)} f(x), \tag{2.84}$$

which is a combination of plane waves in the y and z directions, combined with an unknown function of x, $f(x)$.

To find an equation for this function, $f(x)$ we substitute the trial solution into Eq. 2.83. We find that $f(x)$ obeys

$$-\frac{\hbar^2}{2m^*}\frac{d^2 f}{dx^2} + \left(\hbar\omega_c k_y x + \frac{m^*\omega_c^2}{2}x^2\right)f = (|a| - \frac{\hbar^2(k_y^2 + k_z^2)}{2m^*})f. \tag{2.85}$$

The term in brackets on the left hand side can be rearranged by "completing the square",

$$\left(\hbar\omega_c k_y x + \frac{m^*\omega_c^2}{2}x^2\right) = \frac{m^*\omega_c^2}{2}(x - x_0)^2 - \frac{m^*\omega_c^2}{2}x_0^2 \tag{2.86}$$

where

$$x_0 = -\frac{\hbar k_y}{m\omega_c}. \tag{2.87}$$

Finally, moving all the constants over to the right hand side we find,

$$-\frac{\hbar^2}{2m^*}\frac{d^2 f}{dx^2} + \frac{m^*\omega_c^2}{2}(x - x_0)^2 f = (|a| - \frac{\hbar^2 k_z^2}{2m^*})f. \tag{2.88}$$

Eq. 2.88 is just the Schrödinger equation for a simple Harmonic oscillator, except that the origin of coordinates is shifted from $x = 0$ to $x = x_0$. Therefore the term in square brackets on the right is just the energy of the oscillator,

$$\left(n + \frac{1}{2}\right)\hbar\omega_c = |a| - \frac{\hbar^2 k_z^2}{2m^*}, \tag{2.89}$$

or

$$\left(n + \frac{1}{2}\right)\hbar\omega_c + \frac{\hbar^2 k_z^2}{2m^*} = \dot{a}(T_c - T). \tag{2.90}$$

The corresponding functions $f(x)$ are just the wave functions of a simple Harmonic oscillator for each n, shifted by x_0.

Imagine that we gradually cool a superconductor in an external field, H. At the zero field transition temperature, T_c, it will be impossible to satisfy Eq. 2.90 because of the zero point energy term $\hbar\omega_c/2$ on the right

hand side. A solution will only be possible when the temperature is far enough below T_c to achieve,

$$\frac{1}{2}\hbar\omega_c = \dot{a}(T_c - T),\qquad(2.91)$$

corresponding to the lowest possible energy solution ($n = 0$, $k_z = 0$). This equation determines the depression in transition temperature in the magnetic field,

$$
\begin{aligned}
T_c(H) &= T_c(0) - \frac{1}{2\dot{a}}\hbar\omega_c \\
&= T_c(0) - \frac{2e\hbar\mu_0}{2\dot{a}m*}H.
\end{aligned}
\qquad(2.92)
$$

Alternatively, we can start in a large external field, H, above H_{c2} which we gradually decrease (keeping the temperature fixed) until

$$\frac{1}{2}\hbar\frac{2eB}{m^*} = \dot{a}(T_c - T).\qquad(2.93)$$

Therefore, rearranging,

$$
\begin{aligned}
\mu_0 H_{c2} = B_{c2} &= \frac{2m^*\dot{a}(T_c - T)}{\hbar^2}\frac{\hbar}{2e} \\
&= \frac{\Phi_0}{2\pi\xi(T)^2}.
\end{aligned}
\qquad(2.94)
$$

It is interesting to note that this result implies that at H_{c2} there is exactly one flux quantum (i.e. one vortex line), in each unit area $2\pi\xi(T)^2$. This expression also provides the simplest way to measure the Ginzburg-Landau coherence length $\xi(0)$ experimentally. Since $\xi(T) = \xi(0)t^{-1/2}$ where $t = |T - T_c|/T_c$,

$$\mu_0 H_{c2} = \frac{\Phi_0}{2\pi\xi(0)^2}\frac{T_c - T}{T_c}\qquad(2.95)$$

and so by measuring the gradient of $H_{c2}(T)$ near to T_c one can easily find the corresponding $\xi(0)$.

It is also interesting to compare this expression for H_{c2} with the corresponding result for H_c which we found earlier. Using the Ginzburg-Landau expression for the total energy in the Meissner state we had found that

$$
\begin{aligned}
H_c &= \frac{\dot{a}}{(\mu_0 b)^{1/2}}(T_c - T) \\
&= \frac{\Phi_o}{2\pi\mu_0\sqrt{2}\xi\lambda}
\end{aligned}
$$

$$= \frac{H_{c2}}{\sqrt{2}\kappa}, \tag{2.96}$$

and therefore

$$H_{c2} = \sqrt{2}\kappa H_c \tag{2.97}$$

From this we can deduce that for superconductors with $\kappa > 1/\sqrt{2}$ we will have $H_{c2} > H_c$, and the phase transition will be second order with the order parameter growing continuously from zero at fields just below H_{c2}. I.e. we will have a type II superconductor. On the other hand, for superconductors with $\kappa < 1/\sqrt{2}$ we will have $H_{c2} < H_c$, and the phase transition will be first order phase transition at the field H_c, below which the order parameter jumps discontinuously to a finite value. The Abrikosov theory therefore immediately describes the difference between type I and type II superconductors,

$$\kappa \begin{cases} < \frac{1}{\sqrt{2}} & \text{type I} \\ > \frac{1}{\sqrt{2}} & \text{type II} \end{cases}$$

The linearized Ginzburg-Landau equation allows us to find at H_{c2}, but does not immediately tell us anything about the form of the solution below this field. To do this we must solve the non-linear equation, Eq. 2.80. This is very hard to do in general, but Abrikosov made a brilliant guess and came up with essentially the exact solution! He could see from the solutions to the linearized equation Eq. 2.80 that only the harmonic oscillator ground state solutions $n = 0$ and $k_z = 0$ will be significant. However there are still an infinite number of degenerate states, corresponding to the different possible k_y values,

$$\psi(\mathbf{r}) = Ce^{i(k_y y)}e^{-(x-x_0)^2/\xi(T)^2}, \tag{2.98}$$

where C is a nomalization constant. Here we have used the fact that the ground state wave function of a quantum harmonic oscillator is a gaussian function. The width of the gaussian solution to Eq. 2.88 turns out to be the GL coherence length $\xi(T)$.

Abrikosov's trail solution was to assume that we can combine these solutions into a **periodic** lattice. If we look for a solution which is periodic in y with period l_y, then we can restrict the values of k_y to

$$k_y = \frac{2\pi}{l_y}n \tag{2.99}$$

with n any positive or negative integer. The corresponding Landau level x shift is

$$x_0 = -\frac{2\pi\hbar}{m\omega_c l_y}n = -\frac{\Phi_0}{Bl_y}n. \tag{2.100}$$

Therefore we can try a periodic solution

$$\psi(\mathbf{r}) = \sum_{n=-\infty,\infty} C_n e^{i(2\pi ny/ly)} e^{-(x+n\P hi_0/Bl_y)^2/\xi(T)^2}. \tag{2.101}$$

In this solution we can view the parameters C_n as variational parameters which are to be chosen to minimize the total GL free energy of the system.

The solution above is periodic in y, but not necessarily periodic in x. Abrikosov noted that it can be made periodic in x provided the coefficients obey

$$C_{n+\nu} = C_n \tag{2.102}$$

for some integer ν. The period is l_x, where

$$l_x = \nu \frac{\Phi_0}{Bl_y}. \tag{2.103}$$

Abrikosov studied the simplest case, $\nu = 1$ which corresponds to a simple square lattice lattice. Later it was shown that a slightly lower total energy is obtained for the $\nu = 2$ case and the minimum energy state corresponds to a simple triangular lattice. In each case the order parameter $\psi(\mathbf{r})$ goes to zero at one point in each unit cell, and there is exactly one flux quantum Φ_0 per unit cell. Therefore the solution is a **periodic lattice of vortices**. This is illustrated in Fig. 2.7.

Experimental evidence for the Abrikosov flux lattice comes from a variety of methods. In a "flux decoration" experiment small paramagnetic particles are dusted onto the surface of the superconductor (just like the children's experiment to see magnetic fields of a bar magnet using iron filings on paper above the magnet!). The particles concentrate int he points of highest magnetic field, i.e. the vortices. Other similar methods involve scanning a small SQUID loop or Hall probe just above the surface of the superconductor to directly measure the variation of the local flux density $\mathbf{B}(\mathbf{r})$. For most ordinary type II low T_c superconductors, such as Pb or Nb, these experiments indeed show that the vortices form a fairly regular hexagonal lattice. The lattice can be periodic over quite long length scales, but is disrupted now and then by defects. These defects (exactly analogous to crystal dislocations or point defects) tend to concentrate near defects in the underlying crystal lattice (such as grain boundaries, impurities etc.).

Another method of observing the order in the flux lattice is to use neutron scattering. The neutrons have a magnetic moment, and so are sensitive to the magnetic field $\mathbf{B}(\mathbf{r})$. If this is periodic, as in the Abrikosov flux lattice, then there will be diffraction. The diffraction pattern can be used to find the geometry of the flux lattice. Again the majority of systems studied are found to have triangular lattices. But, interestingly, a square lattice has now been found in a few recently discovered superconductors. These are: the 'borocarbide' system $ErNi_2B_2C$, the high temperature superconductor $YBa_2Cu_3O_{7-\delta}$ and the possible p-wave strontium ruthenate Sr_2RuO_4. All of these have been found to have square vortex lattices in at least some range of external fields. It may be that this is simply because

of small corrections to the original Abrikosov theory (such as terms omitted in the standard GL equations, such as higher powers of ψ, like $|\psi|^6$, or higher order gradients). n fact the square lattice and triangular lattice have energies differing by less than 1% in the Abrikosov solution. But in some cases it seems more likely to be due to the fact that the underlying form of superconductivity is "unconventional", meaning that the Cooper pairs have a different symmetry from the normal BCS case. We shall introduce these ideas briefly in chapter 7.

Finally, we should note that while the Abrikosov solution is essentially exact just below H_{c2}, it cannot necessarily be applied far away from there, such as at H_{c1}. As we have seen, near to H_{c2} the vortices are close together, separated by distances of order the coherence length $\xi(T)$. Effectively they are so densely packed that their cores are essentially touching. On the other hand, just at H_{c1} we have very few vortices in the entire sample, and so they are well separated. We can estimate of the lower critical field H_{c1} from the energy balance for the very first few vortices to enter a superconductor in the Meissner phase. One can show that a single London vortex has an energy of approximately (see exercise 3.3)

$$E = \frac{\Phi_0^2}{4\pi\mu_0\lambda} \ln\left(\frac{\lambda}{\xi}\right) \tag{2.104}$$

per unit length. Therefore in a superconductor with N/A flux lines per unit area and thickness L, there will be a total energy cost EN/A per unit volume due to the vortices. But on the other hand, each vortex carries a flux Φ_0, and so the average magnetic induction in the sample is $B = \Phi_0 N/A$. The magnetic work gained by the presence of the vortices is $\mu_0 H dM = H dB$ (at constant H). Energy balance therefore favours the presence of the vortices when

$$E\frac{N}{A} < H\Phi_0\frac{N}{A}. \tag{2.105}$$

Thus is becomes energetically favourable for the vortices to enter the sample when $H > H_{c1}$, where

$$H_{c1} = \frac{\Phi_o}{4\pi\mu_0\lambda^2} \ln\left(\frac{\lambda}{\xi}\right). \tag{2.106}$$

This is obviously the lower critical field, and can be simply expressed as

$$H_{c1} = \frac{H_c}{\sqrt{2}\kappa} \ln(\kappa). \tag{2.107}$$

This expression is only valid when $\kappa >> 1/\sqrt{2}$, i.e. in the London vortex limit.

2.10 Thermal Fluctuations

The Ginzburg-Landau theory as described above is purely a **mean-field theory**. It neglects **thermal fluctuations**. In this t is therefore similar to the

Curie-Weiss or Stoner models in the theory of magnetism (Blundell 2001). But in fact it is a great strength of the GL theory that it can easily be extended so that these fluctuations can be included. It is much simpler to include these in the GL theory than in the more complex BCS theory.

In the mean-field approach, we must always find the order parameter $\psi(\mathbf{r})$ which minimizes the total free enrgy of the system. As discussed above, this is a functional minimization. The total free energy of the system $F[\psi]$, in Eq. 2.29, is a functional of the complex order parameter, $\psi(\mathbf{r})$, meaning that it depends on an infinite number of variables: the values of ψ all possible points $\mathbf{r}$. As we saw, the condition for minimizing the free energy is that the functional derivatives given in Eq. 2.37 are zero.

To go beyond this mean-field approach we must include fluctuations of $\psi(\mathbf{r})$ close to this minimum. For example if we make a small variation in $\psi(\mathbf{r})$, such as $\psi(\mathbf{r}) \rightarrow \psi'(\mathbf{r}) = \psi(\mathbf{r}) + \delta\psi(\mathbf{r})$, then we expect that the energy of the system represented by $\psi'(\mathbf{r})$ would be very similar to that represented by $\psi(\mathbf{r})$. If the total energy difference is small, or no more than $k_{\mathrm{B}}T$, then we might expect that in thermal equilibrium the system would have some probability to be in state $\psi'(\mathbf{r})$. We need to define an effective probability for each possible state. Clearly this must be based on the usual Boltzmann probability distribution and so we expect that,

$$P[\psi] = \frac{1}{Z}e^{-\beta F[\psi]} \tag{2.108}$$

is the probability density for the system to have order parameter $\psi(\mathbf{r})$. It is again a functional of $\psi(\mathbf{r})$ as indicated by the square brackets.

The partition function Z is the normalization factor in this expression. Formally it is a **functional integral**,

$$Z = \int \mathcal{D}[\psi]\mathcal{D}[\psi^*]e^{-\beta F[\psi]}. \tag{2.109}$$

We can treat the integrals over ψ and ψ^* as formally separate for the same reason that we could view functional derivatives with respect to ψ and ψ^* as formally independent. It is really allowed because in fact we have to specify two independent real functions, the real and imaginary parts of ψ at each point $\mathbf{r}$: $\mathrm{Re}[\psi(\mathbf{r})]$ and $\mathrm{Im}[\psi(\mathbf{r})]$.

What is the meaning of the new integration symbols, like $\mathcal{D}[\psi]$ in Eq. 2.109? We are technically integrating over an infinite number of variables, the values of $\psi(\mathbf{r})$ at every point $\mathbf{r}$. It is difficult (and beyond the scope of this book!) to make this idea mathematically rigorous. But we can find an intuitive idea of what this mens by supposing that we only had a discrete set of points in space, $\mathbf{r}_1, \mathbf{r}_2, \ldots, \mathbf{r}_N$. We could define values of ψ and ψ^* at each point, and then calculate a Boltzmann probability. The approximate partition function for this discrete set would be the multiple integral

$$Z(N) = \int d\psi(\mathbf{r}_1)d\psi(\mathbf{r}_1^*) \int d\psi(\mathbf{r}_2)d\psi(\mathbf{r}_2^*)\ldots \int d\psi(\mathbf{r}_N)d\ psi(\mathbf{r}_N^*)e^{-\beta F[\psi]}.$$
$$(2.110)$$

The full functional integral is a limit in which we make the set of points infinitely dense (in fact even possibly uncountably infinite!), defining

$$Z = \lim_{N\to\infty} Z(N). \tag{2.111}$$

One way that this infinite product of integrals might be accomplished is through the Fourier transforms of $\psi(\mathbf{r})$ and $\psi^*(\mathbf{r})$. If we define $\psi_{\mathbf{k}}$ by

$$\psi(\mathbf{r}) = \sum_{\mathbf{k}} \psi_{\mathbf{k}} e^{i\mathbf{k}.\mathbf{r}} \tag{2.112}$$

then specifying the parameters $\psi_{\mathbf{k}}$ and $\psi_{\mathbf{k}}^*$ at every wave vector $\mathbf{k} = (2\pi n_x/L_x, 2\pi n_y/L_y, 2\pi n_z/L_z)$ (or equivalently the real and imaginary parts), is defines the full functions $\psi(\mathbf{r})$ and $\psi^*(\mathbf{r})$. In this representation we can write the partition function as

$$Z = \prod_{\mathbf{k}} \left(\int d\psi_{\mathbf{k}} d\psi_{\mathbf{k}}^* \right) e^{-\beta F[\psi]}. \tag{2.113}$$

Again there are an infinite number of integrals, two for each point $\mathbf{k}$.

As an example of the sort of thermal fluctuation effects that can be calculated within this formalism we shall consider the specific heat of a superconductor near to T_c. For a superconductor in zero magnetic field we have the free energy functional,

$$F[\psi] = \int d^3r \left(\frac{\hbar^2}{2m^*}|\boldsymbol{\nabla}\psi|^2 + a|\psi|^2 + \frac{b}{2}|\psi|^4 \right) \tag{2.114}$$

(dropping the constant normal state free energy F_n, which will be irrelevant here). Writing this in terms of the Fourier coefficients ψ_{bfk} we find

$$F[\psi] = \sum_{bfk} \left(\frac{\hbar^2 k^2}{2m^*} + +a \right) \psi_{\mathbf{k}}^* \psi_{\mathbf{k}} + \frac{b}{2} \sum_{\mathbf{k}_1,\mathbf{k}_2,\mathbf{k}_3} \psi_{\mathbf{k}_1}^* \psi_{\mathbf{k}_2}^* \psi_{\mathbf{k}_3} \psi_{\mathbf{k}_1+\mathbf{k}_2-\mathbf{k}_3}, \tag{2.115}$$

which could in principle be inserted directly into Eq. 2.113. In general this would be very difficult, and requires either massive numerical Monte Carlo simulation, or some other approximation. The simplest approximation that we can make is to make the **gaussian approximation**, in which we neglect the quartic (b) term in the free energy. In this approximation we find a simple result

$$Z = \prod_{\mathbf{k}} \int d\psi_{\mathbf{k}} d\psi_{\mathbf{k}}^* exp\left\{ -\beta \left(\frac{\hbar^2 k^2}{2m^*} + a \right) \psi_{\mathbf{k}}^* \psi_{\mathbf{k}} \right\}. \tag{2.116}$$

Changing variables to the two real functions, $\text{Re}[\psi_{\mathbf{k}}]$ and $\text{Re}[\psi_{\mathbf{k}}]$ gives

$$Z = \prod_{\mathbf{k}} \int d\text{Re}[\psi_{\mathbf{k}}] d\text{Im}[\psi_{\mathbf{k}}] exp\left\{-\beta\left(\frac{\hbar^2 k^2}{2m^*} + a\right)\left(\text{Re}[\psi_{\mathbf{k}}]^2 + \text{Im}[\psi_{\mathbf{k}}]^2\right)\right\},$$

(2.117)

and so for each $\mathbf{k}$ the integral is just a two dimensional gaussian integral. These can be done exactly, resulting in the partition function

$$Z = \prod_{\mathbf{k}} \frac{\pi}{\beta\left(\frac{\hbar^2 k^2}{2m^*} + a\right)}.$$

(2.118)

From the partition function it is possible to calculate all thermodynamic quantities of interest. For example, the total internal energy is given by Eq. **??**,

$$
\begin{aligned}
U &= -\frac{\partial \ln Z}{\partial \beta} \\
&= +k_{\mathrm{B}}T^2 \frac{\partial \ln Z}{\partial T} \\
&\sim -\sum_{\mathbf{k}} \frac{1}{\left(\frac{\hbar^2 k^2}{2m^*} + a\right)} \frac{da}{dT},
\end{aligned}
$$

(2.119)

where in the last step we have kept only the most important contribution which comes from the change of the Ginzburg Landau parameter a with T, $da/dT = \dot{a}$.

The gaussian approximation for the heat capacity near to T_c is found by differentiating again, giving

$$
\begin{aligned}
C_V = \frac{dU}{dT} &= \sum_{\mathbf{k}} \frac{1}{\left(\frac{\hbar^2 k^2}{2m^*} + a\right)^2} \dot{a}^2. \\
&= \frac{V}{(2\pi^3)} \frac{\dot{a}^2}{a^2} \int d^3k \frac{1}{(1 + \xi(T)^2 k^2)^2} \\
&\sim \frac{V}{(2\pi^3)} \frac{\dot{a}^2}{a^2} \frac{1}{\xi(T)^3} \\
&\sim \frac{1}{(T - T_c)^2} |T_c - T|^{3/2} \\
&\sim \frac{1}{|T - T_c|^{1/2}},
\end{aligned}
$$

(2.120)

(where, for simplicity, we have ignored the numerical multiplying prefactors). This shows that the thermal fluctuations can make a very large contribution to the heat capacity, essentially diverging at the critical temperature T_c. If we sketch this behaviour we see that the thermal fluctuations

make a large difference to the original mean-field specific heat of Fig. 2.4. As can be seen in Fig. **??**. In fact, once the fluctuations are included the the heat capacity of superconductors becomes much more similar to the heat capacity of superfluid ^{4}He at T_c, as shown in Fig. **??**.[8]

Experimentally these thermal fluctuations are very difficult to see in standard "low T_c" superconductors, such as Pb or Nb. It is possible to estimate the range of temperatures near to T_c where these fluctuations are significant. This temperature range, T_G is known as the Ginzburg critereon. In 1960 Ginzburg found that this temperature range is extremely small, i.e. much less than 1μK for most low T_c superconductors. Therefore we can say that the original mean-field approach to the Ginzburg Landau equations is perfectly well justified. However, in the high temperature superconductors, discovered in 1986, the coherence length $\xi(0)$ is very small (Table 2.1), of order just a few Angstroms. It turns out that the corresponding Ginzburg temperature range, T_G, is of order $1 - 2$K. Therefore is is quite possible to see such thermal fluctuation effects in these systems. The specific heat near T_c clearly shows thermal critical fluctuations, as shown in Fig. 2.9. In fact in these experimental results very good agreement is found using the value of the critical exponent α given by the three dimensional XY model predictions, exactly as is the case in superfluid ^{4}He, Fig. **??**. The gaussian model exponent $\alpha = 1/2$ does not fit at all as well. Another example of thermal fluctuation effects can be seen in the resistivity, $\rho(T)$, just above T_c. Thermal fluctuations make $\rho(T)$ begin to bend down towards zero even at temperatures quite far above T_c. This downward bending is clearly visible in the resistivity curve of the $T_c = 135$K superconductor $HgBa_2Ca_2Cu_3O_8 + \delta$ shown in Fig. 1.2.

2.11   Vortex Matter

Another very important consequence of thermal fluctuations occurs in the mixed state of high temperature superconductors. As we have seen, Abrikosov's flux lattice theory shows that the vortices align in a periodic lattice arrangement, essentially like a crystal lattice, either triangular or square. However, this is again a mean field approximation! We must, in principle, again include the effects of thermal fluctuations.

The theories of the resulting **vortex matter** states show a very wide range of possibilities. It is still possible to talk about the vortices, but now they themselves form a variety of different states, including liquid and glassy (random, but frozen) states, as well as nearly perfectly ordered

---

[8]In fact, the gaussian theory, as outlined above, is not truly correct since it dropped the $|\psi|^4$ terms in the Ginzburg-Landau free energy. When these terms are included the resulting theory is known in statistical physics as the XY or $O(2)$ model. Its true critical behaviour near T_c can be calculated with various methods based on the renormalization group. The resulting critical exponent for specific heat α is very small and very different from the $\alpha = 1/2$ which is given by the gaussian approximation of Eq. 2.120.

crystalline states. It is believed that the flux lattice never has true crystalline order, and thermal fluctuations always lead to an eventual loss of long ranged order in the periodic structure (although in practice periodicity can be quite well extended). A full discussion of these topics requires a whole book in itself (Singer and Schneider 2000), and there also are many extensive review papers (Blatter 1994).

Unfortunately these thermal fluctuations have been disastrous for commercial applications of high T_c superconductors in high current wires and electromagnets (Yeshrun 1998).[9] The problem is that thermal fluctuations lead to motion of the vortices, and this leads to a source of energy dissipation. Therefore the resistivity is not zero for high T_c superconductors in a magnetic field. The problem also occurs in low T_c superconductors, but to a much lesser extent. In these systems the energy dissipation due to motion of vortices can be reduced or eliminated by providing **pinning centres** which "pin" the vortex lattice and prevent it from moving. Typically these are just impurities, or naturally occurring crystal defects such as grain boundaries and dislocations.

To see why motion of vortices leads to energy dissipation is is necessary to see that a current density **j** flowing through the vortex lattice (perpendicular to the magnetic field) leads to a Lorentz (or Magnus) force on each vortex. The overall force is

$$\mathbf{f} = \mathbf{j} \times \hat{\mathbf{B}} \tag{2.121}$$

per unit volume of the vortex lattice. This will tend to make the vortex liquid flow in the direction perpendicular to the current as shown below on the left, as illustrated in Fig. **??**.

Unfortunately if the vortices flow in response to this force, work is done and there is energy dissipation. To calculate the work, consider a loop of superconducting wire, with a current flowing around the wire. Vortices will tend to drift transversely across the wire, say entering on the inner side of the wire and drifting over to the outer side. This is illustrated in Fig. **??**. Each vortex carries a magnetic flux Φ_o, and so the total magnetic flux in the ring Φ changes by Φ_o with each vortex that crosses from one side of the wire to the other. But by elementary electromagnetism there is an EMF induced in the wire given by $\mathcal{E} = -d\Phi/dt$. Power is dissipated, at a rate given by $P = \mathcal{E}I$ where I is the total current. Therefore vortex motion directly leads to **finite resistance**! In the mixed state, superconductors only have truly zero resistance when the vortices are pinned and unable to move.

---

[9]Perhaps thisis not the only difficulty with commerical applications of high T_c superconductivity. The materials are brittle and cannot easily be made into wires. Nevertheless these problems have been gradually overcome, and now high T_c superconducting wires are beginning to make a serious entry into commercial applications. For example, at least one US city receives part of its electrical power through underground superconducting cables. Some microwave receivers, such as in some masts for mobile phones beside motorways, also use superconducting devices operating at liquid nitrogen temperatures.

In high T_c superconductors the thermal motion of vortices leads to especially bad pinning and hence a significant resistivity in the mixed state. To make matters worse, the lower critical field H_{c1} is tiny, often less than the Earth's magnetic field, and so vortices can never by truly eliminated. At high temperatures and near to H_{c2} it is believed that the vortex matter is in a liquid state, and so the vortices can move freely and pinning is essentially impossible.[10] Lowering the temperature, or going further away from H_{c2} the vortex matter appears to "freeze" into a glassy state. A glass is random spatially, but frozen in time. Since glass is effectively rigid the vortices cannot move and pinning is able to largely prevent flux motion. Therefore in this state the resistivity is quite low. Unfortunately, even in this glassy vortex state the resistivity is not fully zero, since **flux creep** can occur. The random pinning force provides a set of energy barriers to vortex motion, but thermal motions mean that from time to time the vortices can hop over the local energy barrier and find a new configuration.[11] The line in the (H, T) phase diagram where the glassy phase occurs is called the "irreversibility line", as shown in Fig. 2.10. Something approaching zero resitivity is approached only well below this line. This effectively limits the useful magnetic fields for applications of high T_c superconductivity, to very much less than the hundreds of Tesla that one might have expected from the nominal values of $\mu_0 H_{c2} > 100T$, such as one might expect from Table 2.1.

2.12   Summary

We have seen how the Ginzburg Landau theory provides a mathematically rather simple picture with which to describe quite complex phenomena in superconductivity. In terms of the phenomenological order parameter, $\psi(\mathbf{r})$, and four empirically determined parameters ($\dot{a}$, b, m^* and T_c) we can can construct a full theory of superconductivity which encompasses fully phenomena such as the Abrikosov flux lattice, flux quantization and from which one can "derive" the London equation.

The power of the theory is also apparent in the way it can be modified to incorporate thermal fluctuations, including critical phenomena and vortex matter physics. It should be noted that these areas are still highly active areas of experimental and theoretical activity. Even some very simple and fundamental questions are still hotly debated, such as the various vortex phases occurring in high temperature superconductors. These also have important implications for potential commercial applications of these materials.

---

[10] A liquid can always flow around any impurities and so pinning centres have no effect in the vortex liquid state.

[11] The process is presumably analogous to the way that window glass in medieval cathedrals appears to have gradually flowed downwards over timescales of hundreds of years.

2.13 Further Reading

Magnetic work in thermodymanics is discussed in detail in the textbooks by Mandl (1987) and Callen (1960).

The idea of order parameters and Ginzburg Landau theory in general, including superconductors, are discussed in Chakin and Lubensky (1995) and Anderson (1984). Applications of Ginzburg Landau theory to vortex states and other problems are covered in detail by de Gennes (1966). Other books are also useful, such as Tilley and Tilley (1990), Tinkham (1996). In fact almost all textbooks on superconductivity have at least one chapter dealing with Ginzburg Landau theory and its predictions.

Thermal fluctuations and critical phenomena are in themselves huge fields of study. A good introductory course is Goldenfeld (1992), while the books Amit (1984) and Ma (1976) are very comprehensive. These books discuss very general classes of theoretical models, but the Ginzburg Landau theory we have discussed is equivalent to the model they call XY or $O(2)$.

For a modern view of thremal fluctuation phenomena and the problems of vortex matter physics, especially in its application to high temperature superconductors, see the book by Singer and Schneider (2000), or the review articles by Blatter (1994) and Yeshrun (1996).

2.14 Exercises

(4.1) (a) For a type I superconductor $H_c(T)$ is the boundary between normal metal and superconductor in the H, T phase diagram. Everywhere on this boundary thermal equilibrium requires

$$G_s(T, H) = G_n(T, H).$$

Apply this equation and $dG = -SdT - \mu_0 MdH$ to two points on the $H - T$ phase boundary (T, H) and $(T + \delta T, H + \delta H)$, , as illustrated in Fig. 2.12. Hence show that:

$$-S_s \delta T - \mu_0 M_s \delta H = -S_n \delta T - \mu_0 M_n \delta H$$

when δT and δH are small, and where $S_{s/n}$ $M_{s/n}$ are the superconducting and normal state entropy and magnetization respectively.

(b) Using part (a), and $M_n = 0$, and $M_s = -H$ show that the latent heat per unit volume for the phase transition, $L = T(S_n - S_s)$, is given by

$$L = -\mu_0 T H_c \frac{dH_c(T)}{dT}$$

where the phase boundary curve is $H_c(T)$. (This is exactly analogous to the Clausius-Claperyon equation in a gas-liquid phase change except H replaces P and $-\mu_0 M$ replaces V. See Mandl (1987) p 228).

(4.2) Find $|\psi|^2$, the free energy $F_s - F_n$, the entropy and the heat capacity of a superconductor near T_c, using the bulk Ginzburg-Landau free energy. Sketch their variations with temperature assuming that $a = \dot{a} \times (T - T_c)$ and $\dot{a}$ and b are constant near T_c.

(4.3) (a) Show that for one-dimensional problems, such as the surface discussed in sec. 4.5, the Ginzburg Landau equations for $\psi(x)$ can be rewritten as:

$$-\frac{d^2}{dy^2} f(y) - f(y) + f(y)^3 = 0$$

where $x = y\xi(T)$, $f(y) = \psi(y\xi)/\psi_0$, and $\psi_0 = \sqrt{|a|/b}$.

(b) Verify that

$$f(y) = \tanh\left(y/\sqrt{2}\right)$$

is a solution to the equation in (b) corresponding to the boundary condition $\psi(0) = 0$. Hence sketch $\psi(x)$ near the surface of a superconductor.

(c) Often the surface boundary condition of a superconductor is not $\psi(x) = 0$, but $\psi(x) = C$ where C is a numerical constant. Show that if $C < \psi_0$ we can just translate the solution from Prob. 4.2 sideways to find a valid solution for any value of C in the range $0 \leq C < \psi_0$.

(d) In the proximity effect a metal (in the half-space $x > 0$) is in contact wi th a superconductor (occupying the region $x < 0$). Assuming that the normal metal can be described by a Ginzburg-Landau model but with $a > 0$, show that the order parameter $\psi(x)$ induced in the metal by the contact with the superconductor is approximately

$$\psi(x) = \psi(0)e^{-x/\xi(T)}$$

where $\hbar^2/2m^*\xi(T)^2 = a > 0$, and $\psi(0)$ is the order parameter of the superconductor at the interface.

(4.4) (a) In Eq. 2.120 we showed that the gaussian model gives a divergence in specific heat of the form

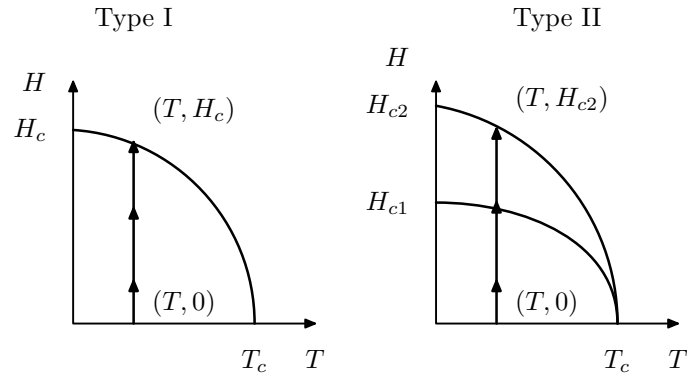$$C_V \sim \frac{1}{|T - T_c|^\alpha}$$

with $\alpha = 1/2$. Repeat the steps given in Eq. 2.120 for the case of a two dimensional system, and show that in this case the gaussian model predicts $\alpha = 1$.

(b) This argument can also be extended easily to the general case of d-dimensions. By replacing the $\mathbf{k}$ sum in Eq. 2.120 by an integral of the form
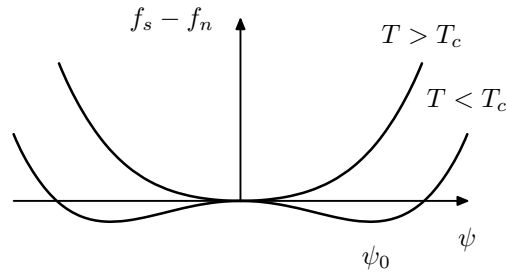
$$\sum_{\mathbf{k}} \rightarrow \frac{1}{(2\pi^d)} \int d^d k$$

show that in d dimensions we have the critical exponent

$$\alpha = 2 - \frac{d}{2}.$$

Type I

Type II

Fig. 2.1 We obtain the condensation energy for superconductors by thermodynamic integration of the Gibbs free energy along the contours in the (T, H) plane, as shown above.

**Fig. 2.2** Free energy difference between the normal and superconducting states (per unit volume) as a function of the order parameter ψ. For $T < T_c$ the free energy has a minimum at ψ_0, while for $T > T_c$ the only minimum is at $\psi = 0$.
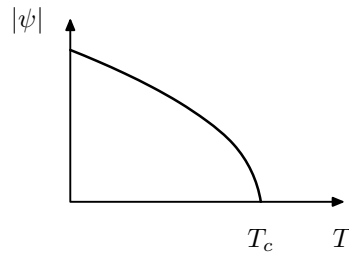

Fig. 2.3 Order parameter magnitude, $|\psi|$, as a function of temperature in the Ginzburg Landau model.
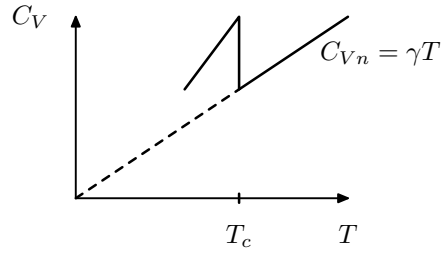
Fig. 2.4 Specific heat of a superconductor near T_c in the Ginzburg Landau model. Above T_c the specific heat is given by the Sommerfeld theory of metals, $C_{Vn} = \gamma T$. At T_c there is a discontinuity and a change of slope.
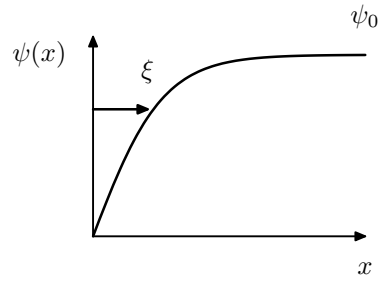
Fig. 2.5 Order parameter of a superconductor near a surface. It recovers to its bulk value ψ_0 over a length scale of the coherence length, ξ.
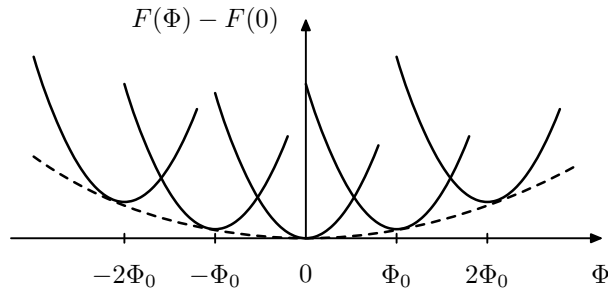
Fig. 2.6 Flux quantization in a superconducting ring. Metastable energy minima exist when the flux is an integer multiple of the flux quantum $\Phi_0 = h/2e$. There is an overall background increase with Φ corresponding to the self-inductance of the ring, making the zero flux state $\Phi = 0$ the global energy minimum. Thermal fluctuations and quantum tunnelling allow transitions between neighbouring meta-stable energy minima.
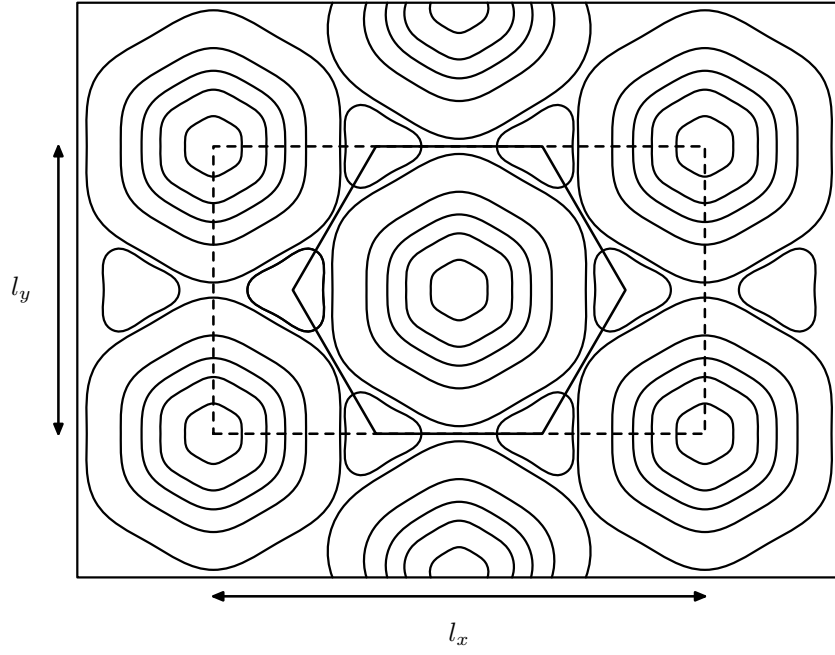
Fig. 2.7 The Abrikosov flux lattice. The figure shows the amplitude of the order parameter, $|\psi(\mathbf{r})|^2$ for the lowest energy triangular lattice. Each triangular unit cell contains on quantum, Φ_0, of magnetic flux and contains on vortex where $\psi(\mathbf{r}) = 0$. In terms of the l_x and l_y lattice periodicities used in Sec. 4.9, $l_y = \sqrt{3}l_x$, and the rectangular unit cell $l_x \times l_y$ contains two vortices and two flux quanta.
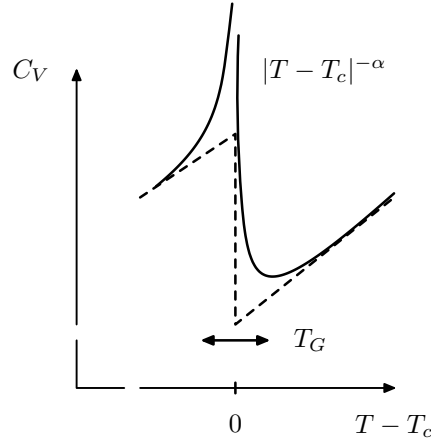
Fig. 2.8 Specific heat of a superconductor near to T_c in the gaussian approximation. The mean field Ginzburg-Landau theory gives a discontinuity at T_c. ut this is supplemented by a thermal fluctuation contribution which diverges like $|T - T_c|^{-\alpha}$ with $\alpha = 1/2$. The full renormalization group treatment (ignoring magnetic field terms) shows that α is given by the three-dimensional XY model value, exactly as in superfluid helium shown in Fig. **??**.

Fig. 2.9 Experimental heat capacity of the high temperature superconductor $YBa_2Cu_3O_{7-\delta}$ near to T_c. In zero magnetic field the experimental data fits very well the predictions of the three dimensional XY model. An external magnetic field (inset) removes the singularity, but does not visibly reduce T_c significantly. Reproduced from Overend, Howson and Lawrie (1994), with permission.
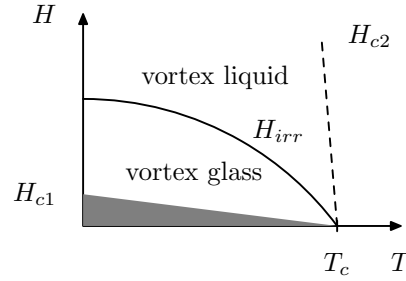
Fig. 2.10 Proposed magnetic phase diagram of some high T_c superconductors. Below H_{c2} vortices form, but are in a liquid state, leading to finite resistance of the superconductor. Below the 'irreversibility line" the vortices freeze (either into a glassy or quasi periodic flux lattice). In this state resistivity is still finite, due to flux creep, but becomes negligible far below the irreversibility line. H_{c1} is extremely small.
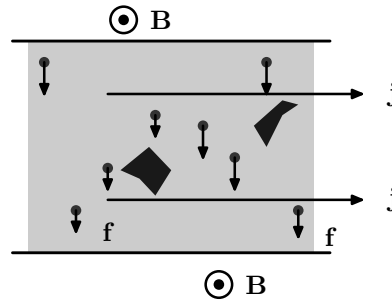
Fig. 2.11 Energy dissipation due to vortex flow in superconductors. Every vortex experiences a Lorentz (Magnus) force perpendicular to the supercurrent direction. This causes the vortices to drift sideways across the wire, unless pinned by defects. For each vortex which crosses the wire from one side to the other, a certain amount of work is done, and energy is dissipated.
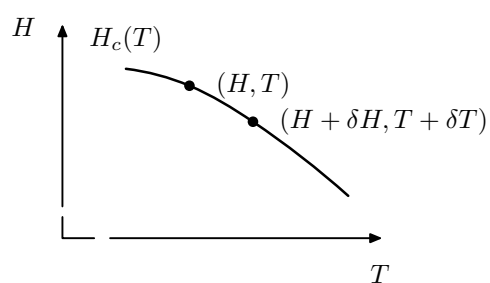
Fig. 2.12 Exercise 4.1. Consider the Gibbs free energy at the points shown on the normal-superconducting phase boundary of a type I superconductor, (T, H) and $T + \delta T, H + \delta H$). At both points equilibrium requires that both normal and superconducting Gibbs free energies must be equal: $G_n(T, H) = G_s(T, H)$.

3

The Macroscopic Coherent State

3.1 Introduction

We have seen in the previous chapters that the concept of the macroscopic wave function,$\psi(\mathbf{r})$, is central to understanding atomic Bose-Einstein condensates, superfluid ^4He, and even superconductivity within the the Ginzburg-Landau theory. But the connection between these ideas is not at all clear, since the atom condensates and ^4He are bosonic systems, while while superconductivity is associated with the conduction electrons in metals which are fermions. The physical meaning of the Ginzburg-Landau order parameter was not at all clear until after 1957 when Bardeen Cooper and Schrieffer (BCS) published the first truly microscopic theory of superconductivity. Soon afterwards the connection was finally established by Gorkov. He was able to show that, at least in the range of temperatures near T_c, the Ginzburg Landau theory can indeed be derived from the BCS theory. Furthermore this provides a physical interpretation of the nature of the order parameter. Essentially is is describing a macroscopic wave function, or condensate, of Cooper pairs.

The purpose of this chapter is to clarify the concept of a macroscopic wave function, and show how it arises naturally from the physics of **coherent states**. Coherent states were first developed in the field of quantum optics, and were especially useful in the theory of the laser. The laser is, of course, yet another type of macroscopic coherent state, with close similarities to atomic BEC. In this chapter we shall first introduce the concept and mathematical properties of coherent states before applying them to bosonic systems. Using this approach we shall rederive the Gross-Pitaevskii equations for the weakly interacting bose gas, as originally introduced above in Chapter 1.

Coherent states can be defined for fermions as well as for bosons. But single fermion coherent states, while very useful in other contexts, are not directly useful in the theory of superconductivity. What is needed is a coherent state of **fermion pairs**. Such coherent states are exactly the type of many-body quantum state first written down in the theory of Bardeen Cooper and Schrieffer in their 1957 theory of superconductivity. We shall

postpone a full discussion of this BCS theory until the following chapter. Here we focus specifically on the physics of the BCS coherent state, without worrying, for example, about why it is a stable ground state. . This separation has the advantage that the key concepts can be presented more clearly and they can be seen to be very general. Indeed it is not necessary to rely on every detail of the BCS theory in order to understand physically the properties of the quantum coherent state. In this approach we can also see very generally the connection between the BCS state and the Ginzburg-Landau theory, since the coherent state of electron pairs provides a direct connection to the order parameter $\psi(\mathbf{r})$.

This logical separation between the full detail of the BCS theory and the physical origin of the order parameter is not just an educational device; it also has a useful purpose more generally. For example, there are several superconductors where we do not know if the BCS theory is applicable, the high T_c superconductors being the most obvious example. However, even though we do not know the **mechanism of pairing** we do know that these systems do have Cooper pairs. For example they have flux quantization in the usual units of $\Phi_0 = h/2e$, showing that the fundamental charge unit is $2e$. We can also assume that there will be a Ginzburg-Landau order parameter whatever the actual pairing mechanism, and this knowledge will provide a sound basis for many theories of the superconducting state (eg theories of the vortex matter states in high T_c superconductors). We can therefore separating the actual mechanism of pairing from its main consequence: the existence of the order parameter.

3.2 Coherent states

To start with, let us just go back to some elementary undergraduate quantum mechanics: the quantum Harmonic oscillator. The Hamiltonian operator is

$$\hat{H} = \frac{\hat{p}^2}{2m} + \frac{m\omega_c^2}{2}x^2 \tag{3.1}$$

where $\hat{p} = i\hbar\frac{d}{dx}$ is the one-dimensional momentum operator, m is the particle mass and ω_c is the classical oscillator angular frequency. The eigenstates and of the oscillator are given by

$$\hat{H}\psi_n(x) = E_n\psi_n(x), \tag{3.2}$$

with energy levels E_n.

The most elegant method of solving this classic problem, to find E_n and $\psi_n(x)$ is to introduce the **ladder operators**,

$$\hat{a}^+ \quad = \quad \frac{1}{(\hbar\omega_c)^{1/2}}\left(\frac{\hat{p}}{(2m)^{1/2}} - i\frac{(m\omega_c^2)^{1/2}x}{(2)^{1/2}}\right)$$

$$\hat{a}^+ \;=\; \frac{1}{(\hbar\omega_c)^{1/2}} \left(\frac{\hat{p}}{(2m)^{1/2}} + i\frac{(m\omega_c^2)^{1/2}x}{(2)^{1/2}} \right). \tag{3.3}$$

These operators have a number of very useful and easily derived properties,[1] which can be summarized as follows:

$$\hat{a}^+ \psi_n(x) \;=\; (n+1)^{1/2}\psi_{n+1}(x) \tag{3.4}$$

$$\hat{a}\psi_n(x) \;=\; (n)^{1/2}\psi_{n-1}(x) \tag{3.5}$$

$$\hat{a}^+\hat{a}\psi_n(x) \;=\; n\psi_n(x) \tag{3.6}$$

$$\left[\hat{a},\hat{a}^+\right] \;=\; 1. \tag{3.7}$$

The first of these relations shows that the operator $\hat{a}^+$ changes any state to the next one higher up the "ladder" of the possible n values. Similarly second shows that $\hat{a}$ moves down the ladder. From the third relation, the combination $\hat{a}^+\hat{a}$ results in no change of n. Therefore Eq. 3.6 shows that we can identify the combination $\hat{n} = \hat{a}^+\hat{a}$ as the **number operator**, which gives the quantum number n of any state,

$$\hat{n}\psi_n(x) = n\psi_n(x). \tag{3.8}$$

The commutator relation, Eq. 3.7,

$$[\hat{a},\hat{a}^+] = \hat{a}\hat{a}^+ - \hat{a}^+\hat{a} = 1 \tag{3.9}$$

is fundamental to the quantumm mechanics of bosonic systems, as we shall see below.

In terms of the latter operators the oscillator Hamiltonian is given by,

$$\hat{H} = \hbar\omega_c \left(\hat{a}^+\hat{a} + \frac{1}{2} \right). \tag{3.10}$$

Combined with Eq. 3.6 it immediately shows that the energy levels are

$$E_n = \hbar\omega_c \left(n + \frac{1}{2} \right). \tag{3.11}$$

exactly as expected.

Using the ladder raising operator, $\hat{a}^+$ repeatedly, Eq. shows that one can construct all of the eigenvectors, $\psi_n(x)$, iteratively by acting repeatedly on an initial ground state $\psi_0(x)$,

$$\psi_n(x) = \frac{1}{(n!)^{1/2}}(\hat{a}^+)^n\psi_0(x). \tag{3.12}$$

Therefore to find the complete set of states it is only necessary to find $\psi_0(x)$ (which elementary quantum mechanics tells us is a simple gaussian

---

[1]See excercise 5.1.

function), and then all of the remaining quantum states can be generated essentially automatically.

But the ladder operators also have many other uses. In particular let us define a **coherent state** by,

$$|\alpha\rangle = C\left(\psi_0(x) + \frac{\alpha}{1!^{1/2}}\psi_1(x) + \frac{\alpha^2}{2!^{1/2}}\psi_2(x) + \frac{\alpha^3}{3!^{1/2}}\psi_3(x) + \ldots\right) \quad (3.13)$$

where α is any arbitrary complex number, and C is a normalization constant. This constant C can be found easily from the normalization condition

$$
\begin{aligned}
1 &= \langle\alpha|\alpha\rangle \\
&= |C|^2\left(1 + \frac{|\alpha|^2}{1!} + \frac{(|\alpha|^2)^2}{2!} + \frac{(|\alpha|^2)^3}{3!} + \ldots\right) \\
&= |C|^2 e^{|\alpha|^2} \quad\quad\quad\quad\quad\quad\quad\quad\quad\quad\quad\quad (3.14)
\end{aligned}
$$

and so we can take $C = e^{-|\alpha|^2/2}$.

Coherent states have many interesting properties. The following expression is a particularly useful relation

$$|\alpha\rangle = e^{-|\alpha|^2/2}\left(1 + \frac{\alpha\hat{a}^+}{1!} + \frac{(\alpha\hat{a}^+)^2}{2!} + \frac{(\alpha\hat{a}^+)^3}{3!} +\right)|0\rangle \quad (3.15)$$

where $|0\rangle = \psi_0(x)$ is the ground state and is also the coherent state with $\alpha = 0$. This expression can be written very compactly as,

$$|\alpha\rangle = e^{-|\alpha|^2/2}\exp\left(\alpha\hat{a}^+\right)|0\rangle. \quad (3.16)$$

Note that the exponential of any operator, $\hat{X}$ is just defined by the usual series expansion of exponential

$$\exp\left(\hat{X}\right) = 1 + \frac{\hat{X}}{1} + \frac{\hat{X}^2}{2!} + \frac{\hat{X}^3}{3!} + \ldots \quad (3.17)$$

Another interesting relation which can be obtained from Eq. 3.13 is

$$\hat{a}|\alpha\rangle = \alpha|\alpha\rangle \quad (3.18)$$

therefore they are eigenstates of the ladder operator $\hat{a}$. To prove this we can write the state $\hat{a}|\alpha\rangle$ explicitly

$$\hat{a}|A\rangle = e^{-|\alpha|^2/2}\hat{a}\left(\psi_0(x) + \frac{\alpha}{1!^{1/2}}\psi_1(x) + \frac{\alpha^2}{2!^{1/2}}\psi_2(x) + \frac{\alpha^3}{3!^{1/2}}\psi_3(x) + \ldots\right). \quad (3.19)$$

But $\hat{a}\psi_n(x) = n^{1/2}\psi_{n-1}(x)$ and so this gives

$$\hat{a}|\alpha\rangle = e^{-|\alpha|^2/2}\left(0 + \frac{\alpha 1^{1/2}}{1!^{1/2}}\psi_0(x) + \frac{\alpha^2 2^{1/2}}{2!^{1/2}}\psi_1(x) + \frac{\alpha^3 3^{1/2}}{3!^{1/2}}\psi_2(x) + \ldots\right) \quad (3.20)$$

which is clearly equal to $\alpha|\alpha\rangle$.

Finally, two further nice properties are also simple consequences of Eq. 3.18,

$$\langle \alpha | \hat{a} | \alpha \rangle = \alpha \tag{3.21}$$
$$\langle \alpha | \hat{a}^+ \hat{a} | \alpha \rangle = |\alpha|^2. \tag{3.22}$$

Therefore the value of $|\alpha|^2$ gives the mean number operator $\langle \hat{n} \rangle$ of the quantum state. Extending this to $\hat{n}^2$ we can find the number uncertainty Δn,

$$
\begin{aligned}
\langle \hat{n}^2 \rangle &= \langle \alpha | \hat{a}^+ \hat{a} \hat{a}^+ \hat{a} | \alpha \rangle \\
&= \langle \alpha | \hat{a}^+ (\hat{a}^+ \hat{a} + 1) \hat{a} | \alpha \rangle \\
&= |\alpha|^4 + |\alpha|^2 \\
\Delta n &= \sqrt{\langle \hat{n}^2 \rangle - \langle \hat{n} \rangle^2} \\
&= |\alpha|.
\end{aligned}
\tag{3.23}
$$
$$\tag{3.24}$$

Coherent states do not have a definite value of the quantum number n, simply because they are not eigenstates of the number operator. In fact the probability of observing the value of n in a quantum measurement of state $|\alpha\rangle$ is actually a Poisson distribution shown in Fig. 3.1

$$P_n = \frac{|\alpha|^{2n}}{n!} e^{-|\alpha|^2} \tag{3.25}$$

as can easily be seen from Eq. 3.13. In this distribution, as given by Eq. 3.24, the standard deviation in the number n is

$$\Delta n = \sqrt{\langle \hat{n} \rangle} \tag{3.26}$$

or

$$\frac{\Delta n}{\langle n \rangle} \sim \frac{1}{\sqrt{\langle n \rangle}}. \tag{3.27}$$

We shall be mostly interested in **macroscopic** coherent states, where $\langle n \rangle$ is essentially infinite. For such states, one can see that the standard deviation Δn becomes essentially negligible compared to $\langle n \rangle$. Therefore to a good approximation we can approximate many operator expectation values by their **mean-field** values derived from the replacement $\hat{n} \approx \langle n \rangle$. In Fig. 3.1 one can see that the distribution becomes strongly peaked about its mean value of $\langle n \rangle$ even for quite small values of $\langle n \rangle$.

Importantly, the coherent state $|\alpha\rangle$ does have a definite **phase**, θ, though not have a definite quantum number n. The coherent state can be defined for any complex number α,

$$\alpha = |\alpha| e^{i\theta}. \tag{3.28}$$

Rewriting Eq. 3.13 in terms of these variables we see that

$$|\alpha\rangle = C\left(\psi_0(x) + e^{i\theta}\frac{|\alpha|}{1!^{1/2}}\psi_1(x) + e^{2i\theta}\frac{|\alpha|^2}{2!^{1/2}}\psi_2(x) + + \dots\right). \qquad (3.29)$$

We see that the term containing ψ_n depends on $e^{in\theta}$. Differentiating with respect to θ one can see that

$$\frac{1}{i}\frac{\partial}{\partial\theta}|\alpha\rangle = \hat{n}|\alpha\rangle. \qquad (3.30)$$

But since the states $|\alpha\rangle$ are a complete set (actually an overcomplete set!), we can make the operator identification

$$\frac{1}{i}\frac{\partial}{\partial\theta} = \hat{n}. \qquad (3.31)$$

So the phase θ and the number n are **conjugate operators**, in a similar way to momentum and position in standard quantum mechanics. It is possible to state a form of the uncertainty principle for these operators[2]

$$\Delta n\Delta\theta \geq \frac{1}{2}. \qquad (3.32)$$

Coherent states have a fixed phase, but do not have definite values of number n. In contrast the energy eigenstates, $\psi_n(x)$, have a well defined value of n, but have an arbitrary (or ill-defined) phase.

Coherent states have many other beautiful mathematical properties, which we will not have time to explore in detail. In particular they are an overcomplete set, since they can be defined for any point in the complex α plane, and so there are uncountably infinite many such states. They are also not orthogonal, and it is easy to show that (exercise 5.2)

$$|\langle\alpha|\beta\rangle|^2 = e^{-|\alpha-\beta|^2}. \qquad (3.33)$$

We can interpret this in terms of the Argand diagram for the complex number α, shown in Fig. 3.2. Every point in the plane represents a valid coherent state. Coherent states at neighbouring points are not orthogonal, but their overlap dies off when $|\alpha - \beta| \sim 1$. Therefore there is effectively one "independent" orthogonal quantum state per unit area of the complex plane. Using polar coordinates, $|\alpha|, \theta$ we see that an element of area contains exactly one quantum state if

$$1 \sim |\alpha|\Delta\theta\Delta|\alpha| \qquad (3.34)$$

which is of order $2\Delta n\Delta\theta$, since $\langle n\rangle = |\alpha|^2$. Therefore the number-phase uncertainty principle gives essentially the minimum area per quantum state in the complex α plane of Fig. 3.2.

[2]A precise proof of this uncertainty relation is a little more tricky than the usual Heisenberg momentum-position uncertainty principle, since θ is only strictly defined in the range between 0 and 2π.

3.3 Coherent States and the Laser

Coherent were first studied extensively in the theory of the laser. In quantum optics the use of the operators $a_{\mathbf{k}s}^+$ and $a_{\mathbf{k}s}$ correspond directly to **creation** and **annihilation** of photons in a particular mode of electromagnetic radiation with wave number $\mathbf{k}$ and polarization s (i.e. left or right circularly polarized). A general quantum state of the system can be represented in the **occupation number representation**

$$|n_{\mathbf{k}_0 s_0}, n_{\mathbf{k}_1 s_1}, n_{\mathbf{k}_2 s_2}, n_{\mathbf{k}_3 s_3}, \ldots\rangle \tag{3.35}$$

where $\mathbf{k}_0$, $\mathbf{k}_1$, $\mathbf{k}_2$ etc. count all the different plane wave states of the system, eg the cavity of the laser.

In the case of light, the creation and annihilation operators arise quite naturally when one quantizes the electromagnetic radiation field. Each specific mode of the classical radiation field $\mathbf{k}$, s obeys Maxwell's equations. When these equations are quantized each mode becomes an independent quantum harmonic oscillator. The quantum states, $n_{\mathbf{k}s}$, of each oscillator are interpreted as the number of "photons" present. The creation operator adds a photon while the annihilation operator destroys one,[3]

$$a_{\mathbf{k}s}^+|\ldots n_{\mathbf{k}_s} \ldots\rangle = (n_{\mathbf{k}s}+1)^{1/2}|\ldots n_{\mathbf{k}_s}+1\ldots\rangle \tag{3.36}$$

$$a_{\mathbf{k}s}|\ldots n_{\mathbf{k}_s} \ldots\rangle = (n_{\mathbf{k}_s})^{1/2}|\ldots n_{\mathbf{k}_s} \ldots\rangle, \tag{3.37}$$

in complete analogy with the harmonic oscillator ladder operators. From these one can deduce that the same commutation law as the ladder operators must apply. But the operators for independent radiation field modes must commute, and therefore we can write,

$$\left[a_{\mathbf{k}_s}, a_{\mathbf{k}'s'}^+\right] = \delta_{\mathbf{k}s,\mathbf{k}'s'} \tag{3.38}$$

$$\left[a_{\mathbf{k}s}, a_{\mathbf{k}'s'}\right] = 0 \tag{3.39}$$

$$\left[a_{\mathbf{k}s}^+, a_{\mathbf{k}'s'}^+\right] = 0. \tag{3.40}$$

In the case of the laser we can naturally shift from the occupation number representation to a coherent state representation. A general coherent state is of the form

$$|\alpha_{\mathbf{k}_0 s_0}, \alpha_{\mathbf{k}_1 s_1}, \alpha_{\mathbf{k}_2 s_2}, \alpha_{\mathbf{k}_3 s_3}, \ldots\rangle \equiv e^{-\sum |\alpha_{\mathbf{k}s}|^2/2} \exp\left(\sum_{\mathbf{k}s} \alpha_{\mathbf{k}s} a_{\mathbf{k}_s}^+\right)|0\rangle. \tag{3.41}$$

Here $|0\rangle$ is the vacuum state, with no photons present. An ideal coherent laser source is one in which just one of these modes has a macroscopic occupation, $\langle \hat{n}_{\mathbf{k}s} \rangle = |\alpha_{\mathbf{k}s}|^2$ while the others have essentially zero occupation.

---

[3]For convenience we will no longer write these as $\hat{a}^+$ and $\hat{a}$, but just as a^+ and a. No ambiguity will arise from this simplified notation, but one must not forget that these are operators and do not commute.

In practical lasers, usually a few closely spaced **k** modes become macroscopically excited, and the system can randomly jump from locking onto one mode to another due to the no n-linear optical pumping which maintains the macroscopic mode occupation. It is the frequency of these jumps and the finite range of **k** values which limits the otherwise prefect optical coherence of a typical laser light source. See Loudon (1979) for a more detailed discussion of optical coherent states and their application to the laser.

3.4 Bosonic Quantum Fields

In this section we shall introduce **quantum field operators** for the case of boson particles. This will allow us to consider the quantum states of atomic BEC and superfluid ^{4}He. The BEC is a **weakly interacting** Bose system, while ^{4}He, as discussed in chapter 2, is a strongly interacting liquid of boson particles. At the same time we shall also see how the coherent state concept can also be applied to boson particles. This will enable us to define the macroscopic wave function $\psi(\mathbf{r})$ which we need in order to describe the condensate of particles. In this way we can generalize the simple intuitive approach of chapters 1 and 2 into something which is both systematic and rigorous.

Understanding BEC and superfluids obviously requires us to work with many-particle quantum states for very large numbers of particles. In elementary quantum mechanics we would write a Schrödinger equation for a wave function of N particles, in order to obtain an N body wave function

$$\Psi(\mathbf{r}_1, \mathbf{r}_2, \ldots, \mathbf{r}_N). \tag{3.42}$$

As discussed in Chapters 1 and 2, if we consider a system of N interacting Bose atoms then we could in principle write a wave function $\psi(\mathbf{r}_1, \ldots, \mathbf{r}_N)$ obeying the 3N-dimensional Schrödinger equation

$$\hat{H}\Psi(\mathbf{r}_1, \ldots, \mathbf{r}_N) = E\Psi(\mathbf{r}_1, \ldots, \mathbf{r}_N) \tag{3.43}$$

where

$$\hat{H} = \sum_{i=1,N} \left(\frac{\hbar^2}{2m} \nabla_i^2 + V_1(\mathbf{r}) \right) + \frac{1}{2} \sum_{i,j=1,N} V(\mathbf{r}_i - \mathbf{r}_j). \tag{3.44}$$

Here $V_1(\mathbf{r})$ is the external potential, and $V(\mathbf{r})$ is the particle-particle interaction. In the case of ^{4}He this interaction could be taken as the Lennard-Jones potential of two helium atoms, Eq. **??** or Eq. **??**, while for an atomic BEC we would use the delta function interaction of Eq. **??**. The fact that the particles are bosons is expressed by the fact the the wave function must be symmetric under permutation of any two of the particle coordinates

$$\psi(\ldots \mathbf{r}_i, \ldots, \mathbf{r}_j \ldots) = \psi(\ldots \mathbf{r}_j, \ldots, \mathbf{r}_i \ldots) \tag{3.45}$$

representing an exchange of the identical particles at $\mathbf{r}_i$ and $\mathbf{r}_j$.

This approach is feasible for systems with a few particles, such as say the electrons in an atom, but it quickly becomes impractical in larger systems. A much more useful method is to adopt the methods of quantum field theory and introduce **field operators** which add or remove particles to the system. If we consider a single particle in a box we know that the wave functions are plane wave states

$$\psi_{\mathbf{k}}(\mathbf{r}) = \frac{1}{(V)^{1/2}} e^{i\mathbf{k}.\mathbf{r}} \tag{3.46}$$

where V is the volume. We saw in chapter 1 that each of these single particle states can be occupied by 0, 1, 2, 3 or any other finite number of Bose particles. We denote these possible by the occupation number, $n_{\mathbf{k}}$. A general quantum many body state of the system will be a superposition of different N-body plane wave states. The complete basis of all possible states can be represented by the set of all possible occupation numbers of each plane wave. In exact analogy with the case of the laser we can creation and annihilation operators $a_{\mathbf{k}}^+$ and $a_{\mathbf{k}}$ which increase or decrease these occupation numbers. In order to satisfy the Bose symmetry condition on the wave function, Eq. 3.45 it turns out that it is necessary that

$$[a_{\mathbf{k}}, a_{\mathbf{k}}^+] = 1.$$

For two different plane wave states the occupation numbers are independent, and hence the creation operators must commute. Therefore the complete set of commutation relations are exactly as given in Eqs. 3.38-3.40. Similarly the occupation operator is given by the number operator,

$$\hat{n}_{\mathbf{k}} = a_{\mathbf{k}}^+ a_{\mathbf{k}} \tag{3.47}$$

These relations completely define the boson quantum field operators.

The set of many-particle states with all possible number operators, $\{n_{\mathbf{k}}\}$, is a complete set of wave functions. But, just as in the case of the harmonic oscillator, we can generate any $n_{\mathbf{k}}$ by successive actions of the operators $a_{\mathbf{k}}^+$, starting with a ground state $|0\rangle$. The interpretation is different now. $|0\rangle$ is the **vacuum state**, i.e. a state with no particles present. Successive actions of $a_{\mathbf{k}}^+$ add more particles to the system. Any many particle quantum state can be represented by a superposition of states generated in this way.

These field operators can also be cast into a real space form. We can define the quantum field operators $\hat{\psi}^+(\mathbf{r})$ and $\hat{\psi}(\mathbf{r})$ which create and annihilate particles at point $\mathbf{r}$. These can be defined by a Fourier transform of the $\mathbf{k}$ space operators,

$$\hat{\psi}(\mathbf{r}) = \frac{1}{\sqrt{V}} \sum_{\mathbf{k}} e^{i\mathbf{k}.\mathbf{r}} a_{\mathbf{k}} \tag{3.48}$$

$$\hat{\psi}^+(\mathbf{r}) \quad = \quad \frac{1}{\sqrt{V}} \sum_{\mathbf{k}} e^{-i\mathbf{k}.\mathbf{r}} a_{\mathbf{k}}^+. \tag{3.49}$$

The function $e^{i\mathbf{k}.\mathbf{r}}/\sqrt{V}$ here is obviously just a free particle plane wave in quantum state, $\mathbf{k}$. The inverse Fourier transforms are

$$\hat{a}_{\mathbf{k}} \quad = \quad \frac{1}{\sqrt{V}} \int e^{-i\mathbf{k}.\mathbf{r}} \hat{\psi}(\mathbf{r}) d^3r \tag{3.50}$$

$$\hat{a}_{\mathbf{k}}^+ \quad = \quad \frac{1}{\sqrt{V}} \int e^{i\mathbf{k}.\mathbf{r}} \hat{\psi}^+(\mathbf{r}) d^3r \tag{3.51}$$

Using these definitions and the Bose commutation law, one can show (exercise 5.4) that these real-space field operators have the commutation laws,

$$\left[\hat{\psi}(\mathbf{r}), \hat{\psi}^+(\mathbf{r}')\right] \quad = \quad \delta(\mathbf{r} - \mathbf{r}') \tag{3.52}$$

$$\left[\hat{\psi}(\mathbf{r}), \hat{\psi}(\mathbf{r}')\right] \quad = \quad 0 \tag{3.53}$$

$$\left[\hat{\psi}^+(\mathbf{r}), \hat{\psi}^+(\mathbf{r}')\right] \quad = \quad 0. \tag{3.54}$$

We can also represent any operator in terms of its actions on quantum states described in terms of these operators. In particular the Hamiltonian, Eq. 3.44 becomes

$$\hat{H} \quad = \quad \int \left(\hat{\psi}^+(\mathbf{r}) \left[\frac{\hbar^2}{2m}\nabla^2 + V_1(\mathbf{r})\right] \hat{\psi}(\mathbf{r})\right) d^3r$$
$$+\frac{1}{2} \int V(\mathbf{r} - \mathbf{r}')\hat{\psi}^+(\mathbf{r})\hat{\psi}(\mathbf{r})\hat{\psi}^+(\mathbf{r}')\hat{\psi}(\mathbf{r}') d^3r d^3r'. \tag{3.55}$$

where the combination $\hat{\psi}^+(\mathbf{r})\hat{\psi}(\mathbf{r})$ is obviously the density operator of particles at $\mathbf{r}$.

It turns out to be convenient to always work in "normal order", in which all the creation operators are on the left and all the annihilation operators are on the left. Commuting two of the field operators above we obtain

$$\hat{H} \quad = \quad \int \left(\hat{\psi}^+(\mathbf{r}) \left[\frac{\hbar^2}{2m}\nabla^2 + V_1(\mathbf{r})\right] \hat{\psi}(\mathbf{r})\right) d^3r$$
$$+\frac{1}{2} \int V(\mathbf{r} - \mathbf{r}')\hat{\psi}^+(\mathbf{r})\hat{\psi}^+(\mathbf{r}')\hat{\psi}(\mathbf{r})\hat{\psi}(\mathbf{r}') d^3r d^3r'$$
$$+\frac{1}{2} \int V(\mathbf{r} - \mathbf{r}')\hat{\psi}^+(\mathbf{r})\delta(\mathbf{r} - \mathbf{r}')\hat{\psi}(\mathbf{r}') d^3r d^3r' \tag{3.56}$$

The final term here arises from the commutator of $[\hat{\psi}(\mathbf{r}), \hat{\psi}^+(\mathbf{r}')]$, and reduces to

$$V(0) \int d^3r \hat{\psi}^+(\mathbf{r})\hat{\psi}(\mathbf{r}) = V(0)\hat{N} \tag{3.57}$$

where

$$\hat{N} = \int d^3r \hat{\psi}^+(\mathbf{r})\hat{\psi}(\mathbf{r}) \tag{3.58}$$

is obviously just the operator for the total number of particles in the system. The $\hat{N}V(0)$ term is a constant can be absorbed into the definition of the chemical potential, μ, and so we shall drop it from now on.

For a bulk fluid we can assume translational invariance, and ignore the external potential $V_1(\mathbf{r})$. Going back to $\mathbf{k}$-space and we can use the Fourier transforms Eqs. 3.48 and 3.49 to represent the Hamiltonian in terms of $a_{\mathbf{k}}^+$ and $a_{\mathbf{k}}$. The kinetic energy term is

$$
\begin{aligned}
\hat{T} &= -\int \left(\hat{\psi}^+(\mathbf{r})\frac{\hbar^2}{2m}\nabla^2\hat{\psi}^+(\mathbf{r}) \right) d^3r \\
&= \frac{1}{V}\sum_{\mathbf{kk}'} \int \left(a_{\mathbf{k}'}^+ e^{-i\mathbf{k}'\cdot\mathbf{r}}\frac{\hbar^2k^2}{2m}a_{\mathbf{k}}e^{i\mathbf{k}\cdot\mathbf{r}} \right) d^3r \\
&= \sum_{\mathbf{k}} \frac{\hbar^2k^2}{2m}a_{\mathbf{k}}^+ a_{\mathbf{k}}.
\end{aligned}
\tag{3.59}
$$

The potential energy term is

$$
\begin{aligned}
\hat{V} &= \frac{1}{2}\int V(\mathbf{r}-\mathbf{r}')\hat{\psi}^+(\mathbf{r})\hat{\psi}^+(\mathbf{r}')\hat{\psi}(\mathbf{r})\hat{\psi}(\mathbf{r}')d^3r d^3r' \\
&= \frac{1}{2V^2}\sum_{\mathbf{k_1 k_2 k_3 k_4}} \int V(\mathbf{r}-\mathbf{r}')a_{\mathbf{k_1}}^+ a_{\mathbf{k_2}}^+ a_{\mathbf{k_3}} a_{\mathbf{k_4}} \\
&\qquad\qquad e^{i(-\mathbf{k_1}\cdot\mathbf{r}-\mathbf{k_2}\cdot\mathbf{r}'+\mathbf{k_3}\cdot\mathbf{r}'+\mathbf{k_4}\cdot\mathbf{r})}d^3r d^3r' \\
&= \frac{1}{2V}\sum_{\mathbf{k_1 k_2 k_3 k_4}} a_{\mathbf{k_1}}^+ a_{\mathbf{k_2}}^+ a_{\mathbf{k_3}} a_{\mathbf{k_4}} \delta_{\mathbf{k_3}+\mathbf{k_4},\mathbf{k_1}+\mathbf{k_2}} \int V(\mathbf{r})e^{i(\mathbf{k_4}-\mathbf{k_1})\cdot\mathbf{r}}d^3r.
\end{aligned}
$$

Introducing the Fourier transform of the interaction

$$V_{\mathbf{q}} = \frac{1}{V}\int V(r)e^{i\mathbf{q}\cdot\mathbf{r}}d^3r \tag{3.60}$$

and making the replacements $\mathbf{k}_1 \rightarrow \mathbf{k} + \mathbf{q}$, $\mathbf{k}_2 \rightarrow \mathbf{k}' - \mathbf{q}$, $\mathbf{k}_3 \rightarrow \mathbf{k}'$, and $\mathbf{k}_4 \rightarrow \mathbf{k}$ we can express the full Hamiltonian as

$$\hat{H} = \sum_{\mathbf{k}} \frac{\hbar^2k^2}{2m}a_{\mathbf{k}}^+ a_{\mathbf{k}} + \frac{1}{2}\sum_{\mathbf{kk}'\mathbf{q}} V_{\mathbf{q}} a_{\mathbf{k}+\mathbf{q}}^+ a_{\mathbf{k}'-\mathbf{q}}^+ a_{\mathbf{k}'} a_{\mathbf{k}}. \tag{3.61}$$

We can interpret the interaction term simply as a process in which a pair of particles are scattered from initial states $\mathbf{k}$, $\mathbf{k}'$ to final states $\mathbf{k} + \mathbf{q}$, $\mathbf{k}' - \mathbf{q}$. The momentum transferred between the particles is $\mathbf{q}$, and the matrix element for the process is $V_{\mathbf{q}}$.

3.5 Off-Diagonal Long Ranged order

The field operators introduced in the previous section provide a general way to discuss quantum coherence in condensates and superfluids. Even though Eq. 3.61 is still too difficult to solve in general, we can still use it explore the consequences of macroscopic quantum coherence in bosonic systems.

Firstly, let us revisit the idea of the macroscopic quantum state, as introduced for BEC and superfluid ^{4}He in chapters 1 and 2. Using the field operators we can redefine the one-particle density matrix as

$$\rho_1(\mathbf{r} - \mathbf{r}') \equiv \langle \hat{\psi}^+(\mathbf{r})\hat{\psi}(\mathbf{r}') \rangle. \tag{3.62}$$

This definition is clearly more compact than the equivalent one given in Chapter 2. Using the Fourier transformations Eqs. 3.48 and 3.49 we find

$$
\begin{aligned}
\rho_1(\mathbf{r} - \mathbf{r}') &= \frac{1}{V} \sum_{\mathbf{k}\mathbf{k}'} e^{i(\mathbf{k}'.\mathbf{r}' - \mathbf{k}.\mathbf{r})} \langle a_{\mathbf{k}}^+ a_{\mathbf{k}'} \rangle \\
&= \frac{1}{V} \sum_{\mathbf{k}} e^{-i(\mathbf{k}.(\mathbf{r} - \mathbf{r}'))} \langle a_{\mathbf{k}}^+ a_{\mathbf{k}} \rangle,
\end{aligned}
\tag{3.63}
$$

which is just the Fourier transform of the momentum distribution

$$n_{\mathbf{k}} \equiv \langle a_{\mathbf{k}}^+ a_{\mathbf{k}} \rangle \tag{3.64}$$

exactly as found in chapter 2.

Now let us consider the consequences of these definitions in the case of a quantum coherent many-particle state. Just as in the case of the laser, we can define a coherent state

$$|\alpha_{\mathbf{k}_1}, \alpha_{\mathbf{k}_2}, \alpha_{\mathbf{k}_3} \ldots\rangle$$

for any set of complex numbers $\alpha_{\mathbf{k}_i}$. Using the standard properties of coherent states we find

$$n_{\mathbf{k}} \equiv \langle |\alpha_{\mathbf{k}}|^2 \rangle \tag{3.65}$$

and hence

$$\rho_1(\mathbf{r} - \mathbf{r}') = \frac{1}{V} \sum_{\mathbf{k}} e^{-i\mathbf{k}.(\mathbf{r} - \mathbf{r}')} |\alpha_{\mathbf{k}}|^2. \tag{3.66}$$

Typically we will be interested in quantum states where only one of the $\mathbf{k}$ states is macroscopically occupied, (usually but not always $\mathbf{k} = 0$). So suppose that state $\mathbf{k}_0$ has occupation $N_0 = |\alpha_{\mathbf{k}_0}|^2$ where N_0 is a macroscopic number (a finite fraction of the total particle number N) and all the other $|\alpha_{\mathbf{k}_i}|^2$ are small. For such a state we will have the momentum distribution

$$n_{\mathbf{k}} = N_0 \delta_{\mathbf{k},\mathbf{k}_0} + f(\mathbf{k}) \tag{3.67}$$

where $f(\mathbf{k}$ is a smooth function of $\mathbf{k}$. The corresponding density matrix is

$$\rho_1(\mathbf{r} - \mathbf{r}') = n_0 + \frac{2}{(2\pi)^3} \int d^3k \, e^{-i\mathbf{k}.(\mathbf{r} - \mathbf{r}')} f(\mathbf{k}) \tag{3.68}$$

where $n_0 = N_0/V$.

These results are exactly the same as we found in chapter 2 by more elementary methods. The presence of the condensate is shown by the constant contribution, n_0 to the density matrix. If the function $f(\mathbf{k}$ is sufficiently smooth, then its Fourier transform will vanish for large $|\mathbf{r} - \mathbf{r}'|$ leaving just the constant contribution,

$$\langle \hat{\psi}^+(\mathbf{r})\hat{\psi}(\mathbf{r}')\rangle \to n_0 \tag{3.69}$$

as $|\mathbf{r} - \mathbf{r}'| \to \infty$. This is what is meant by the term **off diagonal long ranged order** (ODLRO), introduced by Oliver Penrose.

Fig. 3.3 shows the physical interpretation of the ODLRO in superfluids. A particle can be annihilated at $\mathbf{r}$, and absorbed into the condensate, while a second particle is created at $\mathbf{r}'$ out of the condensate. This process has a quantum mechanical amplitude because of the quantum coherence of the condensate, even when the points $\mathbf{r}$ and $\mathbf{r}'$ are separated arbitrarily far apart. In contrast, for a normal liquid (even a normal quantum liquid) these processes would be incoherent except when $\mathbf{r}$ and $\mathbf{r}'$ are close together.

Using the coherent state concept, there is one more step which we can take. If the density matrix

$$\langle \hat{\psi}^+(\mathbf{r})\hat{\psi}(\mathbf{r}')\rangle \tag{3.70}$$

is a constant, however far apart points $\mathbf{r}$ and $\mathbf{r}'$ are, then is seems plausible that we can treat the points as independent statistically. Then we can view the above as an average of a product of independent random variables and hence write is as a product of the two averages computed separately

$$\langle \hat{\psi}^+(\mathbf{r})\hat{\psi}(\mathbf{r}')\rangle \to \langle \hat{\psi}^+(\mathbf{r})\rangle\langle \hat{\psi}(\mathbf{r}')\rangle \tag{3.71}$$

for $|\mathbf{r} - \mathbf{r}'| \to \infty$.

If we were to work in the standard fixed particle number, N, many-body formulation of quantum mechanics then averages such as $\langle \hat{\psi}^+(\mathbf{r})\rangle$ would be automatically zero, since acting on any N particle state $\hat{\psi}^+(\mathbf{r})|N\rangle$ is an $N + 1$ particle state, and is necessarily orthogonal to $\langle N|$. But if we are working in the basis of coherent states, then there is no such problem. The coherent states have definite phase, not definite N, and this type of expectation value is perfectly well allowed.

Therefore we can say that there is an **order parameter** or **macroscopic wave function**, defined by

$$\psi_0(\mathbf{r}) = \langle \hat{\psi}(\mathbf{r})\rangle. \tag{3.72}$$

In term of this function we see that[4]

$$\rho_1(\mathbf{r} - \mathbf{r}') = \psi_0^*(\mathbf{r})\psi_0(\mathbf{r}') \tag{3.73}$$

---

[4]The creation operator $\hat{\psi}^+(\mathbf{r})$ is just the Hermitian conjugate of $\hat{\psi}(\mathbf{r})$ and so $\psi_0^*(\mathbf{r}) = \langle \hat{\psi}^+(\mathbf{r})\rangle$.

for $|\mathbf{r} - \mathbf{r}'| \to \infty$. In a translationally invariant system (the condensation occurs in the $\mathbf{k} = 0$ state), we must therefore have

$$\psi_0(\mathbf{r}) = \sqrt{n_0}e^{i\theta} \tag{3.74}$$

where θ is an arbitrary constant phase angle.

Of course this phase θ is nothing more than the XY model phase angle introduced in chapter 2, Fig. **??**. But now we can see that its true meaning is that we have a coherent quantum state in which the $\mathbf{k} = 0$ state has a macroscopic occupation.

Since we have not yet made any connection to the Hamiltonian, Eq. 3.61 it is impossible to prove from these arguments that such a coherent quantum state will be stable. But at least we can see how to construct coherent many-particle wave functions in which a definite order parameter phase θ is possible. possible. In the case of the ideal Bose condensate discussed in chapter 1 one can still work in the fixed particle number representation, and so there is no advantage to explicitly introduce a coherent state formalism. But as soon as there are any interactions, however weak, the coherent state approach becomes advantageous. In the next section we shall consider the weakly interacting bose gas, in which the advantages of the coherent state approach can be seen explicitly.

3.6   The Weakly Interacting Bose Gas

The theory of the **weakly interacting Bose gas** was originally developed by Bogoliubov in in late 1940's. It was developed as a theory of superfluid helium, although as we have seen, for ^{4}He the interatomic interactions are very strong. In this case the theory has some qualitative features which agree with experimental properties of ^{4}He, most notably the linear phonon like quasiparticle excitation spectrum, $\epsilon_{\mathbf{k}} = ck$, at small wave vectors in fig. **??**. But it fails to reproduce other important features, such as the roton minimum in the spectrum. On the other hand, the theory is believed to be close to exact for the case of atomic BEC, since the conditions under which it is derived are close to the experimental ones.

First of all we shall assume that we are at zero temperature, or close to zero, so that the system is close to its ground state. We assume that the system is in a coherent many-particle state, characterized by a macroscopic wave function $\psi_0(\mathbf{r}$, as in Eq. 3.72. Suppose that the many-particle quantum state $,|\psi\rangle$, is an ideal coherent state at zero temperature. Then it is an eigenstate of the annihilation operator,

$$\hat{\psi}(\mathbf{r})|\psi\rangle = \psi_0(\mathbf{r})|\psi\rangle. \tag{3.75}$$

We can view this as a trial many-particle wave function, and we will vary the parameter $\psi_0(\mathbf{r})$ so as to variationally minimize the total energy. The

variational energy is found by taking the expectation value of the Hamiltonian,

$$
\begin{aligned}
\hat{H} &= \int \hat{\psi}^+(\mathbf{r}) \left(-\frac{\hbar^2 \nabla^2}{2m} + V_1(\mathbf{r}) \right) \hat{\psi}(\mathbf{r}) d^3r \\
&\quad + \frac{1}{2} \int V(\mathbf{r} - \mathbf{r}') \hat{\psi}^+(\mathbf{r}) \hat{\psi}^+(\mathbf{r}') \hat{\psi}(\mathbf{r}) \hat{\psi}(\mathbf{r}') d^3r d^3r'.
\end{aligned} \quad (3.76)
$$

Here the single particle potential $V_1(\mathbf{r})$ is the effective external potential of the atom trap. In the case of bulk superfluids this is obviously zero.

Using the definition of the coherent state $|\psi\rangle$ from Eq. 3.75 we can find immediately that the variational energy is

$$
\begin{aligned}
E_0 &= \langle \psi | \hat{H} | \psi \rangle \\
&= \int \psi_0^*(\mathbf{r}) \left(-\frac{\hbar^2 \nabla^2}{2m} + V_1(\mathbf{r}) \right) \psi_0(\mathbf{r}) d^3r \\
&\quad + \frac{1}{2} \int V(\mathbf{r} - \mathbf{r}') \psi_0^*(\mathbf{r}) \psi_0^*(\mathbf{r}') \psi_0(\mathbf{r}) \psi_0(\mathbf{r}') d^3r d^3r'.
\end{aligned} \quad (3.77)
$$

We can find the minimum by functional differentiation, exactly as for the Ginzburg-Landau equation. Setting

$$
\frac{\partial E_0}{\partial \psi_0^*(\mathbf{r})} = 0
$$

yields,

$$
\left(-\frac{\hbar^2 \nabla^2}{2m} + V_1(\mathbf{r}) - \mu \right) \psi_0(\mathbf{r}) + \int V(\mathbf{r} - \mathbf{r}') \psi_0(\mathbf{r}) \psi_0^*(\mathbf{r}') \psi_0(\mathbf{r}') d^3r' = 0.
$$
$$(3.78)$$

The parameter μ is a Lagrange multiplier, necessary to maintain a constant normalization of the macroscopic wave function

$$
N_0 = \int |\psi_0(\mathbf{r})|^2 d^3r. \quad (3.79)
$$

Clearly Eq. 3.78 is of the form of an effective Schrödinger equation

$$
\left(-\frac{\hbar^2 \nabla^2}{2m} + V_1(\mathbf{r}) + V_{eff}(\mathbf{r}) - \mu \right) \psi_0(\mathbf{r}) = 0 \quad (3.80)
$$

where μ is the chemical potential, and the effective potential is

$$
V_{eff}(\mathbf{r}) = \int V(\mathbf{r} - \mathbf{r}') |\psi_0^*(\mathbf{r}')|^2 . d^3r'
$$

This Schrödinger equation is exactly the Gross-Pitaevski equation again, which we derived by a different method in chapter 2.

To examine the accuracy of this ground state, and to examine the low energy excited states, we need to consider possible quantum states which are close to our trial ground state $|\psi\rangle$, but which do not deviate from it too much. We need to consider many-particle states which do not exactly obey the coherent state conduction, Eq. 3.75, but for which it is nearly obeyed. Bogoliubov introduced an elegant method so achieve this. He assumed that the field operators can be expressed approximately as their constant coherent state value, plus a small deviation,

$$\hat{\psi}(\mathbf{r}) = \psi_0(\mathbf{r}) + \delta\hat{\psi}(\mathbf{r}). \tag{3.81}$$

From the commutation relations for the field operators, it is easy to see that

$$[\delta\hat{\psi}(\mathbf{r}), \delta\hat{\psi}^+(\mathbf{r}')] = \delta(\mathbf{r} - \mathbf{r}'), \tag{3.82}$$

and so the deviation operators $\delta\hat{\psi}(\mathbf{r})$ and $\delta\hat{\psi}^+(\mathbf{r})$ are also bosonic quantum fields.[5] We can then rewrite the hamiltonian in terms of $\psi_0(\mathbf{r})$ and $\delta\hat{\psi}(\mathbf{r})$. We can group terms according to whether $\delta\hat{\psi}(\mathbf{r})$ occurs never, once, twice, three times or four,

$$\hat{H} = \hat{H}_0 + \hat{H}_1 + \hat{H}_2 + \ldots \tag{3.83}$$

and we assume that it is valid to simply ignore terms higher than second order.

In this expansion, the first term, $\hat{H}_0$ is simply the original coherent state energy, Eq. 3.77 which we can minimize using the Gross-Piaevskii equations. Furthermore, if we have variationally minimized the energy there will be no corrections to the energy to linear order in the deviation operators $\delta\hat{\psi}(\mathbf{r})$. the first significant correction term is quadratic in the deviation operators. Several terms contribute, but the net result is that

$$
\begin{aligned}
\hat{H}_2 &= \int \delta\hat{\psi}^+(\mathbf{r}) \left(-\frac{\hbar^2 \nabla^2}{2m} + V_1(\mathbf{r}) \right) \delta\hat{\psi}(\mathbf{r}) d^3r \\
&+ \frac{1}{2} \int V(\mathbf{r} - \mathbf{r}') d^3r d^3r' \left(\delta\hat{\psi}^+(\mathbf{r}) \delta\hat{\psi}^+(\mathbf{r}') \psi_0(\mathbf{r}) \psi_0(\mathbf{r}') \right. \\
&+ 2\delta\hat{\psi}^+(\mathbf{r}) \psi_0^*(\mathbf{r}') \delta\hat{\psi}(\mathbf{r}) \psi_0(\mathbf{r}') + 2\psi_0^*(\mathbf{r}) \delta\hat{\psi}^+(\mathbf{r}') \delta\hat{\psi}(\mathbf{r}) \psi_0(\mathbf{r}') \\
&+ \left. \psi_0^*(\mathbf{r}) \psi_0^*(\mathbf{r}') \delta\hat{\psi}(\mathbf{r}) \delta\hat{\psi}(\mathbf{r}') \right).
\end{aligned} \tag{3.84}
$$

One can visualize the meaning of these various terms in terms of the simple diagrams shown in Fig. 3.4. There are four distinct terms. The first, shown in panel (a), corresponds to the creation of two particles, one at $\mathbf{r}$ and $\mathbf{r}'$ under the action of the potential $V(\mathbf{r} - \mathbf{r}')$. Of course they are

---

[5]A different way to see this is to imagine that we simply translate the origin of the coherent state complex plane, Fig. 3.2. Shifting the origin from $\alpha = 0$ to $\alpha = \psi_0(\mathbf{r})$ we can then describe states which are near to $|\psi\rangle$ in terms of the coherent states α which are in the vicinity of the point $\psi_0(\mathbf{r})$.

not really created, but scattered out of the condensate. The second term corresponds to the scattering of an existing quasiparticle by interaction with particles in the condensate. It has a extra factor of 2 since we can find an identical diagram with $\mathbf{r}$ and $\mathbf{r}'$ interchanged. The third diagram (c) is also a scattering of an existing quasiparticle, but now the quasiparticle at $\mathbf{r}$ is absorbed into the condensate, while at the same time a second quasiparticle appears at $\mathbf{r}'$. Again $\mathbf{r}$ and $\mathbf{r}'$ can be interchanged. leading to an extra factor of 2. The final diagram, (d), shows two quasiparticles being absorbed into the condensate.

To keep the algebra manageable let us specialize to the case (relevant for the atomic BEC) of a pure contact interaction,

$$V(\mathbf{r} - \mathbf{r}') = g\delta(\mathbf{r} - \mathbf{r}'). \tag{3.85}$$

For convenience we will also assume that $\psi_0(\mathbf{r})$ is real, and equal to $\psi_0(\mathbf{r}) = \sqrt{n_0(\mathbf{r})}$, where $n_0(\mathbf{r})$ the spatially varying condensate density in the atom trap. The quadratic Hamiltonian $\hat{H}_2$ simplifies to

$$
\begin{aligned}
\hat{H}_2 &= \int \delta\hat{\psi}^+(\mathbf{r})\left(-\frac{\hbar^2\nabla^2}{2m} + V_1(\mathbf{r}) - \mu\right)\delta\hat{\psi}(\mathbf{r})d^3r \\
&\quad + \frac{g}{2}\int n_0(\mathbf{r})\left(\delta\hat{\psi}^+(\mathbf{r})\delta\hat{\psi}^+(\mathbf{r}) + 4\delta\hat{\psi}^+(\mathbf{r})\delta\hat{\psi}(\mathbf{r}) + \delta\hat{\psi}(\mathbf{r})\delta\hat{\psi}(\mathbf{r})\right)d^3r.
\end{aligned}
\tag{3.86}
$$

This Hamiltonian is a quadratic form in the operators, and it turns out that all such quadratic Hamiltonians can be diagonalized exactly. The procedure makes use of the **Bogoliubov** transformation to eliminate the "anomalous" terms $\delta\hat{\psi}(\mathbf{r})\delta\hat{\psi}(\mathbf{r})$ and $\delta\hat{\psi}^+(\mathbf{r})\delta\hat{\psi}^+(\mathbf{r})$. Define a new pair of operators by

$$
\begin{aligned}
\hat{\varphi}(\mathbf{r}) &= u(\mathbf{r})\delta\hat{\psi}(\mathbf{r}) + v(\mathbf{r})\delta\hat{\psi}^+(\mathbf{r}) \tag{3.87} \\
\hat{\varphi}^+(\mathbf{r}) &= u^*(\mathbf{r})\delta\hat{\psi}^+(\mathbf{r}) + v^*(\mathbf{r})\delta\hat{\psi}(\mathbf{r}). \tag{3.88}
\end{aligned}
$$

These are again bosonic quantum field operators if

$$\left[\hat{\varphi}(\mathbf{r}), \hat{\varphi}^+(\mathbf{r})\right] = \delta(\mathbf{r} - \mathbf{r}'), \tag{3.89}$$

which is true provided that the functions $u(\mathbf{r})$ and $v(\mathbf{r})$ are chosen to obey

$$|u(\mathbf{r})|^2 - |v(\mathbf{r})|^2 = 1. \tag{3.90}$$

The general solution becomes quite complicated, so let us specialize to the case of a uniform Bose liquid, without the atom trap potential $V(\mathbf{r})$. Assuming that the macroscopic wave function is also just a constant, $\psi_0 = \sqrt{n_0}$, and going to $\mathbf{k}$-space Eq. 3.86 becomes

$$\hat{H}_2 = \sum_{\mathbf{k}}\left((\frac{\hbar^2k^2}{2m} - \mu)a_{\mathbf{k}}^+a_{\mathbf{k}} + \frac{n_0g}{2}(a_{\mathbf{k}}^+a_{-\mathbf{k}}^+ + 4a_{\mathbf{k}}^+a_{\mathbf{k}} + a_{-\mathbf{k}}a_{\mathbf{k}})\right). \tag{3.91}$$

The Bogoliubov transformation in k-space gives the new operators

$$b_{\mathbf{k}} = u_{\mathbf{k}}a_{\mathbf{k}} + v_{\mathbf{k}}a_{-\mathbf{k}}^+ \tag{3.92}$$

$$b_{\mathbf{k}}^{+} \quad = \quad u_{\mathbf{k}}^{*} a_{\mathbf{k}} + v_{\mathbf{k}}^{*} a_{-\mathbf{k}} \tag{3.93}$$

where $u_{\mathbf{k}}$ and $v_{\mathbf{k}}$ obey

$$|u_{\mathbf{k}}|^2 - |v_{\mathbf{k}}|^2 = 1. \tag{3.94}$$

The idea is to rewrite the Hamiltonian in terms of these new operators and then to vary the parameters $u_{\mathbf{k}}$ and $v_{\mathbf{k}}$ to make it diagonal. In particular it is necessary to make the coefficients of the anomalous terms, $b_{\mathbf{k}}^{+} b_{-\mathbf{k}}^{+}$ and $b_{-\mathbf{k}} b_{\mathbf{k}}$ equal to zero. Since the calculation is lengthy we shall just quote the results. It turns out that when the anomalous terms are eliminated, the new quasiparticle excitations created by the $b_{\mathbf{k}}^{+}$ operators have the energy spectrum

$$E_{\mathbf{k}} = \left(\frac{\hbar^2 k^2}{2m} \right)^{1/2} \left(\frac{\hbar^2 k^2}{2m} + 2n_0 g \right)^{1/2} . \tag{3.95}$$

For small $|\mathbf{k}|$ (less than $\sim \sqrt{4n_0 g m}/\hbar$) the spectrum is linear

$$E_{\mathbf{k}} \sim ck \tag{3.96}$$

where the "phonon" velocity is

$$c = \left(\frac{\hbar^2 n_0 g}{m} \right)^{1/2} . \tag{3.97}$$

This Bogoliubov quasiparticle spectrum is sketched in Fig. 3.5. The spectrum is linear at small $\mathbf{k}$, and joins smoothly onto the independent particle energy $\hbar^2 k^2/2m$ for large $\mathbf{k}$. The success of this Bogoliubov theory is that it explains the linear dispersion in the excitation spectrum near to $\mathbf{k} = 0$, as we saw in the case of superfluid ^{4}He, Fig. **??**. In chapter 2 we have also seen that a linear spectrum is necessary to prevent quasiparticle scattering from the container walls, and hence to maintain a dissipationless superflow. Therefore we can conclude that even a very weakly interacting Bose gas is a superfliud, even when the ideal non-interacting Bose gas is not. The critical velocity for the superfluid will be less than c, and so by Eq. 3.97 the critical velocity will approach zero in the limits of weak interaction $g \to 0$, or low density $n_0 \to 0$.

Of course there are still huge differences between the Bogoliubov quasiparticle spectrum in Fig. 3.5 and the experimental quasiparticle spectrum of Fig. **??**. Most importantly, there is no roton minimum. The Bogoliubov spectrum is linear at small $\mathbf{k}$ and becomes equal to the free particle spectrum $\hbar^2 k^2/2m$ for large $\mathbf{k}$, but it has no minimum at intermediate $\mathbf{k}$. The roton minimum is therefore an effect emerging only in a strongly interacting Bose liquid. This difference has another effect, namely that the Bogoliubov spectrum $E_{\mathbf{k}}$ has a slight upwards curvature at small $\mathbf{k}$, while the true spectrum has a slight downward curvature. This curvature means that a quasiparticle of momentum $\hbar \mathbf{k}$ and energy $E_{\mathbf{k}}$ has a non-zero cross section

to decay into three quasiparticles of lower energy and momentum. Therefore the Bogoliubov quasiparticle is not an exact eigenstate, but only a long lived resonance.[6]

3.7 Coherence and ODLRO in Superconductors

The above ideas were originally introduced to explain the strongly interacting Bose superfluid ^{4}He. But they also apply to superconductors. However in this case the argument must be modified in order to take account of the fact that the electrons in a superconductor are fermions. Although it is perfectly possible to define coherent states for fermions, they are not immediately useful for superconductivity. This is because a single fermion state can only ever be occupied by either 0 or 1 fermions, due to the exclusion principle. Therefore it is not possible to have a macroscopic number of fermions in a single plane wave state.

It was Robert Schrieffer who first managed to write down a coherent many-particle wave function for fermions. His colleauges Bardeen and Cooper had already realized that electrons bind into pairs in a superconductor. There was even an earlier theory by Schafroth Blatt and Butler in which superconductivity was seen as a Bose condensate of electron pairs.[7] But Bardeen Cooper and Schrieffer (BCS) knew that the pairs of electrons in superconductors could not be simply treated as bosons. The problem was to write down a valid many-body wave function for the electrons in which each electron participate in the pairing. The brilliant solution Schrieffer discovered was effectively another type of coherent state, similar to those we have already seen. But the key point is to have a coherent state in which a macroscopic number of **pairs** are all in the same state.

Nevertheless even in the BCS theory we have a form of ORLRO and an order parameter, as we shall discover in this section. Their appearance is a quite general phenomenon. Here we concentrate on the most general statements about the ODLRO, and leave the actual details of the BCS theory, and its specific predictions until the next chapter.

---

[6]It makes perfect sense here to borrow the concepts of elementary particle physics, and to talk about one particle decaying into a set of others. Just as in particle physics we can call such 'particles' resonances. In this context the Bogoliubov quasiparticles are just the 'elementary particles' of the Bose gas, and the background condensate is the analog of the vacuum.

[7]Unfortunately this theory was not able to make quantitative predictions for the superconductors which were known at that time, and it was generally discarded in favour of the Bardeen Cooper Schrieffer theory which was very much more successful in making quantitative predictions. The electron pairs in the Bardeen Cooper and Schrieffer theory **are not bosons**. In general a pair of fermions is not equivalent to a boson. In the BCS case the bound electon pairs are very large, and so different pairs strongly overlap each other. In this limit it is not possible to describe the pair as a boson, and so the BCS theory is not normally expressed in terms of bose condensation. However in recent years theories based upon the ideas of the Schafroth, Blatt and Butler theory have been somewhat revived as a possible models of high T_c superconductors.

First we must define the correct quantum field operators to describe the conduction electrons in a solid. In single-particle quantum mechanics of solids we know that the wave functions are Bloch waves

$$\psi_{n\mathbf{k}}(\mathbf{r}) = e^{i\mathbf{k}.\mathbf{r}} u_{n\mathbf{k}}(\mathbf{r}). \tag{3.98}$$

Here the crystal wave vector $\mathbf{k}$ must lie within the first Brillouin zone. For simplicity of notation we shall assume that only one of the energy bands, n, is relevant (i.e. the one at the Fermi surface) and so we will drop the index n from now on.

A particular Bloch state of a given spin σ, $\psi_{\mathbf{k}\sigma}(\mathbf{r})$, can either be empty or occupied by an electron. A quantum state of N particles can be specified by saying for each individual state whether it is occupied or not. This is **the occupation number representation** of quantum mechanics. We can introduce operators which change these occupation numbers. Suppose we label the state as $|0\rangle$ or $|1\rangle$ if the given Bloch state $\psi_{\mathbf{k}\sigma}(\mathbf{r})$. Then we can define operators which change the occupation numbers

$$\begin{aligned} c^+|0\rangle &= |1\rangle \\ c|1\rangle &= |0\rangle. \end{aligned}$$

These are obviously similar to the similar Bose field operators, or the Harmonic oscillator ladder operators, $\hat{a}^+$ and $\hat{a}$. The only difference is that the state of a harmonic oscillator can have $n = 0, 1, 2, \ldots$, while for fermions the occupation number is only 0 or 1. The operators c^+ and c are again called the creation' and annihilation' operators. Since electrons are neither being created or annihilated in solids these names may seem a bit misleading, however the operators work the same way in particle physics where particles are indeed being created or annihilated back into the vacuum (eg. electron-positron pairs annihilating each other). In a solid one can imagine adding electrons to the solid (e.g. with an external current source into the surface), or removing them from the solid (eg. in photo-emission).

These operators have a couple of important properties. Firstly, just as for bosons, the combination c^+c measures the occupation number $|n\rangle$ since

$$\begin{aligned} c^+c|0\rangle &= 0 \\ c^+c|1\rangle &= |1\rangle \end{aligned}$$

i.e. $c^+c|n\rangle = n|n\rangle$. Secondly the exclusion principle implies that we cannot occupy a state with more than one fermion, and hence $c^+c^+|n\rangle = 0$ and $cc|n\rangle = 0$. This fermion nature of the particles means that

$$\{c, c^+\} \equiv cc^+ + c^+c = 1 \tag{3.99}$$

where $\{A, B\} = AB + BA$ is the **anti-commutator** of operators A and B. The antisymmetry of the many-particle wave function for fermions means

that the operators for different Bloch states or spin states **anti-commute**, and so in general we have the anti-commutation relations,

$$\{c_{\mathbf{k}\sigma}, c^+_{\mathbf{k}'\sigma'}\} = \delta_{\mathbf{k}\sigma,\mathbf{k}'\sigma'} \qquad (3.100)$$

$$\{c_{\mathbf{k}\sigma}, c_{\mathbf{k}'\sigma'}\} = 0 \qquad (3.101)$$

$$\{c^+_{\mathbf{k}\sigma}, c^+_{\mathbf{k}'\sigma'}\} = 0 \qquad (3.102)$$

where $\sigma = \pm 1$ denotes the two different spin states. Naturally, just as for bosons, we can also represent these operators in real space, by a Fourier transformation, obtaining

$$\{\hat{\psi}_\sigma(\mathbf{r}), \hat{\psi}^+_{\sigma'}(\mathbf{r}')\} = \delta(\mathbf{r} - \mathbf{r}')\delta_{\sigma\sigma'} \qquad (3.103)$$

$$\{\hat{\psi}_\sigma(\mathbf{r}), \hat{\psi}_{\sigma'}(\mathbf{r}')\} = 0 \qquad (3.104)$$

$$\{\hat{\psi}^+_\sigma(\mathbf{r}), \hat{\psi}^+_{\sigma'}(\mathbf{r}')\} = 0. \qquad (3.105)$$

In some sense this is also like a Bose condensate of the Cooper pairs. However because the fermion antisymmetry is fully taken account of the wave function leads to quite different predictions than one might just expect with a Bose condensation picture. The BCS predictions turned out to be extremely accurate numerically, despite it being a simplified mean-field model wave function. Its accuracy lies in the large size of the Cooper pairs, with their characteristic size ξ (the coherence length) being much larger than the typical inter-electron spacings in a solid r_s, where $N/V = n = 4\pi r_s^3/3$.

Now the mathematical challenge which BCS needed to solve was to write down a many-particle wave function in which every electron near the Fermi surface participates in the pairing. They knew that a single pair of electrons would bind into a spin singlet state with two body wave function

$$\Psi(\mathbf{r}_1\sigma_1, \mathbf{r}_2\sigma_2) = \varphi(\mathbf{r}_1 - \mathbf{r}_2)\frac{1}{\sqrt{2}}\left(\left|\uparrow\downarrow\right\rangle - \left|\downarrow\uparrow\right\rangle\right) \qquad (3.106)$$

They first wrote down a many-particle wave function in which every particle is paired,

$$\Psi(\mathbf{r}_1\sigma_1, \ldots, \mathbf{r}_N\sigma_N) = \frac{1}{\sqrt{N!}}\sum_P (-1)^P \Psi(\mathbf{r}_1\sigma_1, \mathbf{r}_2\sigma_2)\Psi(\mathbf{r}_3\sigma_3, \mathbf{r}_4\sigma_4)\ldots$$
$$\ldots \Psi(\mathbf{r}_{N-1}\sigma_{N-1}, \mathbf{r}_N\sigma_N). \qquad (3.107)$$

Here the sum over P denotes the sum over all the $N!$ permutations of the N particle labels $\mathbf{r}_1\sigma_1$, $\mathbf{r}_2\sigma_2$ etc. The sign $(-1)^P$ is positive for an even permutation and -1 for odd permutations. This alternating sign is necessary so that the many-body wave function has the correct fermion antisymmetry

$$\Psi(\ldots, \mathbf{r}_i\sigma_i, \ldots, \mathbf{r}_j\sigma_j, \ldots) = -\Psi(\ldots, \mathbf{r}_j\sigma_j, \ldots, \mathbf{r}_i\sigma_i, \ldots). \qquad (3.108)$$

But this fixed N many-body quantum mechanics is unwieldy. By fixing N we cannot have a definite overall phase, unlike in a coherent state representation. But if we use coherent states then it is possible to describe a condensate with a definite phase, and the key step achieved by Schrieffer was to find a way to write down a coherent state of fermion pairs. First we need to write down operators which create or annihilate pairs of electrons. Defining,

$$\hat{\varphi}^+(\mathbf{R}) \equiv \int d^3r \int \varphi(\mathbf{r})\hat{\psi}_\uparrow^+(\mathbf{R}+\mathbf{r}/2)\hat{\psi}_\downarrow^+(\mathbf{R}-\mathbf{r}/2). \qquad (3.109)$$

we can see that acting with this operator on a quantum state with N electrons gives a new quantum state with $N+2$ electrons. It creates a spin singlet electron pair, where the electrons are separated by $\mathbf{r}$ and with centre of mass at $\mathbf{R}$.[8]

Naively one might regard such a fermion pair as a boson. But this is not correct. If we try to evaluate the commutator we find that

$$\left[\hat{\varphi}(\mathbf{R}), \hat{\varphi}^+(\mathbf{R}')\right] \;\neq\; \delta(\mathbf{R}-\mathbf{R}') \qquad (3.110)$$

$$\left[\hat{\varphi}(\mathbf{R}), \hat{\varphi}(\mathbf{R}')\right] \;\neq\; 0 \qquad (3.111)$$

$$\left[\hat{\varphi}^+(\mathbf{R}), \hat{\varphi}^+(\mathbf{R}')\right] \;\neq\; 0. \qquad (3.112)$$

The operators only commute when $\mathbf{R}$ and $\mathbf{R}'$ are far apart, corresponding to non-overlapping pairs. For this reason we cannot simply make a Bose condensate out of these pairs.

But even though these are not true boson operators, we can still define the analogue of ODLRO corresponding to Bose condensation. Now it **is** a state of ODLRO of **Cooper pairs**. We can define a new density matrix by,

$$\rho_1(\mathbf{R}-\mathbf{R}') = \langle \hat{\varphi}^+(\mathbf{R}), \hat{\varphi}(\mathbf{R}') \rangle. \qquad (3.113)$$

This is a one particle density matrix for pairs, and so it is related to the two particle density matrix for the electrons

$$\rho_2(\mathbf{r}_1\sigma_1, \mathbf{r}_2\sigma_2, \mathbf{r}_3\sigma_3, \mathbf{r}_4\sigma_4) = \langle \hat{\psi}_{\sigma_1}^+(\mathbf{r}_1)\hat{\psi}_{\sigma_2}^+(\mathbf{r}_2)\hat{\psi}_{\sigma_3}(\mathbf{r}_3)\hat{\psi}_{\sigma_4}^+(\mathbf{r}_4) \rangle. \qquad (3.114)$$

Inserting the definition of the pair operator gives the pair density matrix in terms of the electron one

$$\rho_1(\mathbf{R}-\mathbf{R}') = \int \varphi(\mathbf{r})\varphi(\mathbf{r}')\rho_2(\mathbf{R}+\frac{\mathbf{r}}{2}\uparrow, \mathbf{R}-\frac{\mathbf{r}}{2}\downarrow, \mathbf{R}'-\frac{\mathbf{r}'}{2}\downarrow, \mathbf{R}'+\frac{\mathbf{r}'}{2}\uparrow)d^3rd^3r'. \qquad (3.115)$$

The pair wave function $\varphi(\mathbf{r})$ is a quantum mechanical bound state, and so it will become zero for large $|\mathbf{r}|$. If the scale of its range is defined by a length,

---

[8]Note that we assume here that the wave function for the bound electron pair obeys $\varphi(\mathbf{r}) = \varphi(-\mathbf{r})$. This is simply because a spin singlet bound state wave function must be even under exchange of particle coordinates, because the spin single state is odd under exchange.

ξ_0, (which turns out to be the BCS coherence length of the superconductor), then the the main contributions to the pair density matrix comes from the parts of electron density matrix where $\mathbf{r}_1$ and $\mathbf{r}_2$ are separated by less than ξ_0, and similarly $\mathbf{r}_3$ and $\mathbf{r}_4$ are separated by less than ξ_0. But the pair $\mathbf{r}_1,\mathbf{r}_2$ and the pair $\mathbf{r}_3,\mathbf{r}_4$ can be separated by any arbitrarily large distance.

Now we can can have ODLRO in the pair density matrix, provided that

$$\rho_1(\mathbf{R} - \mathbf{R}') \rightarrow const. \tag{3.116}$$

as $|\mathbf{R} - \mathbf{R}'| \rightarrow \infty$. The BCS theory does therefore correspond to a similar macroscopic quantum coherence to the ordinary theory of ODLRO in super-fluids. However is is an ODLRO of Cooper pairs, not single electrons.

In terms of the electron density matrix $\rho_2(\mathbf{r}_1\sigma_1, \mathbf{r}_2\sigma_2, \mathbf{r}_3\sigma_3, \mathbf{r}_4\sigma_4)$ this ODLRO corresponds to the density matrix approaching a constant value in a limit where the two coordinates $\mathbf{r}_1$ and $\mathbf{r}_2$ are close to each other, and $\mathbf{r}_3$ and $\mathbf{r}_4$ are close, but these two pairs are separated by an arbitrarily large distance. Fig. 3.6 illustrates this concept.

Following the same approach to ODLRO as in the weakly interacting Bose gas, we can make the assumption that very distant points $\mathbf{R}$ and $\mathbf{R}'$ should behave independently. Therefore we should be able to write

$$\rho_1(\mathbf{R} - \mathbf{R}') \sim \langle \hat{\varphi}^+(\mathbf{R}) \rangle \langle \hat{\varphi}(\mathbf{R}') \rangle \tag{3.117}$$

for $|\mathbf{R} - \mathbf{R}'| \rightarrow \infty$. We can therefore also define a **macroscopic wave function** by

$$\psi(\mathbf{R}) = \langle \hat{\varphi}(\mathbf{R}) \rangle. \tag{3.118}$$

Effectively this is the **Ginzburg-Landau order parameter** for the superconductor.

Of course, we have still not actually shown how to construct a many-electron quantum state which would allow this type of Cooper pair ODLRO. We leave that until the next chapter. Nevertheless we can view the above discussion as stating the requirements for the sort of quantum state which could exhibit superconductivity. It was possibly the most significant achievement of the BCS theory that it was possible to explicitly construct such a non-trivial many-body quantum state. In fact we can see immediately from Eq. 3.118 that we must have a coherent state with a definite quantum mechanical phase θ, and conversely that we should not work with fixed particle number N. At the time of the original publication of the BCS theory in 1957 this aspect was one of the most controversial of the whole theory. The explicit appearance of the phase θ also caused concern, since it appeared to violate the principle of gauge invariance. It was only the near perfect agreement between the predictions of the BCS theory and experiments, as well as clarification of the gauge invariance issue by Anderson and others which led to the final acceptance of the BCS theory.

3.8 The Josephson Effect

The Josephson effect is a direct physical test of the quantum coherence implied by superconducting ODLRO. Soon after the BCS theory was published Brian Josephson, then a young PhD student at Cambridge, considered the effect of electrons tunnelling between two different superconductors.[9]

Consider two superconductors, separated by a thin insulating layer, as shown in Fig. 3.7. If each superconductor has a the macroscopic wave function as defined in, 3.118, then we can assign definite values to the wave functions on either side of the tunnel barrier, say ψ_L and ψ_R for the left and right hand side respectively,

$$\psi_L(\mathbf{R}_L) = \langle L|\hat{\varphi}(\mathbf{R}_L)|L\rangle$$
$$\psi_R(\mathbf{R}_R) = \langle R|\hat{\varphi}(\mathbf{R}_R)|R\rangle$$

where $\mathbf{R}_L$ and $\mathbf{R}_L$ are points on either side of the tunnel barrier, and $|L\rangle$ and $|R\rangle$ are the many-particle quantum states of the superconductors on the left and right side respectively. Josephson assumed that electron tunnelling takes place for electrons crossing the barrier. In terms of electron field operators we can write

$$\hat{H} = \sum_{\sigma} \int T(\mathbf{r}_L, \mathbf{r}_R)(\hat{\psi}_{\sigma}^+(\mathbf{r}_L)\hat{\psi}_{\sigma}(\mathbf{r}_R) + \hat{\psi}_{\sigma}^+(\mathbf{r}_R)\hat{\psi}_{\sigma}(\mathbf{r}_L)d^3r_L d^3r_R \quad (3.119)$$

as the operator which tunnels electrons of spin σ from points $\mathbf{r}_L$ and $\mathbf{r}_R$ on either side of the barrier. Using the BCS many-body wave functions on either side of the junction and second order perturbation theory in the tunnelling Hamiltonian $\hat{H}$, Josephson was able to find the remarkable result that a current flows in the junction, given by

$$I = I_c \sin(\theta_1 - \theta_2) \quad (3.120)$$

where θ_1 and θ_2 are the phases of the macroscopic wave functions on either side of the junction.

The details of how Josephson found this result will not be important here. But it is worth noting very roughly how this might come about. If we consider effects to second order in the tunnelling Hamiltonian $\hat{H}$ we can see that $\hat{H}^2$ contains many terms, but includes some four fermion terms of the following form,

$$\hat{H}^2 \sim T^2(\qquad \hat{\psi}_{\sigma}^+(\mathbf{r}_L)\hat{\psi}_{\sigma'}^+(\mathbf{r}_L')\hat{\psi}_{\sigma}(\mathbf{r}_R)\hat{\psi}_{\sigma'}(\mathbf{r}_R')$$

---

[9]Brian Josephson received the Nobel prize in 1973 for this discovery, possibly one of the few Nobel prizes to have arisen from a PhD project. After Josephon's first prediction of the effect in 1962, established experts in the superconductivity field at first objected to the theory, believing that the effect was either not present or would be too weak to observe. But Josephson's PhD adviser Anderson encouraged Rowell to look for the effect experimentally. Anderson and Rowell together announced the first observation of the Joephson effect in 1963.

$$+\hat{\psi}_\sigma^+(\mathbf{r}_R)\hat{\psi}_{\sigma'}^+(\mathbf{r}_R')\hat{\psi}_\sigma(\mathbf{r}_L)\hat{\psi}_{\sigma'}(\mathbf{r}_L') + \ldots). \qquad (3.121)$$

The net effect of the first of these terms is to transfer a pair of electrons from the right hand superconductor to the left. Conversely the second term transfers a pair from left to right. Because the many-body states on both sides of the junction are coherent pair states, these operators will have non-zero expectation values consistent with the ODLRO

$$\langle L|\hat{\psi}_\sigma^+(\mathbf{r}_L)\hat{\psi}_{\sigma'}^+(\mathbf{r}_L')|L\rangle \neq 0$$
$$\langle R|\hat{\psi}_\sigma(\mathbf{r}_R)\hat{\psi}_{\sigma'}^+(\mathbf{r}_R')|R\rangle \neq 0. \qquad (3.122)$$
$$(3.123)$$

In fact we expect the first of these expectation values proportional to $e^{-i\theta_1}$ and the second to $e^{i\theta_2}$. The overall quantum mechanical amplitude for tunnelling a pair from right to left is thus has a phase $e^{i(\theta_2-\theta_1)}$. The reverse process, tunnelling from left to right has the opposite phase. When they are added together the net current is proportional to $\sin(\theta_1 - \theta_2)$ as given by Eq. 3.120.

Eq. 3.120 shows that the current flows in response to the phase difference $\theta_1 - \theta_2$. Therefore it is in some sense a direct proof of the existence of such coherent state phases in superconductors. The proportionality constant I_c is the maximum Josephson current that can flow, and is called the **critical current** of the junction.

For currents I below I_c the Josephson current is perfectly dissipation-less, i.e. it is a supercurrent. But if current is driven to a higher value, $I > I_c$, a finite voltage drop V develops across the junction. Therefore the typical $I-V$ characteristic of the junction is as shown in Fig. 3.8.

In the case that $I > I_c$ Josephson found a second surprising consequence of this tunnel current. The finite voltage difference V between the superconductors, means that the macroscopic wave functions become time dependent. Using a version of the Heisenbeg equation of motion for the left and right hand side macroscopic wave functions,

$$i\hbar\frac{\partial\psi_L(t)}{\partial t} = -2eV_L\psi_L(t)$$
$$i\hbar\frac{\partial\psi_R(t)}{\partial t} = -2eV_R\psi_R(t), \qquad (3.124)$$

Josephson was able to show that the finite voltage drop $V = V_L - V_R$ leads to a steadily increasing phase difference,

$$\Delta\theta(t) = \Delta\theta(0) + \frac{2eV}{\hbar}t \qquad (3.125)$$

and hence the Josephson current,

$$I = I_c\sin\left(\Delta\theta(0) + \frac{2eV}{\hbar}t\right) \qquad (3.126)$$

oscillates at a frequency

$$\nu = \frac{2eV}{\hbar}. \tag{3.127}$$

This surprising effect is called the a.c. Joesphson effect (in contrast to the d.c. Josephson effect for $I < I_c$, $V = 0$).

The experimental observation of the a.c. Josephson effect not only confirmed the theory and the validity of the BCS macroscopic quantum coherent state, but also provided another direct empirical confirmation that the relevant particle charge is $2e$ and not e. Thus it again confirmed the Cooper pairing hypothesis. Even more surprising is that the Josephson frequency appears to be **exactly** given by Eg. 3.127. In fact, it is so accurate that the Josephson effect has been incorporated into the standard set of measurements used to define the SI unit system. By measuring the frequency (which can be measured with accuracies of one part in 10^{12} or better) and the voltage V one can obtain the ratio of fundamental constants $e/\hbar$ with high precision. Alternatively one can use the given values of $e/\hbar$ and the Josephson effect to define a reliable and portable voltage standard, V.

The Josephson effect is also at the heart of many different practical applications of superconductivity. One of the simplest devices to make is a SQUID ring; where SQUID stands for Superconducting QUantum Interference Device. This is simply a small (or large) superconducing ring in which there are two weak links. Each half of the ring is then connected to external leads, as shown in Fig. 3.9. By "weak link" one can mean either a tunnel barrier, such as Fig. 3.7 (an SIS junction), or a thin normal metallic spacer (an SNS junction). The current through each junction depends on the phase difference across it and so,

$$I = I_{c1} \sin\left(\Delta\theta_1\right) + I_{c2} \sin\left(\Delta\theta_2\right) \tag{3.128}$$

is the sum of the currents of each Josephson junction. The phases differences $\Delta\theta_1$, $\Delta\theta_2$ correspond to the macroscopic wave function phases differences at the points to the left and right of each junction in Fig. 3.9.

In the junctions are perfectly balanced, so $I_{c1} = I_{c2}$ and a small external current I ($< I_c$) is applied to the SQUID, then we would expect an equal steady state current to flow in both halves of the ring, and a constant phase difference equal to $\Delta\theta = \sin^{-1}\left(I/2I_c\right)$ will develop across both junctions. But this is only true if there is no magnetic flux through the ring. Using the principle of gauge invariance we find that a flux Φ implies that the phase differences are no longer equal.

$$
\begin{aligned}
\Phi &= \int \mathbf{B}.d\mathbf{S} \\
&= \oint \mathbf{A}.d\mathbf{r} \\
&= \frac{2e}{\hbar} \oint (\boldsymbol{\nabla}\theta).d\mathbf{r}
\end{aligned}
$$

$$\begin{aligned}
&= \frac{2e}{\hbar} \left(\Delta\theta_1 - \Delta\theta_2 \right) \\
&= 2\pi\Phi_0 \left(\Delta\theta_1 - \Delta\theta_2 \right).
\end{aligned} \tag{3.129}$$

Therefore the magnetic flux through the ring leads to a difference between the two phases. For a balanced SQUID ring system we can assume that

$$\begin{aligned}
\Delta\theta_1 &= \Delta\theta + \frac{\pi\Phi}{\Phi_0} \\
\Delta\theta_2 &= \Delta\theta - \frac{\pi\Phi}{\Phi_0}.
\end{aligned} \tag{3.130}$$

therefore the total current in the SQUID is

$$\begin{aligned}
I &= I_c \sin\left(\Delta\theta_1\right) + I_c \sin\left(\Delta\theta_2\right) \\
&= I_c \sin\left(\Delta\theta + \frac{\pi\Phi}{\Phi_0}\right) + I_c \sin\left(\Delta\theta - \frac{\pi\Phi}{\Phi_0}\right) \\
&= 2I_c \sin\left(\Delta\theta\right) \cos\left(\frac{\pi\Phi}{\Phi_0}\right).
\end{aligned} \tag{3.131}$$

The critical current is therefore modulated by a factor depending on the net flux through the ring,[10]

$$I_c(\Phi) = I_0 \left| \cos\left(\frac{\pi\Phi}{\Phi_0}\right) \right|. \tag{3.132}$$

This modulation of the observed SQUID ring critical current is shown in Fig. 3.10. This current is essentially an ideal Fraunhoffer interference pattern, exactly analogous to the interference pattern one observes in optics with Young's two slit experiment. Here the two Josephson junctions are playing the role of the two slits, and the interference is between the supercurrents passing through the two halves of the ring. The supercurrents acquire different phases due to the magnetic field. One can say that this effect is also analogous to the Ahronov Bohm effect (Feynman 1964), in which a single electron passes on either side of a of a solenoid of magnetic flux.

The SQUID device provides a simple, but highly accurate, system for measuring magnetic flux. Since the flux quantum Φ_0 is only about $2 \times 10^{-15}Wb$ in the SI unit system, and one can make SQUID devices approaching $1cm^2$ in area, it is in principle possible to measure magnetic fields to an accuracy below $B \sim 10^{-10}T$. In particular it is easy to measure **changes** in field to this accuracy by simply counting the number of minima in the SQUID critical current.

---

[10]The SQUID ring critical current will always have the same sign as the driving current and hence the modulus signs appearing in Eq. 3.132.

3.9 Macroscopic Quantum Coherence

To what extent does the Joesphson effect or the SQUID represent true evidence quantum coherence? Even though it is very cold, operating at a temperature below T_c, say at one or two degrees Kelvin, a SQUID ring is hardly isolated from its environment. In fact one can make perfectly good SQUIDs using high temperature superconductors. These operate at temperatures of over 100K. SQUID rings are usually fabricated on some sort of insulating substrate, and are usually subject to normal external electromagnetic noise in the laboratory, unless well shielded.

Given this relatively noisy thermal environment, the SQUID shows a remarkable insensitivity to these effects. This is fundamentally because the macroscopic wave function $\psi(\mathbf{r})$ which we have defined above, and its phase θ, is not a true wave function in the sense of elementary quantum mechanics. In particular it does not obey the fundamental **principle of superposition**, and one cannot apply the usual **quantum theory of measurement** or Copenhagen interpretation to it. The macroscopic wave function behaves much more like a thermodynamic variable, such as the magnetization in a ferromagnet, than a pure wave function, even though it has a phase and obeys local gauge invariance.

But since the early 1980's there have been attempts to observe true quantum superpositions in superconductors (Leggett 1980). I.e. can one construct a "Schrödinger cat" like quantum state? For example is a state such as

$$|\psi\rangle = \frac{1}{\sqrt{2}} \left(|\psi_1\rangle + |\psi_2\rangle \right) \tag{3.133}$$

meaningful in a SQUID ring? If $|\psi_1\rangle$ and $|\psi_2\rangle$ are two pure quantum states, then the general principle of linearity of quantum mechanics, implies that any superposition such as $|\psi\rangle$ must also be a valid quantum state. Only by measuring some observable can one "collapse" the wave function and find out whether the system was in $|\psi_1\rangle$ or $|\psi_2\rangle$. for small system, such as single atoms or photons, such superpositions are a standard part of quantum mechanics. But in his famous 1935 paper Schrödinger showed that this fundamental principle leads to paradoxes with our everyday understanding of the world when we apply it to macroscopic systems such as the famous cat in a box!

Even since Schrödinger's paper it has not been clear where to put the dividing line between the "macrosopic" world (governed by classical physics and without superposition) and the microscopic (governed by quantum mechanics). The ideas of **decoherence** provide one possible route by which quantum systems can acquire classical behaviour. Interactions with the environment lead to entanglement between the quantum sates of the system and those of the environment, and (in some of the most modern approaches) "quantum information" is lost.

In this context one can say that a large SQUID ring, say $1cm$ (or $100m$!) in diameter will be subject to decoherence from its environment, and hence

will be effectively in the classical realm. But if one makes the ring smaller, or operates at lower temperatures, is there a regime where true quantum superpositions occur? In fact the answer to this question is yes! Indeed strong evidence for quantum superposition states has now been seen in three different systems.

The first system where quantum superposition states were observed was in Bose-Einstein condensates, in 1996 (Ketterle 2002). Since these exist in a very low temperature state (a micro Kelvin or less) and are isolated from most external thermal noise sources (since they are trapped in vacuum) one could expect a high degree of quantum coherence to occur. Indeed it has proved possible to "split" a single condensate into two halves, in a similar way to which a beam splitter separates photons. When the two halves of the condensate are subsequently brought back together again, then one observes an interference pattern. The experiment is effectively the exact analogue of the Young's slit interference experiment with light.

The second type of experiment which showed true quantum interference was done using a superconducting island or "Cooper pair box". This consists of a small island of superconductor (Al was used) of order 0.1μm on a side, as shown in Fig. 3.12. Operating at temperatures of a few mK, well below the superconducting T_c, the quantum states of the box can be characterized entirely by the number of Cooper pairs present. For example the box can have a state $|N\rangle$ of N Cooper pairs, or a state $|N+1\rangle$ etc. The energies of these different states can be manipulated through external voltage gates, since they are states of different total electronic charge on the box. The analogue of the Schrodinger cat state for this system is to place it in a superposition, such as

$$|\psi\rangle = \frac{1}{\sqrt{2}}\left(|N\rangle + |N+1\rangle\right). \tag{3.134}$$

Nakamura Pashkin and Tsai (1999) were able to demonstrate the presence of just such superpositions in their device. By connecting the Cooper pair box to a second superconductor, via a Josephson junction, they effectively allowed quantum mechanical transitions between these two states, as Cooper pairs tunnel onto or off the island. By pulsing external voltage gates connected to the system they observed beautiful interference fringes associated with the superposition states, as shown in Fig. 3.13. The figure shows the final charge on the box (i.e. $N+1$ or N) as a function of the voltage pulse amplitude and duration. The results observed oscillations agree excellently with the theoretical predictions based on the existence of macroscopic quantum superposition states.

The third systems in which macroscopic quantum coherence has been demonstrated are small superconducting rings, as in Fig. 2.6. As we saw in chapter 3, a superconducting ring has a set of different ground states corresponding to different winding numbers of the order parameter around the ring. These can again be represented by abstract many-particle states

such as $|n\rangle$ and $|n+1\rangle$. In a large ring there will be no way for the system to tunnel from one of these states to another, but if the ring is made small enough (below 1μm in diameter) such transitions become possible. Two experiments in the year 2000 observed direct evidence for quantum mechanical coherence in such syaytems (van der Wal *et al.* 2000, (Friedman *et al.* 2000). (Earlier reports unconfirmed reports of the effect were also made). In any case these results are fascinating, since they represent a coherent quantum tunnelling of a system containing 10^{10} or more electrons. Fig. 3.14 shows an electron microscope image of a small superconducting circuit, approximately 2μm across, superimposed on an image of the quantum (Rabi) oscillations observed in this circuit (Chiorescu *et al.* 2003). These oscillations demonstrate the existence of quantum superposition states in which two the system is simultaneously in two macroscopically different quantum states!

Do these quantum superposition states have any practical uses? In recent years there has been a huge growth in the field of **quantum information** and **quantum computation**. The idea is that "information" as used and manipulated in computer bits is actually always a physical quantity, e.g. the charges on the capacitors in a RAM computer memory. Therefore it is subject to the laws of physics. But conventional computer bits are essentially based on classical physics. For example a computer bit can be measured without disturbing its state. But is we imagine eventually making the physical computer bits smaller and smaller with each new generation of computer, then eventually we will have to use devices which are so small that quantum mechanics applies, not classical physics. For such a quantum bit, or **qubit**, information is carried by its full quantum state, not just by a classical 0 or 1. Surprisingly it even turns out the computers based on manipulation of these qubits would be far more efficient than classical computers for certain types of algorithms. But whether this goal can be ever achieved depends on finding suitable physical systems in which to realize the qubit. While there are many possibilities under active investigation, superconducting devices or BEC have several possible advantages for these types of problem. At the very least, the experiments described above demonstrating macroscopic quantum superposition states show that BEC or superconducting devices are at least one viable option for a physical qubit. See Mahklin Schön and Shnirman (2001) and Annett Gyorffy and Spiller (2002) for more discussion of possible superconducting qubit devices.

3.10 Summary

In this chapter we have explored the implications of **quantum coherent states** in the theory of Bose and Fermi systems. We have seen how Bose coherent states provide an effective way to understand the laser and the weakly interacting Bose gas. The key point being that the coherent state representation allows one to discuss quantum states with definite phase

θ, rather than with definite particle number N. Using the coherent state approach the ideas of an effective macroscopic quantum wave function and off diagonal long ranged order (ODLRO) also become quite natural.

For fermion systems the coherent state approach is also quite natural, provided that one deals with coherent states of Cooper pairs, not single electrons. We have not yet seen how to explicitly construct such a coherent state (see the next chapter!), but we have already been able to see how ORLRO and the Ginzburg-Landau order parameter both arise naturally from this formalism. The Josephson effect, and its applications to SQUID devices can also be understood qualitatively even without the full description of the BCS wave function.

Finally we have seen that both BEC and superconductors do indeed exhibit **macroscopic quantum coherence**. But in the case of superconductors this is only evident when the devices are small enough and cold enough to avoid the effects of decoherence. Although the usual Josephson effect and the SQIUD interference patters are both interference effects, they do not in themselves show the existence of quantum superposition states such as the Schrödinger cat.

3.11 Further Reading

See Loudon (1979) for a more detailed discussion of optical coherent states and their application to the laser. A more advanced and general review of all applications of coherent states is given by Klauder and Skagerstam (1985).

The theory of the weakly interacting Bose gas is discussed in detail in Pines (1961), a book which also includes a reprint of the original paper by Bogoliubov (1947). More mathematically advanced approaches using many-body Green's function techniques are given by Fetter and Walecka (1971), and the Abrikosov, Gorkov and Dzyaloshinski (1963).

P.W Anderson made many key contributions to the development of the ideas of ODLRO and macroscopic coherence in superconductors. His book *Basic Notions in Condensed Matter Physics*, (Anderson 1984), includes several reprints of key papers in the discovery of ODLRO in superconductors, the Josephson effect and related topics. Tinkham (1996) also has a very detailed discussion about the Josephson effect and SQUID devices.

The problems and paradoxes posed by macroscopic quantum coherence are discussed by Leggett (1980), with a recent up date in Leggett (2002). The possibilities of making superconducting qubit devices for quantum computation are discussed in Mahklin Schön and Shnirman (2001) and Annett Gyorffy and Spiller (2002).

3.12 Exercises

(5.1) (a) Using the definitions of the ladder operators given in Eq. 3.12 show that

$$[\hat{a}, \hat{a}^+] = 1$$

and

$$\hat{H} = \hbar\omega_c \left(\hat{a}^+\hat{a} + \frac{1}{2} \right).$$

(b) Show that

$$[\hat{H}, \hat{a}^+] = \hbar\omega_c \hat{a}^+.$$

Hence show that if $\psi_n(x)$ is an eigenstate of the Hamiltonian with energy E_n, then ψ_{n+1} (defined by Eq. 3.2) is also an eigenstate with energy

$$E_{n+1} = E_n + \hbar\omega_c.$$

(c) Assuming that $\psi_n(x)$ is normalized, show that ψ_{n+1} as defined by Eq. 3.2 is also a correctly normalized quantum state.

(5.2) Using the fundamental defining equation of the coherent state Eq. 3.13, show that two coherent states $|\alpha\rangle$ and $|\beta\rangle$ have the overlap,

$$\langle\alpha|\beta\rangle = e^{-|\alpha|^2/2}e^{-|\beta|^2/2}e^{\alpha^*\beta},$$
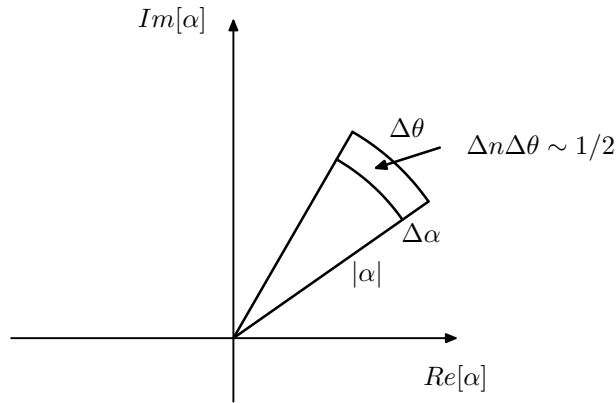
and hence derive Eq. 3.33.

(5.3) Show that for a coherent state $|\alpha\rangle$

$$\langle\alpha|((\hat{a}^+)^p\hat{a}^q|\alpha\rangle = (\alpha^*)^p\alpha^q$$

for any positive integers p and q.
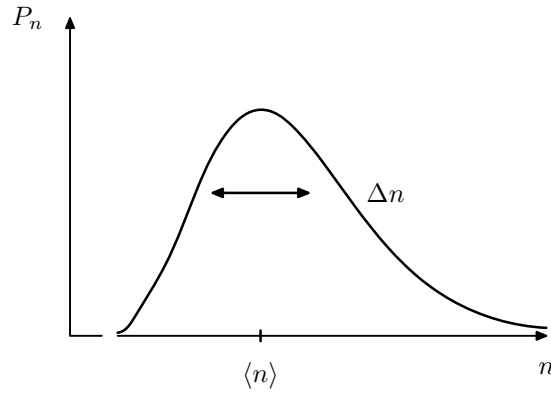
Fig. 3.1 The probability of the a coherent state containing quantum number N is a Poisson distribution. The width Δn is of order $\sqrt{\langle n \rangle}$, and so $\Delta n / \sqrt{\langle n \rangle} \to 0$ for large $\langle n \rangle$. Therefore Δn becomes negligible for coherent states with macroscopic numbers of particles.


Fig. 3.2 Complex plane of coherent states, $|\alpha\rangle$, with $\alpha = |\alpha|e^{i\theta}$. The area $\Delta\theta\Delta n$ contains approximately one independent orthogonal quantum state.
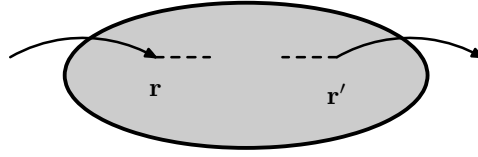
Fig. 3.3 Schematic illustrating the interpretation of the one particle density matrix $\rho_1(\mathbf{r} - \mathbf{r}')$. A particle is inserted into the condensate at $\mathbf{r}$, and a particle is removed from it at $\mathbf{r}'$. In a condensate, this process has a coherent quantum amplitude and phase however great the separation btween $\mathbf{r}$ and $\mathbf{r}'$.
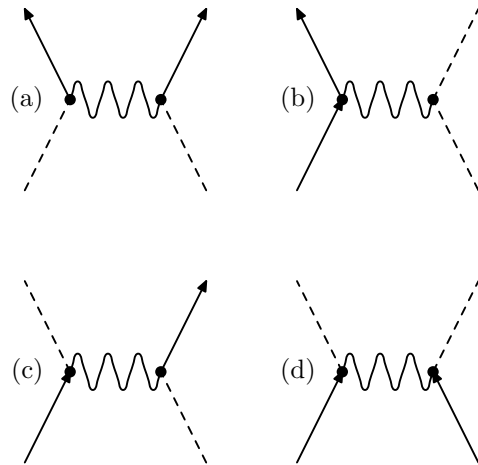

Fig. 3.4 Four types of interactions between quasiparticles and a Bose condensate. The quasiparticles are denoted by the solid lines, the condensate particles by the dashed line, and the interaction $V(\mathbf{r})$ by the wavy line. (a) Two particles are excited out of the condensate. (b) An existing quasiparticle interacts with the condensate. (c) An existing quasiparticle is absorbed into the condensate, while simultaneously a second quasiparticle becomes excited out of it. (d) Two quasiparticles are absorbed into the condensate.
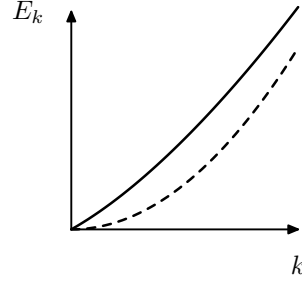
Fig. 3.5 The quasiparticle spectrum of a weakly interacting Bose gas, as found by Bogoliubov. The spectrum is linear at small $\mathbf{k}$, and approaches the free particle energy $\hbar^2 k^2/2m$ for large $\mathbf{k}$. Unlike the case of superfluid ^{4}He, Fig. **??** there is no roton minimum, and there is a slight upward curvature near to $\mathbf{k} = 0$.
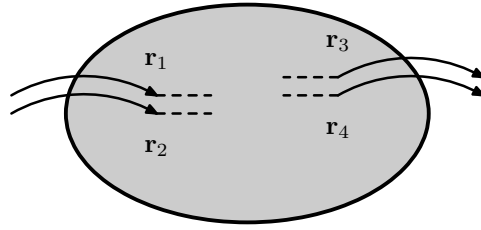
Fig. 3.6 The two body density matrix for electrons in a metal, $\rho_2(\mathbf{r}_1\sigma_1, \mathbf{r}_2\sigma_2, \mathbf{r}_3\sigma_3, \mathbf{r}_4\sigma_4)$. Off diagonal long ranged order (ODLRO) for electron pairs appears when this has a finite value however far apart the pair $\mathbf{r}_1$ and r_2, is from $\mathbf{r}_3$ and r_4. In contrast, the points within each pair must be no more than a coherence length, ξ_0 apart.
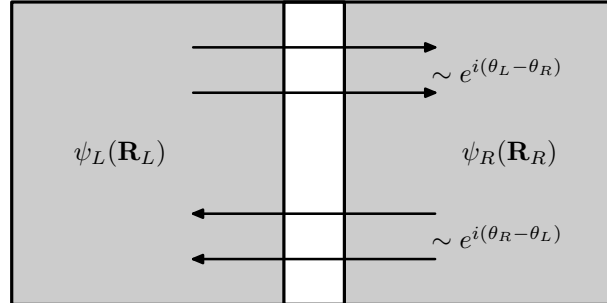
Fig. 3.7 A schematic Josephson tunnel junction between two superconductors. To second order in the tunnelling Hamiltonian there are two possible processes for a Cooper pair to tunnel from one side to another. If θ_L and θ_R denote the order parameter phases on either the left and right hand sides of the junction, then the amplitudes for processes depend on $e^{-(\theta_L - \theta_R)}$ and $e^{-(\theta_R - \theta_L)}$. When these are added together the net tunnel current is proportional to $\sin(\theta_L - \theta_R)$. .
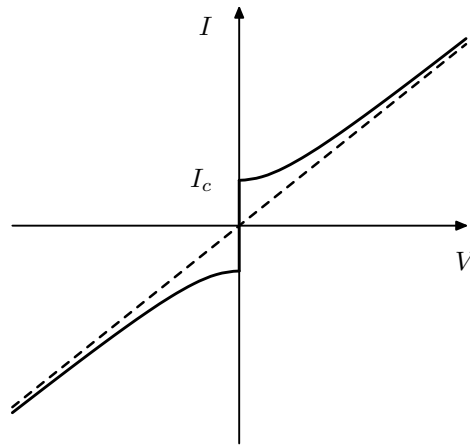
Fig. 3.8 I-V characteristic of a Josephson junction. There is no voltage drop, $V = 0$, provided that the junction current is less than the critical current I_c. Above this value a finite voltage drop occurs. This approaches the normal state Ohm's law result $I = V/R$ for large currents. The a.c. Joesphson effect occurs in the $V \neq 0$ regime above I_c.
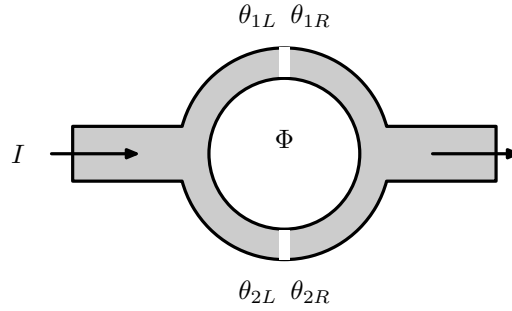
Fig. 3.9 Schematic geometry of a SQUID ring. The two Josephson junctions have currents governed by the phase differences $\Delta\theta_1 = \theta_{1L} - \theta_{1R}$ and $\Delta\theta_2 = \theta_{2L} - \theta_{2R}$. The total critical current of the whole device is modulated by the total magnetic flux through the ring Φ.
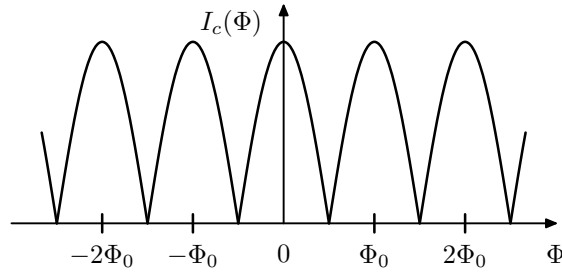
Fig. 3.10 Modulation of critical current in a SQUID ring. This is effectively equivalent to the Fraunhoffer interference pattern of a two slit optical interference pattern. Effectively there is interference between the two currents flowing through the opposite sides of the SQUID ring in Fig. 3.9.

Fig. 3.11 Macroscopic quantum coherence demonstrated in a Bose-Einstein condensate. A condensate is split into two halves, which then interfere with each other, analogous to an optical beam splitter experiment. The interference fringes are clearly visible as horizontal bands of light and dark absorption, corresponding to a spatially modulated condensate density. Reproduced from Ketterle (2002) with permission.

Fig. 3.12 An electron micrograph image of the Cooper pair box device used to demonstrate macroscopic quantum coherence in superconductors. The Cooper pair box, is connected to its environment via Josephson coupling to the charge reservoir, as indicated, and to a probe device, which is used to measure the number of Coooper pairs, N on the box. The device is manipulated through the two electrical gates indicated, one providing a d.c. bias, and the second delivering pico-second pulses which switch the device from one quantum state to another. Reproduced from Nakamua, Pashkina nd Tsai (1999) with permission.

Fig. 3.13 Quantum oscillations of charge observed in the Cooper pair box of fig. 3.12. The measured device current, I, is proportional to the Cooper pair number N on the box, and so the oscillations demonstrate quantum superpositions of states $|N\rangle$ and $|N + 1\rangle$. The oscillations depend on the amplitude and duration of the gate pulses, corresponding to the two axes showin in the diagram. Reproduced from Nakamura, Pashkin and Tsai (1999) with permission.

Fig. 3.14 A small superconducting SQUID type circuit, approximately 2μm across. This device shows coherent oscillations which which are direct consequences of quantum superposition states. In the two states a current either current circulates clockwise or anti-clockwise, as illustrated by the arrows drawn. Because the ring is macroscopic (containing or order 10^{10} superconducting electrons) this demonstrates the existence of "Schrödinger cat" quantum superposition states of macroscopically different states.reproduced from Chiorescu *et al.* (2003) with permission.

4

The BCS Theory of Superconductivity

4.1 Introduction

In 1957 Bardeen Cooper and Schrieffer (BCS) published the first truly microscopic theory of superconductivity. The theory was soon recognized to be correct in all the essential aspects, and to correctly explain a number of important experimental phenomena. For example the theory correctly explained the isotope effect:

$$T_c \propto M^{-\alpha} \tag{4.1}$$

in which the transition temperature changes with the mass of the crystal lattice ions, M. The original BCS theory predicts that the isotope exponent α is 1/2. Most common superconductors agree very well with this prediction, as one can see in Table 4.1. However it is also clear that there are exceptions to this prediction. Transition metals such as Molybdenum, and Osmium (Mo, Os) show a reduced effect, and others such as Ruthenium, Ru, have essentially zero isotope effect. In these it is necessary to extend the BCS theory to include what are called strong coupling effects. In other systems, such as the high temperature superconductor, $YBa_2Cu_3O_7$, the absence of the isotope effect may indicate that the lattice phonons are not involved at all in the pairing mechanism.[1]

The second main prediction of the BCS theory is the existence of an energy gap 2Δ at the Fermi level, as shown in Fig. 4.1. In the normal metal the electron states are filled up to the Fermi energy, ϵ_F, and there is a finite density of states at the Fermi level, $g(\epsilon_F)$. But in a BCS superconductor below T_c the electron density of states acquires a small gap 2Δ separating the occupied and unoccupied states. This gap is fixed at the Fermi energy,

---

[1] Even here the situation is complicated. In fact if the material is prepared with less than optimal oxygen content, e.g. $YBa_2Cu_3O_{6.5}$, then there is again a substantial isotope effect, although less than the BCS prediction. The significance of these is still a matter of strong debate. Do they indicate a phonon role in the pairing mechanism, or do they just relate to variations in lattice properties, band structure etc. which only influence T_c indirectly?

Table 4.1 Isotope effect in some selected superconductors.

	T_c (K)	α
Zn	0.9	0.45
Pb	7.2	0.49
Hg	4.2	0.49
Mo	0.9	0.33
Os	0.65	0.2
Ru	0.49	0.0
Zr	0.65	0.0
Nb_3Sn	23	0.08
MgB_2	39	0.35
$YBa_2Cu_3O_7$	90	0.0

and so (unlike a band gap in a semiconductor or insulator) it does not prevent electrical conduction.

This energy gap was discovered experimentally at essentially the same time as BCS theory was developed. Immediately after the BCS theory was published various different experimental measurements of the energy gap, 2Δ were shown to be excellent agreement with the predictions. Perhaps most important of all of these was electron tunnelling spectroscopy. This not only showed the existence of the energy gap, 2Δ, but also showed extra features which directly showed that the gap arises from electron-phonon coupling. The gap parameter Δ also had another important role. In 1960 Gorkov was able to use the BCS theory to derive the Ginzburg-Landau equations, and hence give a microscopic explanation of the order parameter ψ. He not only found that ψ is directly related to the wave function for the Cooper pairs, but that it is also directly proportional to the gap parameter Δ.

BCS theory built upon three major insights. (i) Firstly it turns out that the effective forces between electrons can sometimes be **attractive** in a solid rather than repulsive. This is due to coupling between the electrons and the phonons of the underlying crystal lattice. (ii) Secondly, in the famous "Cooper problem", Cooper considered the simple system of just two electrons outside an occupied Fermi surface. Surprisingly, he found that he electrons form a stable pair bound state, and this is true **however weak the attractive force**! (iii) Finally Schrieffer constructed a many-particle wave function which all the electrons near to the Fermi surface are paired up. This has the form of a coherent state wave function, similar to those we have seen in the previous chapter. The BCS energy gap 2Δ comes out of this analysis, since 2Δ corresponds to the energy for breaking up a pair into two free electrons.

The full derivation of BCS theory requires more advanced methods of many-body theory than we can cover properly in this volume. For example BCS theory can be elegantly formulated in terms of many-body Green's

functions and Feynman diagrams (Abrikosov, Gorkov and Dzyaloshinski 1963, Fetter and Walecka 1991). But, on the other hand it is possible to at least get the main flavour of the theory with just basic quantum mechanics. Here we shall just follow this simpler approach to develop the outline of the BCS theory and to summarize the key points. Those wishing to extend their knowledge to a deeper level should consult these more advanced texts.

4.2 The electron-phonon interaction

The first key idea in BCS theory is that there is an effective attraction for electrons near the Fermi surface. This idea was first formulated by Frölich in 1950. At first is very surprising to find an attractive force, because electrons "obviously" repel each other strongly with the electrostatic Coulomb repulsion,

$$V(\mathbf{r} - \mathbf{r}') = \frac{e^2}{4\pi\epsilon_0|\mathbf{r} - \mathbf{r}'|}. \tag{4.2}$$

While this is obviously always true, for the **bare electrons**, in a metal we should properly think about **quasiparticles** not bare electrons. A quasiparticle is an excitation of a solid consisting of a moving electron together with a surrounding **exchange correlation hole**. This idea is illustrated in Fig. 4.2. The point is that when the electron moves other electrons must move out of the way. They must do this both both because the exclusion principle prevents two electrons of the same spin being at the same point (this is called the exchange interaction) and because they must also try to minimize the repulsive Coulomb energy of Eq. 4.3.[2] The idea of a quasiparticle was developed by Landau, and we call such a system of strongly interacting fermions a **Landau Fermi liquid**. We shall explore the Fermi liquid idea in more depth in the next chapter.

   If we consider both the electron and its surrounding exchange correlation hole, then in a metal it turns out that between quasiparticles the effective Coulomb force is substantially reduced by **screening**. sing the simplest model of screening in metals, the Thomas Fermi model, we would expect an effective interaction of the form,

$$V_{TF}(\mathbf{r} - \mathbf{r}') = \frac{e^2}{4\pi\epsilon_0|\mathbf{r} - \mathbf{r}'|}e^{-|\mathbf{r}-\mathbf{r}'|/r_{TF}}. \tag{4.3}$$

r_{TF} is the Thomas Fermi screening length. One can see that the effect of screening is to substantially reduce the Coulomb repulsion. In particular the effective repulsive force is now short ranged in space, vanishing for $|\mathbf{r} - \mathbf{r}'| > r_{TF}$. The overall repulsive interaction is therefore much weaker than the original $1/r$ potential.

---

[2]The exchange interaction arises if one treats the many-electron state of the metal using Hartree-Fock theory. But this is not adequate for metals, and modern methods of **Density Functional Theory**, DFT, include both exchange and correlation effects explicitly.

Secondly the electrons interact with each other via their interaction with the phonons of the crystal lattice. In the language of Feynman diagrams an electron in Bloch state $\psi_{n\mathbf{k}}(\mathbf{r})$ can excite a phonon of crystal momentum $\hbar\mathbf{q}$, leaving the electron in a state $\psi_{n\mathbf{k}'}(\mathbf{r})$ with crystal momentum $\hbar\mathbf{k}' = \hbar\mathbf{k} - \hbar\mathbf{q}$. Later a second electron can absorb the phonon and pick up the momentum $\hbar\mathbf{q}$. This gives rise to Feynman diagrams as drawn in Fig. 4.3, which correspond to an effective interaction between the electrons.[3]

How does this electron-phonon interaction arise? Consider a phonon of wave vector bfq in a solid. The effective Hamiltonian for the phonons in the solid will be just a set of quantum Harmonic oscillators, one for each wave vector $\mathbf{q}$ and phonon mode

$$\hat{H} = \sum_{\mathbf{q},\lambda} \hbar\omega_{\mathbf{q}\lambda} \left(a_{\mathbf{q}\lambda}^{+} a_{\mathbf{q}\lambda} + \frac{1}{2} \right) \tag{4.4}$$

where the operators $a_{\mathbf{q}\lambda}^{+}$ and $a_{\mathbf{q}\lambda}$ create or annihilate a phonon in mode λ respectively. There are $3N_a$ phonon modes (branches) in a crystal with N_a atoms per unit cell. For simplicity let us assume that there is only one atom per unit cell, in which case there are just three phonon modes (one longitudinal mode and two transverse). Using the expressions for the ladder operators Eq. 3.12, the atoms located at $\mathbf{R}_i$ will be displaced by

$$\delta\mathbf{R}_i = \sum_{\mathbf{q}\lambda} \mathbf{e}_{\mathbf{q}\lambda} \left(\frac{\hbar}{2M\omega_{\mathbf{q}\lambda}} \right)^{1/2} (a_{\mathbf{q}\lambda}^{+} + a_{-\mathbf{q}\lambda})e^{i\mathbf{q}\cdot\mathbf{R}_i} \tag{4.5}$$

Here $\mathbf{e}_{\mathbf{q}\lambda}$ is a unit vector in the direction of the atomic displacements for mode $\mathbf{q}\lambda$. For example for the longitudinal mode this will be in the direction of propagation, $\mathbf{q}$.

Such a displacement of the crystal lattice will produce a modulation of the electron charge density and the effective potential for the electrons in the solid, $V_1(\mathbf{r})$. We can define the **deformation potential** by

$$\delta V_1(\mathbf{r}) = \sum_i \frac{\partial V_1(\mathbf{r})}{\partial \mathbf{R}_i} \delta\mathbf{R}_i, \tag{4.6}$$

as illustrated in Fig. 4.4.

This is a periodic modulation of the potential, with wavelength $2\pi/q$. An electron moving through the crystal lattice will experience this periodic potential and undergo diffraction. If it is initially in Bloch state $\psi_{n\mathbf{k}}(\mathbf{r})$, it can be diffracted to another Bloch state $\psi_{n'\mathbf{k}-\mathbf{q}}(\mathbf{r})$. The net effect of this

---

[3]In fact this type of Feynman diagram is familiar from particle physics. It is exactly the same as the diagram for the electromagnetic force in quantum electrodynamics, only that then it is a photon not a phonon which is exchanged. Similarly the same diagram gives the weak nuclear force between where the particle exchanged is a W or Z, or the strong nuclear force when gluons are exchange between quarks.

is that an electron has been scattered from a state with crystal momentum $\mathbf{k}$ to one with momentum $\mathbf{k} - \mathbf{q}$. The extra 'momentum' has been provided by the phonon. One can see that either one has created a phonon of momentum $\mathbf{q}$, or annihilated one of momentum $-\mathbf{q}$, or consistent with overall conservation of crystal momentum.[4] We can draw such an interaction as a **vertex** of a Feynman diagram, as shown in Fig. 4.5. In the vertex an electron is scattered from one momentum state to another while simultaneously a phonon is created or destroyed.

Putting together two such vertices we arrive at the diagram shown in Fig. 4.3. The meaning of this diagram is that one electron emits a phonon, it propagates for a while, and it is then absorbed by a second electron. The net effect of the process is to transfer momentum $\hbar\mathbf{q}$ from one electron to the other. Therefore it implies an effective interaction between electrons. Note that we do not have to specify which of the electrons created or destroyed the phonon. Therefore there is no need to draw an arrow on the phonon line showing which way it propagates. This effective interaction between the electrons due to exchange of phonons turns out to be of the form:

$$V_{eff}(\mathbf{q}, \omega)) = |g_{\mathbf{q}}|^2 \frac{1}{\omega^2 - \omega_{\mathbf{q}}^2} \tag{4.7}$$

where the virtual phonon has wave vector $\mathbf{q}$ and frequency $\omega_{\mathbf{q}}$. The parameter $g_{\mathbf{q}}$ is related to the matrix element for scattering an electron from state $\mathbf{k}$ to $\mathbf{k} + \mathbf{q}$ as shown in Fig. 4.5.

An important result due to Migdal is that the electron phonon vertex, $g_{(\mathbf{q}}$ is of order

$$g_{\mathbf{q}} \sim \sqrt{\frac{m}{M}} \tag{4.8}$$

where m is the effective mass of the electrons at he Fermi surface and M is the mass of the ions. Since m_e/M is of order 10^{-4}, typically, the electrons and phonons are only weakly coupled. We are therefore justified in only using the basic electron-phonon coupling diagram Fig. 4.3 and we can neglect and higher order diagrams which would contain more vertices.

The full treatment of this effective interaction is still too complex for analytic calculations. For this reason BCS introduced a highly simplified form of the above effective interaction. They first neglected dependence of the interaction the wave vector $\mathbf{q}$. Replacing the interaction by an approximate one which effectively averages over all values of $\mathbf{q}$. The frequency $\omega_{\mathbf{q}}$ is replaced by, ω_D, which is a typical phonon frequency, usually taken to be

---

[4]There are also **Umklapp** processes, where it is simultaneously scattered by a reciprocal lattice vector of the crystal from $\psi_{n\mathbf{k}}(\mathbf{r})$ to $\psi_{n'\mathbf{k}+\mathbf{q}+\mathbf{G}}(\mathbf{r})$. We shall not consider such processes here. Although they do contribute to the total electron phonon interaction, their effect is generally less important than the direct scattering terms.

the Debye frequency of the phonons, and the $\mathbf{q}$ dependent electron phonon interaction vertex, $g_{\mathbf{q}}$, is replaced by a constant, g_{eff}, giving

$$V_{eff}(\mathbf{q}, \omega) = |g_{eff}|^2 \frac{1}{\omega^2 - \omega_D^2}. \tag{4.9}$$

This is an attractive interaction for phonon frequencies ω which are less than ω_D, and repulsive for $\omega > \omega_D$. But BCS recognized that the repulsive part is not important. We are only interested in electrons which lie within $\pm k_\mathrm{B} T$ of the Fermi energy, and at the temperatures of interest to superconductivity we are int he regime $\hbar \omega_D >> k_\mathrm{B} T$. Therefore BCS assumed the final, simple form

$$V_{eff}(\mathbf{q}, \omega) = -|g_{eff}|^2 \qquad |\omega| < \omega_D. \tag{4.10}$$

The corresponding effective Hamiltonian for the effective electron-electron interaction is

$$\hat{H}_1 = -|g_{eff}|^2 \sum c_{\mathbf{k}_1 + \mathbf{q}\sigma_1}^+ c_{\mathbf{k}_2 - \mathbf{q}\sigma_1}^+ c_{\mathbf{k}_1, \sigma_1} c_{\mathbf{k}_2 \sigma_2} \tag{4.11}$$

where the sum is over all values of $\mathbf{k}_1$, σ_1, $\mathbf{k}_2$, σ_1 and $\mathbf{q}$ with the restriction that the electron energies involved are all within the range $\pm \hbar \omega_D$ of the Fermi surface,

$$|\epsilon_{\mathbf{k}_i} - \epsilon_F| < \hbar \omega_D.$$

Therefore we have interacting electrons near the Fermi surface, but the Bloch states far inside or outside the Fermi surface are unaffected, as shown in Fig. 4.6. The problem is that of electons in this thin shell of states around ϵ_F.

Note that combining the fact that the Migdal vertex is $\sim 1/M^{1/2}$ and the $1/\omega_D^2$ in the effective interaction, one finds that $|g_{eff}|^2 \sim 1/(M\omega_D^2)$. This turns out to be independent of the mass of the ions, M, since $\omega_D \sim (k/M)^{1/2}$, where k is an effective harmonic spring constant for the lattice vibrations. Therefore in the BCS model the isotope effect arises because the thickness of the energy shell around the Fermi surface is $\hbar \omega_D$, and not from changes in the coupling constant, $|g_{eff}|^2$.

4.3 Cooper pairs

Having found that there is an attraction between electron near the Fermi level is still a long way from a theory of superconductivity. The next key step was carried out by Cooper. He noted that the effective interaction is attractive only near to the Fermi surface, Fig. 4.6, and asked what the effect of this attraction would be for just a single pair of electrons outside the occupied Fermi sea. He found that they form a bound state. This result was somewhat unexpected, since two electrons in free space would not bind with the same weak attractive interaction. This "Cooper problem" thus shows

that the Fermi liquid state (i.e. independent Bloch electrons) is unstable to even weak attractive interactions between the particles. This idea thus led the way to the full BCS state in which every electron at the Fermi surface is part of a pair.

Cooper's model is the following. Assume a spherical Fermi surface at zero temperature, where all the states with $k < k_F$ are occupied. Then place an extra two electrons outside of the Fermi surface. These interact by the electron-phonon interaction and in Fig. 4.6.

The two particle wave function of these extra electrons is

$$\Psi(\mathbf{r}_1, \sigma_1, \mathbf{r}_2, \sigma_2) = e^{i\mathbf{k}_{cm} \cdot \mathbf{R}_{cm}} \varphi(\mathbf{r}_1 - \mathbf{r}_2) \phi^{spin}_{\sigma_1, \sigma_2} \qquad (4.12)$$

where $\mathbf{R}_{cm}$ is the centre of mass $(\mathbf{r}_1 + \mathbf{r}_2)/2$ and $\hbar\mathbf{k}_{cm}$ is the total momentum of the pair. It turns out that the minimum energy will correspond to a pair with no centre of mass motion, so in the ground state, $\mathbf{k}_{cm} = 0$, and we shall assume this is so from now on.

The spin wave function can be either spin singlet:

$$\phi^{spin}_{\sigma_1, \sigma_2} = \frac{1}{\sqrt{2}}(|\uparrow\downarrow\rangle - |\downarrow\uparrow\rangle) \qquad (4.13)$$

(total spin $S = 0$) or spin triplet ($S = 1$)

$$\phi^{spin}_{\sigma_1, \sigma_2} = \begin{cases} |\uparrow\uparrow\rangle \\ \frac{1}{\sqrt{2}}(|\uparrow\downarrow\rangle + |\downarrow\uparrow\rangle) \\ |\downarrow\downarrow\rangle \end{cases} . \qquad (4.14)$$

Almost all known superconductors (with a few very interesting exceptions) have singlet Cooper pairs and so we shall assume this from now on.

Fermion antisymmetry implies that

$$\Psi(\mathbf{r}_1, \sigma_1, \mathbf{r}_2, \sigma_2) = -\Psi(\mathbf{r}_2, \sigma_2, \mathbf{r}_1, \sigma_1). \qquad (4.15)$$

Since the spin singlet is an odd function of σ_1 and σ_2 the wave function $\varphi(\mathbf{r}_1 - \mathbf{r}_2)$ must be even, i.e. $\varphi(\mathbf{r}_1 - \mathbf{r}_2) = +\varphi(\mathbf{r}_2 - \mathbf{r}_1)$. Conversely, for a spin triplet state bound it would have to be an odd function.

Expanding $\phi(\mathbf{r}_1 - \mathbf{r}_2)$ in terms of the Bloch waves (assumed to be simply free electron plane wave states) we have

$$\varphi(\mathbf{r}_1 - \mathbf{r}_2) = \sum_{\mathbf{k}} \varphi_{\mathbf{k}} e^{i\mathbf{k} \cdot (\mathbf{r}_1 - \mathbf{r}_2)} \qquad (4.16)$$

where $\varphi_{\mathbf{k}}$ are some expansion coefficients to be found. $\varphi_{\mathbf{k}} = \varphi_{-\mathbf{k}}$ because of the function $\varphi(\mathbf{r})$ is even. The full pair wave function is thus a sum of Slater determinants:

$$\Psi(\mathbf{r}_1, \sigma_1, \mathbf{r}_2, \sigma_2) = \sum_{\mathbf{k}} \varphi_{\mathbf{k}} \begin{vmatrix} \psi_{\mathbf{k}\uparrow}(\mathbf{r}_1) & \psi_{\mathbf{k}\downarrow}(\mathbf{r}_2) \\ \psi_{-\mathbf{k}\uparrow}(\mathbf{r}_1) & \psi_{-\mathbf{k}\downarrow}(\mathbf{r}_2) \end{vmatrix} \qquad (4.17)$$

where the single particle Bloch state is $\psi_{\mathbf{k}}(\mathbf{r}) = e^{i\mathbf{k} \cdot \mathbf{r}}$. Each Slater determinant includes an up spin and a down spin, and an electron at $\mathbf{k}$ and

$-\mathbf{k}$. The state is thus a pairing of electron waves at $\mathbf{k}$ with those at $-\mathbf{k}$. The restriction that all the states below k_F are already filled is imposed by restricting the sum over $\mathbf{k}$ to the range $k > k_F$.

Substituting this trial wave function into the Schrödinger equation gives:

$$E\varphi_{\mathbf{k}} = -2|g_{eff}|^2 \epsilon_{\mathbf{k}}\varphi_{\mathbf{k}} \sum_{\mathbf{k}'} \varphi_{\mathbf{k}'} \tag{4.18}$$

where E is the total energy of the two particle state. For simplicity the energy $\epsilon_{\mathbf{k}}$ is measured relative to ϵ_F. To obtain this equation write

$$|\Psi\rangle = \sum_{\mathbf{k}} \varphi_{\mathbf{k}}|\Psi_{\mathbf{k}}\rangle \tag{4.19}$$

where $|\Psi_{\mathbf{k}}\rangle$ is the two particle Slater determinant given above

$$|\Psi_{\mathbf{k}}\rangle = \left| \begin{array}{cc} \psi_{\mathbf{k}\uparrow}(\mathbf{r}_1) & \psi_{\mathbf{k}\downarrow}(\mathbf{r}_2) \\ \psi_{-\mathbf{k}\uparrow}(\mathbf{r}_1) & \psi_{-\mathbf{k}\downarrow}(\mathbf{r}_2) \end{array} \right| \tag{4.20}$$

The two body Schrödinger equation is

$$\hat{H}|\Psi\rangle = E|\Psi\rangle. \tag{4.21}$$

Multiplying this equation on the left by $\langle\Psi_{\mathbf{k}}|$ picks out the terms for a given $\mathbf{k}$. The Hamiltonian consists of the two energies of the Bloch states $\epsilon_{\mathbf{k}}$ (and note $\epsilon_{\mathbf{k}} = \epsilon_{-\mathbf{k}}$) together with the effective interaction $-|g_{eff}|^2$. The effective interaction takes a momentum $\mathbf{q} = \mathbf{k}' - \mathbf{k}$ from one of the electrons and transfers it to the other. A pair of electrons $\mathbf{k}, -\mathbf{k}$ thus becomes a pair $\mathbf{k}', -\mathbf{k}'$ with a matrix element $-|g_{eff}|^2$. The limitation that $\epsilon(\mathbf{k}) < \hbar\omega_D$ places another restriction on the possible values of $\mathbf{k}$ limiting them to a thin shell between $k = k_F$ and $k = k_F + \omega_D/v$, with v the Bloch wave group velocity at the Fermi surface.

The energy E can be found by a self-consistency argument. Let us define

$$C = \sum_{\mathbf{k}} \varphi_{\mathbf{k}}. \tag{4.22}$$

Then we can solve for the $\varphi_{\mathbf{k}}$ giving

$$\varphi_{\mathbf{k}} = -C|g_{eff}|^2 \frac{1}{E - 2\epsilon_{\mathbf{k}}}. \tag{4.23}$$

Self-consistency requires

$$C = \sum_{\mathbf{k}} \varphi_{\mathbf{k}} = -C|g_{eff}|^2 \sum_{\mathbf{k}} \frac{1}{E - 2\epsilon_{\mathbf{k}}} \tag{4.24}$$

or

$$1 = -|g_{eff}|^2 \sum_{\mathbf{k}} \frac{1}{E - 2\epsilon(\mathbf{k})}. \qquad (4.25)$$

Converting the sum over $\mathbf{k}$ into an integral over the density of states gives

$$1 = -|g_{eff}|^2 g(\epsilon_F) \int_0^{\hbar\omega_D} d\epsilon \frac{1}{E - 2\epsilon} \qquad (4.26)$$

The integration limits are present because of the restriction of $\mathbf{k}$ to the thin shell around the Fermi surface, as discussed above. The integration is easy, and the result can be rearranged to find E,

$$-E = 2\hbar\omega_D e^{-1/\lambda} \qquad (4.27)$$

where the **electron-phonon coupling parameter**, λ

$$\lambda = |g_{eff}|^2 g(\epsilon_F) \qquad (4.28)$$

is assumed to be small, $\lambda \ll 1$.

Thus a bound state does exist, and its energy is exponentially small when λ is small. As in the full BCS solution the energy scale for superconductivity is set by the Debye energy, but multiplied by a very small exponential factor. This explains why the transition temperatures T_c are so small compared to other energy scales in solids. The Debye energies usually correspond to energy scales of order $100 - 300\mathrm{K}$, and it is the very small exponential factor which leads to $T_c \sim 1\mathrm{K}$ for most metallic superconductors.

Interestingly, the bound state exists however small the interaction constant λ is. This would not have been the case without the filled Fermi sea. In general, an attractive interaction in three dimensions does not always lead to the existence of a bound state. The presence of the filled Fermi sea is thus a key aspect of the BCS theory.

Finally, notice that obviously we could have made two particle states with different quantum numbers. For example we could have made spin triplets instead of singlets. The relative coordinate wave function $\varphi(\mathbf{r}_1 - \mathbf{r}_2)$ we had above was independent of the direction of the vector $\mathbf{r}_1 - \mathbf{r}_2$, i.e. the pair are found in an s-wave state (like the ground state of the hydrogen atom). On the other hand it might have been possible to find solutions with p or d type wave functions,

$$\varphi(\mathbf{r}_1 - \mathbf{r}_2) = f(|\mathbf{r}_1 - \mathbf{r}_2|)Y_{lm}(\theta, \phi)$$

where Y_{lm} is a spherical Harmonic function. In general these different pairing states are all quite possible, however it seems that almost all superconductors choose a s-wave singlet pairing state. In fact the BCS model electron-electron interaction we chose above only allows solutions of that

type, since it is independent of the phonon wave vector $\mathbf{q}$. Fourier transforming to real space, this corresponds to a point contact interaction

$$V_{eff}(\mathbf{r_1} - \mathbf{r}_2) = -|g_{eff}|^2 \delta(\mathbf{r_1} - \mathbf{r}_2).$$

Only s-wave spherical Harmonic functions, $l = 0$, allow pair wave function which is finite at $\mathbf{r}_1 = \mathbf{r}_2$. However more general types of interactions, perhaps not due to electron-phonon coupling, can allow other pair types to occur. Superfluid helium-3 (^{3}He) occurs because of Cooper pairing of the (fermion) ^{3}He atoms. These Cooper pairs turn out to be $p-wave$ and spin triplet. The nature of the Cooper pairs in the high T_c superconductors is still controversial, but there is now a lot of evidence suggesting spin singlet, but $d-wave$ Cooper pairs. We shall return to this topic in the next chapter.

4.4 The BCS wave function

Using the insight from the Cooper problem, Bardeen Cooper and Schrieffer realized that the whole Fermi surface would be unstable to the creation of such pairs. As soon as there is an effective attractive interaction essentially every electron at the Fermi surface will become bound into a Cooper pair.

The next problem was to write down a many particle wave function in which every electron is paired. At first one could try a sort of product state of the form given in Eq. 3.107. However this function is not very convenient to work with. It also does not make clear the concept of the macroscopic quantum coherence which, as we have seen, is essential to the formation of a condensate an hence to the idea of superconductivity.

Instead, Schrieffer wrote down a **coherent state** of Cooper pairs. As discussed in the previous chapter, is is possible to construct operators which create or annihilate electron pairs centred at $\mathbf{R}$,

$$\hat{\varphi}^+(\mathbf{R}) \qquad \hat{\varphi}(\mathbf{R}).$$

As we have seen, these operators **do not** obey normal Bose commutation laws, and so they cannot be regarded as creating or destroying boson particles.

We will look for a uniform translationally invariant soulution, and so it is more convenient to work in $\mathbf{k}$ space. Let us defining the pair creation operator by,

$$\hat{P}_{\mathbf{k}}^+ = c_{\mathbf{k}\uparrow}^+ c_{-\mathbf{k}\downarrow}^+. \tag{4.29}$$

This creates a pair of electrons of zero total crystal momentum, and opposite spins. In terms of this operator Schrieffer proposed the following coherent state many-body wave function,

$$|\Psi_{BCS}\rangle = const. \exp\left(\sum_{\mathbf{k}} \alpha_{\mathbf{k}}\right)\hat{P}_{\mathbf{k}}^+)|0\rangle. \tag{4.30}$$

where the complex numbers, α_{bfk}, are parameters which can be adjusted to minimize the total energy. Here the "vacuum" state, $|0\rangle$, is a state with

a completely filled Fermi sea, i.e. the $T = 0$ non-interacting electron gas, a ground state with no electron or hole excitations.

Even though these pair operators do not obey Bose commutation laws

$$\left[\hat{P}_{\mathbf{k}}^+, \hat{P}_{\mathbf{k}}\right] \neq 1 \tag{4.31}$$

they **do** commute with each other. It is easy to confirm that

$$\left[\hat{P}_{\mathbf{k}}^+, \hat{P}_{\mathbf{k}'}^+\right] = 0 \tag{4.32}$$

for different $\mathbf{k}$ points, $\mathbf{k} \neq \mathbf{k}'$. On the other hand, for the same $\mathbf{k}$ point, $bfk = \mathbf{k}'$, the product $\hat{P}_{\mathbf{k}}^+ \hat{P}_{\mathbf{k}}^+$ contains four electron creation operators for the same $\mathbf{k}$ point,

$$\hat{P}_{\mathbf{k}}^+ \hat{P}_{\mathbf{k}}^+ = c_{\mathbf{k}\uparrow}^+ c_{-\mathbf{k}\downarrow}^+ c_{\mathbf{k}\uparrow}^+ c_{-\mathbf{k}\downarrow}^+ = 0, \tag{4.33}$$

and it is therefore always zero because $c_{\mathbf{k}\uparrow}^+ c_{\mathbf{k}\uparrow}^+ = 0$. It will also be useful to note that this implies

$$\left(\hat{P}_{\mathbf{k}}^+\right)^2 = 0. \tag{4.34}$$

Using the fact that these operators commute we can rewrite the coherent state in Eq. 4.30 as as a product of exponentials, one for each $\mathbf{k}$ point,

$$|\Psi_{BCS}\rangle = const. \prod_{\mathbf{k}} \exp{(\alpha_{\mathbf{k}})\hat{P}_{\mathbf{k}}^+}|0\rangle \tag{4.35}$$

Then, using property, Eq. 4.34, we can also expand out each of the operator exponentials. In the expansion of all terms containing $\hat{P}_{\mathbf{k}}^+$ to quadratic or higher powers are zero. Therefore we obtain

$$|\Psi_{BCS}\rangle = const. \prod_{\mathbf{k}} \left(1 + \alpha_{\mathbf{k}}\hat{P}_{\mathbf{k}}^+\right)|0\rangle. \tag{4.36}$$

The normalizing constant is found from

$$1 = \langle 0| \left(1 + \alpha_{\mathbf{k}}^* \hat{P}_{\mathbf{k}}\right) \left(1 + \alpha_{\mathbf{k}}\hat{P}_{\mathbf{k}}^+\right) |0\rangle = 1 + |\alpha_{\mathbf{k}}|^2. \tag{4.37}$$

So we can finally write the normalized BCS state as

$$|\Psi_{BCS}\rangle = \prod_{\mathbf{k}} \left(u_{\mathbf{k}} + v_{\mathbf{k}}\hat{P}_{\mathbf{k}}^+\right)|0\rangle \tag{4.38}$$

where

$$u_{\mathbf{k}} = \frac{1}{1 + |\alpha_{\mathbf{k}}|^2} \tag{4.39}$$

$$v_{\mathbf{k}} = \frac{\alpha_{\mathbf{k}}}{1 + |\alpha_{\mathbf{k}}|^2} \tag{4.40}$$

and where

$$|u_{\mathbf{k}}|^2 + |v_{\mathbf{k}}|^2 = 1. \tag{4.41}$$

Notice that the constants $\alpha_{\mathbf{k}}$ can be any complex numbers, as is usual in a coherent state. Therefore we can associate a complex phase angle θ

with the BCS state. On the other hand, the wave function does not have a definite particle number, N, since it is a superposition of the original Fermi sea, $|0\rangle$, and the sea plus $2, 4, 6, \ldots$ electrons. Of course this number-phase uncertainty is typical of coherent states. As BCS argued, the total number of electrons involved, N, is macroscopic and of order the system size. For this state the uncertainty in N, ΔN, is of order $N^{1/2}$ and is therefore absolutely negligible compared to N. Nevertheless it was only several years after the original BCS paper that this become fully accepted as a valid argument.

Finally, the way the BCS state was originally written, as described above, treats electrons and holes in a relatively unsymmetrical manner. We start with a filled Fermi sea $|0\rangle$ and add pairs of electrons. But what about pairs of holes? In fact these are also included in the theory. We just have to see that by a suitable redefinition of the original reference state $0\rangle$ we can write the BCS state in a form which treats electrons and holes more evenly,

$$|\Psi_{BCS}\rangle = \prod_{\mathbf{k}} \left(u_{\mathbf{k}} c_{-\mathbf{k}\downarrow} + v_{\mathbf{k}} c^{+}_{\mathbf{k}\uparrow} \right) |0\rangle \qquad (4.42)$$

where

One can equally well view the BCS state as a condensate of electron pairs above a filled electron Fermi sea, of a condensate of hole pairs below an empty "hole sea". In fact electrons and holes contribute more or less equally.[5]

4.5   The mean-field Hamiltonian

With the trial wave function given above, the next task is to find the parameters $u_{\mathbf{k}}$ and $u_{\mathbf{k}}$ which minimize the energy.

Using the BCS approximation for the effective interaction, Eq. 4.11, the relevant Hamiltonian is

$$\hat{H} - \mu N = \sum_{\mathbf{k},\sigma} (\epsilon_{\mathbf{k}} - \epsilon_F) c^{+}_{\mathbf{k}\sigma} c_{\mathbf{k}\sigma} - |g_{eff}|^2 \sum c^{+}_{\mathbf{k}_1+\mathbf{q}\sigma_1} c^{+}_{\mathbf{k}_2-\mathbf{q}\sigma_2} c_{\mathbf{k}_1,\sigma_1} c_{\mathbf{k}_2\sigma_2},$$

$$(4.43)$$

where, as discussed above, we restrict the interaction to values of $\mathbf{k}$ so that $\epsilon_{\mathbf{k}}$ is within $\pm\hbar\omega_D$ of the Fermi energy.

If we assume that the most important interactions are those involving Cooper pairs $\mathbf{k}, \uparrow$ and $-\mathbf{k}, \downarrow$ the most important terms are those for which

---

[5]The same duality arises in Dirac's theory of the electron sea. Do the positive energy electrons move above a filled Dirac sea of filled negative energy electron states? In this picture positrons are holes in this Dirac sea of electrons. But an equally valid point of view is the opposite! We could view positive energy postitrons as moving above a filled sea of negative energy positrons. Then electrons are just holes in this filled sea of postitrons! Neither point of view is any more correct than the other.

$\mathbf{k}_1 = -\mathbf{k}_2$ and $\sigma_1 = -\sigma_2$. Dropping all other interactions the Hamiltonian becomes

$$\hat{H} - \mu N = \sum_{\mathbf{k},\sigma}(\epsilon_{\mathbf{k}} - \epsilon_F)c^+_{\mathbf{k}\sigma}c_{\mathbf{k}\sigma} - |g_{eff}|^2 \sum_{\mathbf{k},\mathbf{k}'}c^+_{\mathbf{k}\uparrow}c^+_{-\mathbf{k}\downarrow}c_{-\mathbf{k}'\downarrow}c_{\mathbf{k}'\uparrow} \qquad (4.44)$$

using the same model form of the interaction V_{eff} as we used in the Cooper problem above.

If we assume that the most important interactions are those involving Cooper pairs $\mathbf{k}, \uparrow$ and $-\mathbf{k}, \downarrow$ this becomes

$$\hat{H} = \sum_{\mathbf{k},\sigma}(\epsilon_{\mathbf{k}} - \epsilon_F)c^+_{\mathbf{k}\sigma}c_{\mathbf{k}\sigma} - |g_{eff}|^2 \sum_{\mathbf{k},\mathbf{k}'}c^+_{\mathbf{k}\uparrow}c^+_{-\mathbf{k}\downarrow}c_{-\mathbf{k}'\downarrow}c_{\mathbf{k}'\uparrow} \qquad (4.45)$$

using the same model form of the interaction V_{eff} as before.

The above Hamiltonian is still an interacting electron problem and is too hard to solve exactly. But making use of the trail BCS wave function it can by solved variationally to minimize the free energy. This is equavalent to making a **mean-field** approximation. The idea is that each Cooper pair is much larger than the typical spacing between particles, and so in the above sum over $\mathbf{k}'$ we can replace the operators with their average value. Introducing

$$\Delta = -|g_{eff}|^2 \sum_{\mathbf{k}'}\langle c_{-\mathbf{k}'\downarrow}c_{\mathbf{k}'\uparrow}\rangle \qquad (4.46)$$

then the Hamiltonian becomes approximately

$$\hat{H}_{BCS} = \sum_{\mathbf{k},\sigma}(\epsilon_{\mathbf{k}} - \epsilon_F)c^+_{\mathbf{k}\sigma}c_{\mathbf{k}\sigma} + \sum_{\mathbf{k}}(c^+_{\mathbf{k}\uparrow}c^+_{-\mathbf{k}\downarrow}\Delta + \Delta^* c_{-\mathbf{k}\downarrow}c_{\mathbf{k}\uparrow}). \qquad (4.47)$$

The last term is needed to keep $\hat{H}$ Hermitian ($\hat{H}^+ = \hat{H}$). This BCS Hamiltonian is now sufficiently simple that everything can be solved exactly from now on.

The BCS Hamiltonian can be diagonalized by a change of variables. It is necessary to introduce a new set of operators which are linear combinations of the original operators,

$$b^+_{\mathbf{k}\uparrow} = u_{\mathbf{k}}c^+_{\mathbf{k}\uparrow} + v_{\mathbf{k}}c_{-\mathbf{k}\downarrow}$$
$$b_{-\mathbf{k}\downarrow} = -v_{\mathbf{k}}c^+_{\mathbf{k}\uparrow} + u_{\mathbf{k}}c_{-\mathbf{k}\downarrow} \qquad (4.48)$$

It turns out that these operators also anti-commute, provided that $|u|^2 + |v|^2 = 1$. In fact assuming real valued u and v, writing $u = \cos\theta$, $v = \sin\theta$ the new operators are just a 2x2 rotation of the original ones

$$\begin{pmatrix} b^+_{\mathbf{k}\uparrow} \\ b_{-\mathbf{k}\downarrow} \end{pmatrix} = \begin{pmatrix} \cos\theta & \sin\theta \\ -\sin\theta & \cos\theta \end{pmatrix} \begin{pmatrix} c^+_{\mathbf{k}\uparrow} \\ c_{-\mathbf{k}\downarrow} \end{pmatrix} \qquad (4.49)$$

If the u and v are chosen to be an eigenvector of the following 2x2 matrix,

$$\left(\begin{array}{cc} \epsilon_{\mathbf{k}} - \epsilon_F & \Delta \\ \Delta^* & -(\epsilon_{\mathbf{k}} - \epsilon_F) \end{array} \right) \left(\begin{array}{c} u_{\mathbf{k}} \\ v_{\mathbf{k}} \end{array} \right) = E_{\mathbf{k}} \left(\begin{array}{c} u_{\mathbf{k}} \\ v_{\mathbf{k}} \end{array} \right). \tag{4.50}$$

The eigenvalues are the energies

$$E_{\mathbf{k}} = \sqrt{(\epsilon_{\mathbf{k}} - \epsilon_F)^2 + |\Delta|^2}. \tag{4.51}$$

In terms of the new diagonalized operators, it turns out that the BCS Hamiltonian has the simple form:

$$\hat{H}_{BCS} = \sum_{\mathbf{k}} E_{\mathbf{k}} b_{\mathbf{k}\uparrow}^+ b_{\mathbf{k}\uparrow} - E_{\mathbf{k}} b_{-\mathbf{k}\downarrow} b_{-\mathbf{k}\downarrow}^+. \tag{4.52}$$

This is diagonal, i.e. each term just involves the numbers of b particles in a given state $(b_{-\mathbf{k}\downarrow} b_{-\mathbf{k}\downarrow}^+ = 1 - n_{-\mathbf{k}\downarrow})$. The excitations of the system involve either adding or removing b particles, with corresponding changes of energy $\pm E_{\mathbf{k}}$.

4.6   The BCS energy gap and quasiparticle states

Fig. 4.8 shows energies of the excitations created by the $b^+\mathbf{k}$ operators $\pm E_{\mathbf{k}}$ as a function of $\mathbf{k}$. It gives the following physical picture. In the normal state $\Delta = 0$ and the excitation energies are $+\epsilon_{\mathbf{k}}$ for adding an electron to an empty state, or $-\epsilon_{\mathbf{k}}$ for removing an electron (adding a hole).

In the superconducting state these become modified to $+E_{\mathbf{k}}$ for adding a b particle, or $-E_{\mathbf{k}}$ for removing one. Because $+E(\mathbf{k})$ is greater than Δ and $-E_{\mathbf{k}}$ is less than $-\Delta$ the minimum energy to make an excitation is 2Δ. Thus this is the energy gap of the superconductor. The b particles are called quasi-particles.

The b^+, b operators are a strange mixture of the creation c^+ and annihilation c operators. This implies that the states they create or destroy are neither purely electron or purely hole excitations, instead they are a quantum superposition of electron and hole. In fact u and v have the physical interpretation that

$$|u_{\mathbf{k}}|^2$$

is the probabilities that the excitation is an electron if one measures its charge, and

$$|v_{\mathbf{k}}|^2$$

is the probability that it is a hole.[6]

---

[6] Again there are nice analogies to particle physics. The neutral K-meson, K_0, has an antiparticle, $\overline{K}_0$. Neither of them are eigenstates of total energy (mass), and so when the particle propagates is oscillates between these two states. If it is measured at any point there is a certain probability that it will be found to be K_0 and another for it to be $\overline{K}_0$. Here, the BCS quasiparticles are the energy (mass) eigenstates, and they are quantum superpositions of electrons and holes states.

Finally in order to find Δ it is again necessary to invoke self-consistency. Δ was defined by

$$\Delta = g \sum_{\mathbf{k}} \langle c_{-\mathbf{k}\downarrow} c_{\mathbf{k}\uparrow} \rangle \tag{4.53}$$

Determining the expectation value from the solutions to the BCS Hamiltonian Bardeen Cooper and Schrieffer obtained

$$\Delta = |g_{eff}|^2 \sum_{\mathbf{k}} \frac{\Delta}{2E_{\mathbf{k}}} \tanh\left(\frac{E_{\mathbf{k}}}{2k_{\mathrm{B}}T}\right), \tag{4.54}$$

or converting the sum into an integral over energy we arrive at **the BCS gap equation**,

$$1 = \lambda \int_0^{\hbar\omega_D} d\epsilon \frac{1}{E} \tanh\left(\frac{E}{2k_{\mathrm{B}}T}\right) \tag{4.55}$$

where $E = \sqrt{\epsilon^2 + |\Delta|^2}$ and $\lambda = |g_{eff}|^2 g(\epsilon_F)$ is the dimensionless electron-phonon coupling parameter.

The BCS gap equation implicitly determines the gap $\Delta(T)$ at any temperature T. It is the central equation of the theory, since it predicts both the transition temperature T_c and the value of the energy gap at zero temperature $\Delta(0)$.

From the BCS gap equation, taking the limit $\Delta \to 0$ one can obtain an equation for T_c

$$k_B T_c = 1.13 \hbar\omega_D \exp\left(-1/\lambda\right) \tag{4.56}$$

which has almost exactly the same form as the formula for the binding energy in the Cooper problem. Also at $T = 0$ one can also do the integral and determine $\Delta(0)$. The famous BCS result

$$2\Delta(0) = 3.52 k_B T_c \tag{4.57}$$

is obeyed very accurately in a wide range of different superconductors.

4.7 Predictions of the BCS theory

The BCS theory went on to predict many other physical properties of the superconducting state. For most simple metallic superconductors, such as Al, Hg etc., these agreed very well with experimental facts, providing strong evidence in support of the theory. For example two key predictions where the behaviour of the nuclear magnetic resonance (NMR) relaxation rate, $1/T_1$ below the critical temperature T_c, and the temperature dependence of the attenuation coefficient for ultrasound. These are both sensitive to the electronic density of states in the superconductor, Fig. 4.1, but also depend on **coherence factors**, which are certain combinations of the BCS parameters $u_{\mathbf{k}}$ and $v_{\mathbf{k}}$. it turns out (Schrieffer 1964), that the good agreement between theory and experiment depends in detail on the values of these parameters. Therefore one can say that the BCS theory has been

tested not just at the level of the quasiparticle energies, $E_{\mathbf{k}}$, but also at a more fundamental level. Therefore one can say that not only the existence of Cooper pairs, but also their actual wave functions, $u_{\mathbf{k}}$ and $v_{\mathbf{k}}$, have been confirmed experimentally.

A further confirmation of both the existence of Cooper pairs, and the BCS energy gap is provided by **Andreev Scattering**. Consider an interface between a normal metal and a superconductor, as shown in Fig. 4.11. Consider an electron moving in the metal in a Bloch state $\mathbf{k}$ with energy $\epsilon_{\mathbf{k}}$. If its energy is below the superconductor energy gap,

$$\epsilon_{\mathbf{k}} - \epsilon_F < \Delta \tag{4.58}$$

then the electron cannot propagate into the superconductor, and so it is perfectly reflected at the interface. This is normal particle reflection. But Andreev noticed that another process is possible. The electron can combine with another electron and form a Cooper pair, which will pass freely into the superconductor. By conservation of charge, a hole must be left behind. By conservation of momentum this hole will have to have momentum exactly opposite to the original electron, $-\mathbf{k}$. For the same reason it will also have opposite spin. therefore we have the situation shown in Fig. 4.11. The incoming electron can be reflected either as an electron, with a specularly reflected $\mathbf{k}$ vector, or it can be reflected as a hole of opposite spin and momentum, which travels back exactly along the original electron's path! Direct evidence for such scattering events can be found by injecting electrons into such an interface, say by electron tunnelling. Since the returning hole carries a positive charge and is moving in the opposite direction to the injected electron the tunnel current is actually twice what it would have been if $\Delta = 0$, or if the tunnelling electron is injected with at a voltage above the energy gap, $V > \Delta$.

An interesting feature of Andreev reflection is that the electron and hole are exactly **time reversed** quantum states,

$$
\begin{aligned}
-e &\rightarrow e \\
\mathbf{k} &\rightarrow -\mathbf{k} \\
\sigma &\rightarrow -\sigma
\end{aligned}
\tag{4.59}
$$

in charge, momentum and spin. Fundamentally this is arises because the Cooper pairs in the BCS wave function are pairs of time reversed single particle states. A very surprising implication of this fact was pointed out by P.W. Anderson. He noted that if the crystal lattice is disordered due to impurities, then Bloch's theorem no longer applies and the crystal momentum $\mathbf{k}$ is not a good quantum number. But, even in a strongly disordered system the single particle wave functions still come in **time reversed pairs**

$$\psi_{i\uparrow}(\mathbf{r}) \qquad \psi_{i\downarrow}^*(\mathbf{r}). \tag{4.60}$$

The single particle Hamiltonian operator $\hat{H} = \hbar^2\nabla^2/2m + V(\mathbf{r})$ is real even if the potential $V(\mathbf{r})$ is not periodic, and it turns out that this implies that $\psi_{i\uparrow}(\mathbf{r})$ and $\psi_{i\downarrow}^*(\mathbf{r})$ must be both eigenstates and be **exactly degenerate**. Anderson argued that that one could reformulate BCS theory entirely in terms of these new states of the disordered crystal lattice, and that to a first approximation quantities like T_c (which depend only on $g(\epsilon_F$ and $\lambda)$ will be essentially unchanged. This explains why the BCS theory works well even in highly disordered systems, such as metallic alloys. If the mean free path l for the electrons in the solid is greater than the coherence length,

$$l > \xi_0$$

then the alloy is said to be in the **clean limit**, but if it is shorter,

$$l < \xi_0$$

the alloy is said to be in the **dirty limit**. On the other hand, Anderson's argument does not apply if the crystal impurities themselves break the time-reversal symmetry, such as magnetic impurities[7] Therefore superconductivity is heavily influenced (and rapidly destroyed) by magnetic impurities. They are said to be **pair breaking** since they break up the Cooper pairs.[8]

Finally, in some superconductors one has to extend the original BCS theory to allow for **strong coupling**. The assumptions made by BCS are essentially exact in the weak-coupling limit, namely when $\lambda << 1$. But when the coupling parameter λ becomes larger, say $0.2 - 0.5$, then one has to self-consistently take into account both the effects of the phonons on the electrons, and the effects of the electrons on the phonons. For example, the phonon frequencies are affected by the coupling to the electrons. All of these effects can be included consistently, systematically keeping all effects which are of order m_e/M, where M is the mass of the crystal lattice ions. In terms of the Migdal theorem stated above, that each electron-phonon vertex is of order $\sqrt{m_e/M}$, it is only necessary to systematically include all Feynman diagrams which have two electron-phonon vertices. When all such effects are included it is also necessary to fully include the phonon denstity of states, and the electron phonon coupling matrix elements. The theory developed by Eliashberg characterizes both of these with a single function $\alpha^2(\omega)F(\omega)$, where $F(\omega)$ is the phonon density of states and $\alpha(\omega)$

---

[7]Under time reversal and spin becomes reversed, so magnetic impurity atoms break time reversal symmetry. An external magnetic field would also break the symmetry.

[8]Interestingly, for superconductors with magnetic impurities states start to fill in the energy gap, Δ. As more impurities are added the transition temperature T_c decreases and more and more states fill the gap. It turns out that there is a small regime of **gapless superconductivity** in which the energy gap has completely disappeared, even though the system is still superconducting and below T_c. Therefore the presence of the energy gap is not completely essential to the existence of superconductivity.

is an effective electron-phonon matrix element. In terms of these quantities the electron-phonon coupling constant becomes

$$\lambda = 2 \int_0^\infty \frac{\alpha^2(\omega)F(\omega)}{\omega} d\omega. \tag{4.61}$$

An approximate expression for the critical temperature was found by McMillan,

$$k_{\mathrm{B}}T_c = \frac{\hbar\omega_D}{1.45} \exp\left(\frac{1.04(1+\lambda)}{\lambda - \mu^*(1+0.62\lambda)} \right). \tag{4.62}$$

Here the parameter μ^* is the **Coulomb pseudopotential**, which takes into account the direct (screened) Coulomb repulsion between the electrons. This formula works well in superconductors such as Pb and Nb, where there are significant deviations from BCS theory. For example, it explains the reduced isotope effect in these materials, as shown in Table 4.1.

4.8 Further Reading

There are many excellent text books on the BCS theory. These include Schrieffer (1964), de Gennes (1966), Tinkham (1996), Ketterson and Song (1999) and Waldram (1996), as well as many others. These include many more details which we have not had space to include here. The description of the BCS state given here is similar to those given in most of these books.

At a more advanced level one should first learn many-body theory formally. Books at this level include Fetter and Walecka (1971), Abrikosov Gorkov Dzyaloshinski (1963), and Rickayzen (1980). Schrieffer (1964) also introduces these methods as part of his discussion of the BCS theory.

4.9 Exercises

(6.1) (a) Show that the pair operators $\hat{P}_{\mathbf{k}}^+$ and $\hat{P}_{\mathbf{k}'}^+$ commute, as given in Eqs. 4.32.

Show that they do not obey boson commutator equations, i.e.

$$\left[\hat{P}_{\mathbf{k}}, \hat{P}_{\mathbf{k}'}^+ \right] \neq \delta_{\mathbf{k},\mathbf{k}'}.$$

(6.3) Confirm that the quasiparticle operators $b_{\mathbf{k}}^+$ and $b_{\mathbf{k}}$ obey fermionic anticommutation rules

$$\{b_{\mathbf{k}}, b_{\mathbf{k}'}^+\} = \delta_{\mathbf{k},\mathbf{k}'}.$$

(6.4) (a) Show that the coherent state, Eq. 4.42, is equivalent to

$$|\Psi\rangle = \prod_{\mathbf{k}} \left(b_{\mathbf{k}\uparrow}^{+} \right) |0\rangle.$$

Hence show that

$$\langle \Psi | b_{\mathbf{k}\uparrow}^{+} b_{\mathbf{k}\uparrow} | \Psi \rangle = 1.$$

(b) Write $c_{\mathbf{k}\uparrow}^{+} c_{-\mathbf{k}\downarrow}^{+}$ in terms of the $b_{\mathbf{k}}^{+}$ and $b_{-\mathbf{k}}^{+}$ operators. Hence show that

$$\langle \Psi | b_{\mathbf{k}\uparrow}^{+} b_{-\mathbf{k}\downarrow}^{+} | | \Psi \rangle = u_{\mathbf{k}} v_{\mathbf{k}}$$

(6.5) (a) The BCS gap equation becomes

$$1 = \lambda \int_{0}^{\hbar\omega_D} \frac{1}{\epsilon} \tanh \left(\frac{\epsilon}{2k_{\mathrm{B}}T_c} \right) d\epsilon$$

at the critcal temperature T_c. Show that the integrand can be reasonably well approximated by

$$\frac{1}{\epsilon} \tanh \left(\frac{\epsilon}{2k_{\mathrm{B}}T_c} \right) \approx \begin{array}{ll} 1/\epsilon & \epsilon > 2k_{\mathrm{B}}T_c \\ 0 & \text{otherwise} \end{array}.$$

Hence, write down a simple analytical estimate of T_c. How close is your estimate to the exact BCS value?

(b) Show that the gap equation becomes

$$1 = \lambda \int_{0}^{\hbar\omega_D} \frac{1}{(\epsilon^2 + |\Delta|^2)^{1/2}} d\epsilon$$

at $T = 0$. Making the approximation

$$\frac{1}{(\epsilon^2 + |\Delta|^2)^{1/2}} \approx \begin{array}{ll} 1/\epsilon & \epsilon > |\Delta| \\ 0 & \text{otherwise} \end{array}.$$

find a simple analytical estimate of $|\Delta|$. Compare your results with the famous BCS result $|\Delta| = 1.76 k_{\mathrm{B}} T_c$.
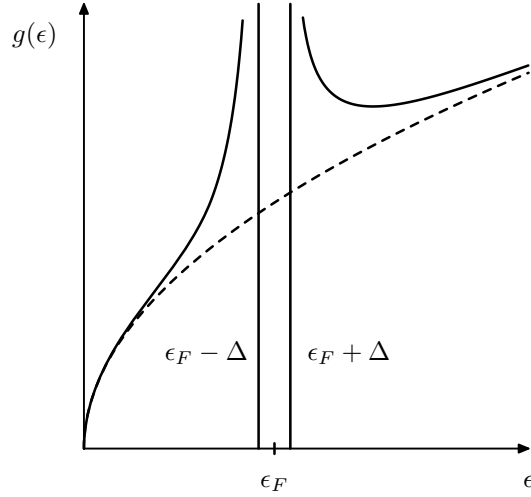
Fig. 4.1 The BCS energy gap, 2Δ in a superconductor. The gap is always pinned at the Fermi level, unlike the gap in an insulator or a semiconductor, and hence electrical conduction always remains possible.
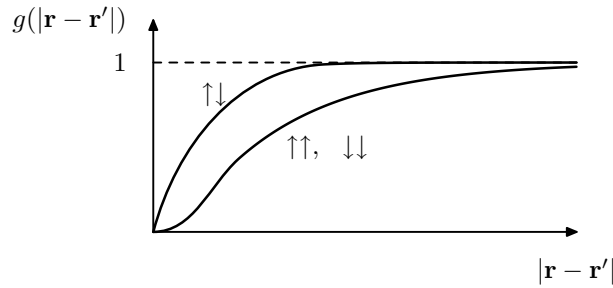

Fig. 4.2 The exchange-correlation hole for an electron moving in a metal. $g(|\mathbf{r} - \mathbf{r}'|)$ is the pair-correlation function of the electron gas. It measures the relative probability of finding an electron at $\mathbf{r}'$ given that one is at $\mathbf{r}$. By the Pauli exclusion principle this must vanish for $\mathbf{r} - \mathbf{r}'$ in the case of parallel spin particles, $\uparrow\uparrow$ and $\downarrow\downarrow$. This is the **exchange**-hole. But the $e^2/4\pi\epsilon_0 r$ repulsive Coulomb interaction gives an additional high energy cost for two electrons to be close together, whatever their spins. This is the **correlation** part of the exchange-correlation hole.
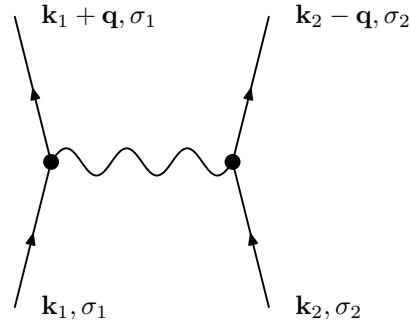
Fig. 4.3 Interaction of fermions via exchange of a gauge boson. In particle physics such diagrams could represent interactions between quarks due to exchange of gluons, interactions between electrons by exchange of photons or by exchange of W or Z bosons. In the BCS theory the same principle gives the interaction between electrons at the Fermi surface due to exchange of crystal lattice phonons.
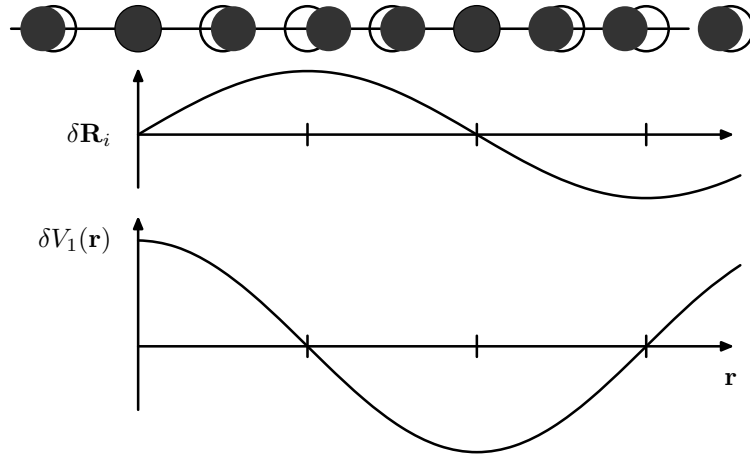

Fig. 4.4 A phonon in a solid and the resulting atomic displacements, $\delta abf R_i$, and deformation potential, $\delta V_1(\mathbf{r})$. For eaxmple, one can see that in the diagram the atom at the origin is not displaced, and locally its neighbours are further apart than average. This leads to a locally repulsive potential for the electrons, since there is a reduced positive charge density from the ions. In contrast, in regions where the atom density is higher than average the deformation potential is attractive for electrons.
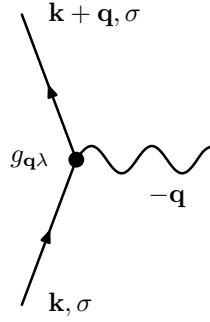
Fig. 4.5 The vertex for the electron phonon-interaction. The electron is scattered from **k** to **k**+**q** by the annihilation of a phonon of wave vector **q**, or the destruction of a phonon of wave vector −**q**. The phonon can be real or virtual, depending on the available energy.
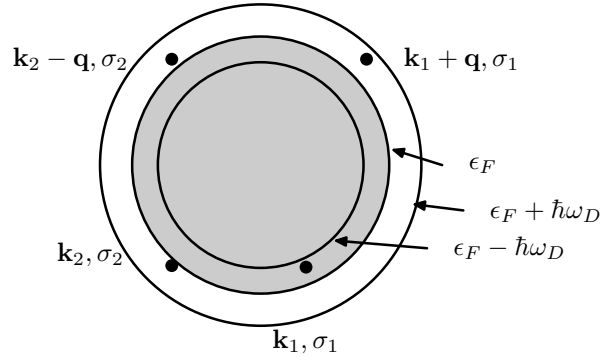

Fig. 4.6 The effective electron-electron interaction near the Fermi surface. The electrons at $\mathbf{k}_1, \sigma_1$ and $\mathbf{k}_2, \sigma_2$ are scattered to $\mathbf{k}_1 + \mathbf{q}, \sigma_1$ and $\mathbf{k}_1 + \mathbf{q}, \sigma_2$. The interaction is attractive provided that all of the wave vectors lie in the range where $\epsilon_{\mathbf{k}}$ is within energy $\pm \hbar \omega_D$ of the Fermi energy.
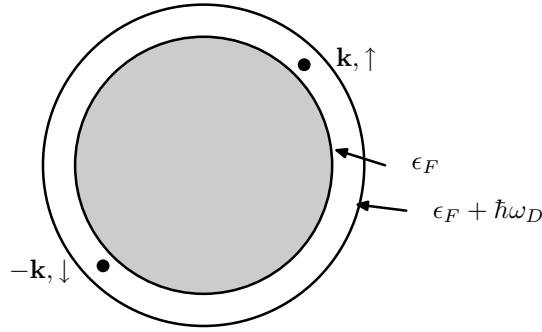
Fig. 4.7 The Cooper problem: two electrons outside a fully occupied Fermi sea. The interaction is attractive provided that the electron energies are in the range $\epsilon_F < \epsilon_{\mathbf{k}} < \epsilon_F + \hbar\omega_D$.
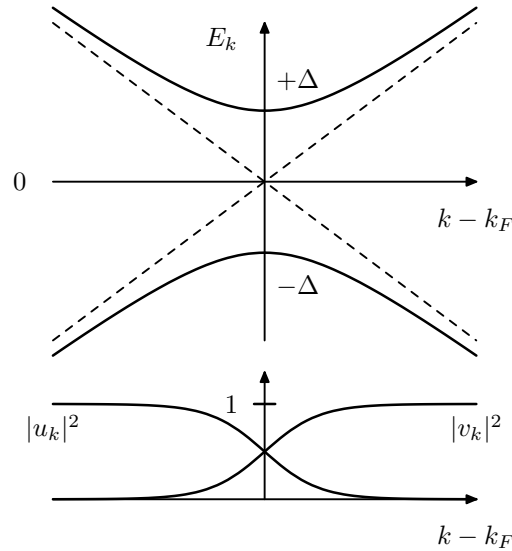

Fig. 4.8 Top: Energy eigenvalues $E_{\mathbf{k}}$ as a function of $\mathbf{k}$ near the Fermi wave vector $\mathbf{k}_F$. The dashed lines show the electron and hole energy levels $\epsilon_{\mathbf{k}} - \epsilon_F$ and $-\epsilon_{\mathbf{k}} + \epsilon_F$ in the normal metal. In the superconductor these states become hybridized, and the resulting eigenvalues are $\pm E_{\mathbf{k}}$ relative to ϵ_F. One can see that there are no states with energy less than $\pm\Delta$ near the Fermi energy. **Bottom:** The BCS wave function parameters $|u_{\mathbf{k}}|^2$ and $|v_{\mathbf{k}}$ for $\mathbf{k}$ near to the Fermi surface. The state is predominantly electron like well beow k_F ($|u_{\mathbf{k}}|^2 \approx 1$) and predominantly hole like far above the Fermi surface, ($|v_{\mathbf{k}}|^2 \approx 1$). But near to $\mathbf{k}_F$ the quasiparticle has mixed electron and hole character.
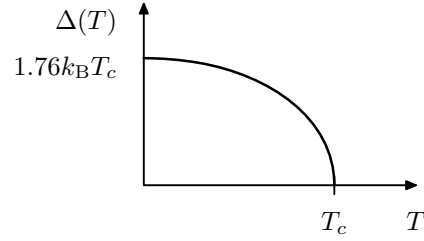
Fig. 4.9 Δ as a function of temperature in the BCS theory.

Fig. 4.10 NMR relaxation rate $1/T_1$ in the BCS theory. The peak below T_c is called the Hebel-Slichter peak, and is a consequence of specific **coherence factors** associated with the form of the BCS pair wave function. The drop to zero at low temperatures is due to the BCS energy gap. In contrast, in ultrasound the BCS coherence factors are different and imply a sudden drop immediately below T_c. Agreement between experiments and theory shows that the BCS state is an excellent description of the state.
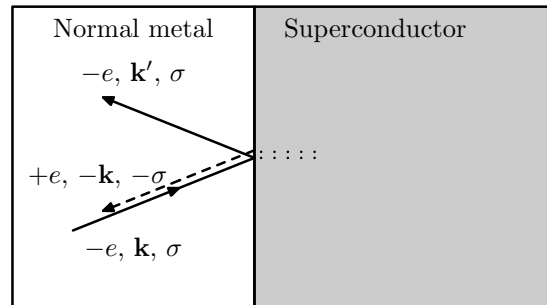
Fig. 4.11 Andreev scattering of electrons in a normal metal. The electron incident on the superconductor can either be reflected normally, remaining an electron of the same spin, or it can be Andreev reflected, becoming a hole of opposite momentum and spin. In the Andreev scattering process a net charge of $-e$ is passed into the superconducting condensate. The conductivity of the junction is two times that for electrons with energies V above the gap Δ.

Bibliography

Abo-Shaeer, J.R., Raman, C., Vogels, J.M., Ketterle, W., *Science* **292**, 476-479.

Abrikosov, A.A., Gorkov, L.P., Dzyaloshinski, I.E., (1963). *Methods of quantum field theory in statistical physics.* Dover, New York.

Abaramowitz, M., and Stegun, I.A. (1965), *Handbook of Mathematical Functions*, Dover, New York.

Amit, D.J. (1984), *Field Theory Renormalization Group, and Critical Phenomena*, World Scientific.

Annett, J.F. (1990), *Advances in Physics* **39**, 83-126.

Annett, J.F., Goldenfeld, N.D. and Renn, S.R., (1996), in *Physical Properties of High Temperature Superconductors V*, D.M. Ginsberg (ed.), World Scienfific.

Annett, J.F., Gyorffy, B.L. and Spiller T.P. (2002), in *Exotic States in Quantum Nanostructures*, S. Sarkar (Ed.), Kluwer.

Ashcroft, N. and Mermin, N.D. 1976, *Solid State Physics*, W.B. Saunders.

Anderson, P.W. (1984). *Basic Notions of Condensed Matter Physics.* Benjamin/Cummings, Melno Park.

Blatter, G., Feigel'man, M. V., Geshkenbein, V. B., Larkin A. I. and Vinokur, V. M. (1994), *Rev. Mod. Phys.* **66**, 1125-1388.

Blundell, S. (2001). *Magnetism in Condensed Matter.* Oxford Univ ersity Press, Oxford.

Boas, M.L. (1983), *Mthematical Methods in the Physical Sciences*, 2nd ed., John Wiley & Sons.

Bogoliubov, N. (1947), *Journal of Physics*, **11** 23.

Callen, H.B., (1960).*Thermodynamics.* John Wiley and Sons, New York.

Ceperley, D.M. (1995). *Rev. Mod. Phys.* **67**, 279-355.

Chakin, P.M. and and Lubensky, T.C.(1995). *Principles of Condensed Matter Physics.* Cambridge University Press.

Chu, C.W., Gao, L., Chen, F., Huang, L.J., Meng, R.L. and Xue, Y.Y. (1993), *Nature* **365**, 323-5.

Chiorescu *et al.* (2003), *Science* **299**, 1869.

Dalfovo,F., Giorgni,S., Pitaevskii,L.P., and Stringari,S. (1999). *Rev. Mod. Phys.* **71**, 463-513 (1999).

Fetter, A.L. and Walecka, J.D. (1971).*Quantum many-particle theory.* McGraw Hill, New York.

Feynman R.P., Leighton, R.B. and Sands M. (1964), *The Feynman Lectures on Physics, Volume II*, Addison Wesley.

Feynman, R.P., (1972). *Statistical Mechanics.* Addison Wesley, Redwood City.

Friedman J.R. *et al.* (2000), *Nature* **406** 43.

de Gennes, P.-G., (1966). *Superconductivity of Metals and Alloys*, Addison Wesley Advanced Book Programme, Redwood City.

Goldendeld, N.D. (1992), *Lectures on Phase Transitions and the R enormalization Group*, Addison-Wesley, Reading, MA.

Home, D. and Gribbin, J. (1994). *New Scientist*, 9 January, page 26.

Huang, K., (1987). *Statistical Physics.* 2nd Edition, J. Wiley, New York.

Jones, R.A.L., (2002). *Soft Condensed Matter* . Oxford University Press, Oxford.

Ketterle, W. (2002). *Rev. Mod. Phys.* **74**, 1131-1151.

Ketterle, W. (2003), http://cua.mit.edu/ketterle_group/Nice_pics.ht m.

Ketterson, J.B. and Song, S.N. (1999). *Superconductivity.* Cambridge University Press, Cambridge.

Kittel, C. (1996). *Introduction to solid State Physics*, 7th ed., John Wiley & Sons.

Klauder, J.R. and Skagerstam, B-S (1985), *Coherent States: Applications in Physics and Mathematical Physics*, World Scientific.

Leggett, A.J. (1975), *Rev. Mod. Phys.*, **47** 332-414.

Leggett, A.J. (1980), *Suppl. Prog. Theor. Phys.* **69**, 80-100.

Leggett, A.J. (2001). *Reviews of Modern Physics* **73**, 307-356.

Leggett, A.J. (2002), *J. Phys.: Condens. Matter* **14**, R415.

Loudon, R. (1979), *The Quantum Theory of Light*, Oxford.

Ma, S-K. (1974), *Modern Theory of Critical Phenomena*, Benjamin/Cummings.

Mahklin, Y., Schön, G., and Shnirman A. (2001), *Rev. Mod. Phys.* **73**, 357.

Mandl, F. (1987). *Statistical Physics* (2nd edn.). J. Wiley, Chicester.

Matthews J., and Walker, R.L. (1970), *Mathematical Methods of Physics*, 2nd ed., Addison Wesley.

Nakamura, Y., Pashkin, Y.A., and Tsai, J.S. (1999), *Science* **398** 786-788.

Overend N., Howson M.A. and Lawrie I. D. (1994), Phys. Rev. Lett. 72, 3238-3241.

Pines, D. (1961), *The Many Body Problem*, Benjamin Cummings, Reading Massachusetts.

Phillips, W.D. (1998). *Rev. Mod. Phys.* **70**, 721-741.

Poole, C.P. (2000), *Handbook of Superconductivity*, Academic Press.

Ramakrishnan, T.V., and Rao, C.N.R., (1992). *Superconductivity Today.* Wiley Eastern, New Dehli.

Rickayzen, G. (1980). *Green's functions and condensed matter.* Academic Press, London.

Sauls, J.A. (1994), *Advances in Physics* **43**, 113-141.

Silver, R.N., and P.E. Sokol, P.E. (eds.) (1989).*Momentum Distributions.* Plenum, New York.

Schrieffer, J.R. (1964). *Theory of Superconductivity*. Benjamin/Cummings, Reading Massachusets.

Schneider, T. and Singer, J.M. , (2000). *Phase Transition Approach to High Temperature Superconductors*, Imperial College Press, UK.

Singleton, J., (2002). *Band theory and electronic properties of solids.* Oxford University Press, Oxford.

Tilley, D.R. and Tilley, J (1990). *Superfluidity and Superconductivity* (3rd Edition), Adam Hilger and IOP Publishing, Bristol.

Tinkham, M. (1996). *Introduction to Superconductivity* 2nd Ed. McGraw-Hill, New York.

van der Wal, C. *et al.* (2000), *Science* **290** 773.

Tsuei, C.C. and Kirtley, J.R. (2000), *Rev. Mod. Phys.* **72** 969-1016.

Waldram, J.R. (1996). *Superconductivity of Metals and Cuprates*, Institute of Physics, Bristol.

Wheatley, J.C. A.J. (1975), *Rev. Mod. Phys.*, **47** 415-470.

Yeshurun, Y., Malozemoff, A. P. and Shaulov , A. (1996), *Rev. Mod. Phys.* **68**, 911-949.

Ziman, J.M. (1979), *Principles of the Theory of Solids*, 2nd Ed., Cambridge University Press.